2005-11-21

Acoustics of the Salt Lake Tabernacle: Characterization and Study of Spatial Variation

Sarah Rollins
Brigham Young University - Provo

THE SALT LAKE TABERNACLE: ACOUSTIC CHARACTERIZATION AND STUDY OF SPATIAL VARIATION

by

Sarah Rollins

A thesis submitted to the faculty of

Brigham Young University

in partial fulfillment of the requirements for the degree of

Master of Science

Department of Physics and Astronomy

Brigham Young University

December 2005

BRIGHAM YOUNG UNIVERSITY

GRADUATE COMMITTEE APPROVAL

of a thesis submitted by

Sarah Rollins

This thesis has been read by each member of the following graduate committee and by majority vote has been found to be satisfactory.

_____	_____
Date	Timothy W. Leishman, Chair
_____	_____
Date	Scott D. Sommerfeldt
_____	_____
Date	Jonathan D. Blotter

BRIGHAM YOUNG UNIVERSITY

As chair of the candidate's graduate committee, I have read the thesis of Sarah Rollins in its final form and have found that (1) its format, citations, and bibliographical style are consistent and acceptable and fulfill university and department style requirements; (2) its illustrative materials including figures, tables, and charts are in place; and (3) the final manuscript is satisfactory to the graduate committee and is ready for submission to the university library.

_____	_____
Date	Timothy W. Leishman Chair, Graduate Committee

Accepted for the Department

_____	_____
Date	Ross L. Spencer Graduate Coordinator

Accepted for the College

_____	_____
Date	G. Rex Bryce Associate Dean, College of Physical and Mathematical Sciences

ABSTRACT

ACOUSTICS OF THE SALT LAKE TABERNACLE:

CHARACTERIZATION AND STUDY OF

SPATIAL VARIATION

Sarah Rollins

Department of Physics and Astronomy

Master of Science

In order to preserve the acoustics of the Salt Lake Tabernacle after the seismic renovation of 2005-2006, it was necessary to characterize these acoustics immediately preceding the renovation. This thesis discusses the characterization process that began with the measurement of hundreds of impulse responses for five different source positions and several receiver locations throughout the hall seating areas. The acoustics were further characterized by deriving various parameters from these responses that correlate with subjective preferences for music and speech. Impulse responses were also generated by a CATT-Acoustic™ computer model of the Tabernacle for the same purpose. The parameter values were then mapped over diagrams of the seating areas of the hall to show the spatial variation of the acoustics. To further investigate the variation, statistics were calculated for each parameter and an algorithm was developed to

determine the minimum number of receiver locations necessary to adequately characterize the hall. Computer models were also used to investigate focusing effects of the curved ceiling and historical comments made about the improvements to the acoustics with addition of the balcony in 1870.

ACKNOWLEDGMENTS

I would like to thank the following people for their encouragement and support during the research and writing of this thesis:

* Dr. Leishman, Dr. Sommerfeldt, and Dr. Blotter for their helpful suggestions and encouragement.
* The Physical Facilities Department of The Church of Jesus Christ of Latter-Day Saints, the Department of Physics and Astronomy, and the Copley family, for funding this research.
* FFKR Architects, for AutoCAD drawings and historical photographs.
* Tim Gulsrud of Kirkegaard Associates, for data on occupied measurements in the Tabernacle.
* Heather Smith, for her suggestions for improving the CATT-Acoustic™ computer model.
* Micah Shepherd, for his help with ray-tracing in the EASE® computer model.
* Students of the Acoustic Research Group, for measuring hundreds of impulse responses in the Tabernacle.
* My family and friends, for their constant encouragement and prayers.

Table of Contents

List of Tables

List of Figures

1 Introduction

The Salt Lake Tabernacle has been well known for its unique acoustics since it was completed in 1867. Every day, people from all over the world visit this historic building and hear a demonstration of its acoustics. During the demonstration, a speaker is located at the front of the room, usually about 30 m or more from the audience. Even at this distance, the speaker can be heard without a microphone and the audience can easily hear pins drop on a wooden table. Such demonstrations have led to the Tabernacle's reputation among the general public for ideal acoustics. However, while those who better understand its acoustics recognize that they are interesting, they also recognize that they are not perfect. A few acousticians have measured the hall on a more technical level. Wayne Hales measured the reverberation time, intensity, and perception of echoes throughout the hall in the early 1920s.[1,2] In the early 1960s Vern Knudsen and Harvey Fletcher observed a flutter echo across the width of the hall and a dramatic decrease in reverberation time when the hall was occupied.[3] However, few if any detailed measurements have been made and published using modern equipment and techniques.

The hall is currently undergoing a major seismic renovation that could have an impact on its acoustics.[4,5] In order to preserve their uniqueness and historical significance, modern techniques were used in this study immediately preceding the renovation to characterize the hall as a benchmark for future comparisons. Several acoustic parameters were also analyzed to investigate the spatial variation of the sound field.

The study of architectural or room acoustics began in 1895 when Wallace Clement Sabine developed the formula for calculating the reverberation time of a room.[6] Later, Manfred Schroeder derived the reverberation time from the measured impulse response of a room, using reverse integration.[7] For this and other reasons, the measurement of impulse responses in rooms is central to modern techniques in architectural acoustics. It depends upon the room, the receiver position, and the source position. To further characterize sound quality in speech and musical performance spaces, many objective parameters have been developed in recent years that correlate with subjective descriptions and preferences.[8,9,10] These parameters are also derived from impulse responses measured at different locations using specific source and receiver configurations. In addition, new techniques have been developed for measuring the impulse responses that are superior to early methods of popping balloons and firing starter pistols to generate the impulses. The modern methods typically use a computer to generate a signal, which is sent through a loudspeaker in the hall. A microphone subsequently measures the response of the hall and provides a response signal to the computer. The signal is compared to the original signal to derive the impulse response for this particular source-receiver combination. The maximum-length sequence (MLS) signal[11,12] was chosen for this study because of its convenience and ability to produce impulse responses consistently and accurately, even in the presence of background noise.

The unique geometry of the Tabernacle makes it especially interesting for measuring and characterizing room acoustics. Its floor plan is rectangular with semicircular extensions on both short sides. The ceiling is a barrel-vaulted ceiling over the rectangular portion of the floor, with approximate quarter spheres over the

semicircular extensions of the floor. Whispering gallery effects can be heard in many locations of the hall from these large concave surfaces. Accordingly, one might expect the sound field in the hall to be less uniform over the seating areas than in many other halls. Figure 1.1 shows the various seating areas in the Tabernacle. The domed ceiling and the quasi-elliptical footprint of the hall focus sound to different areas of the main floor and balcony.

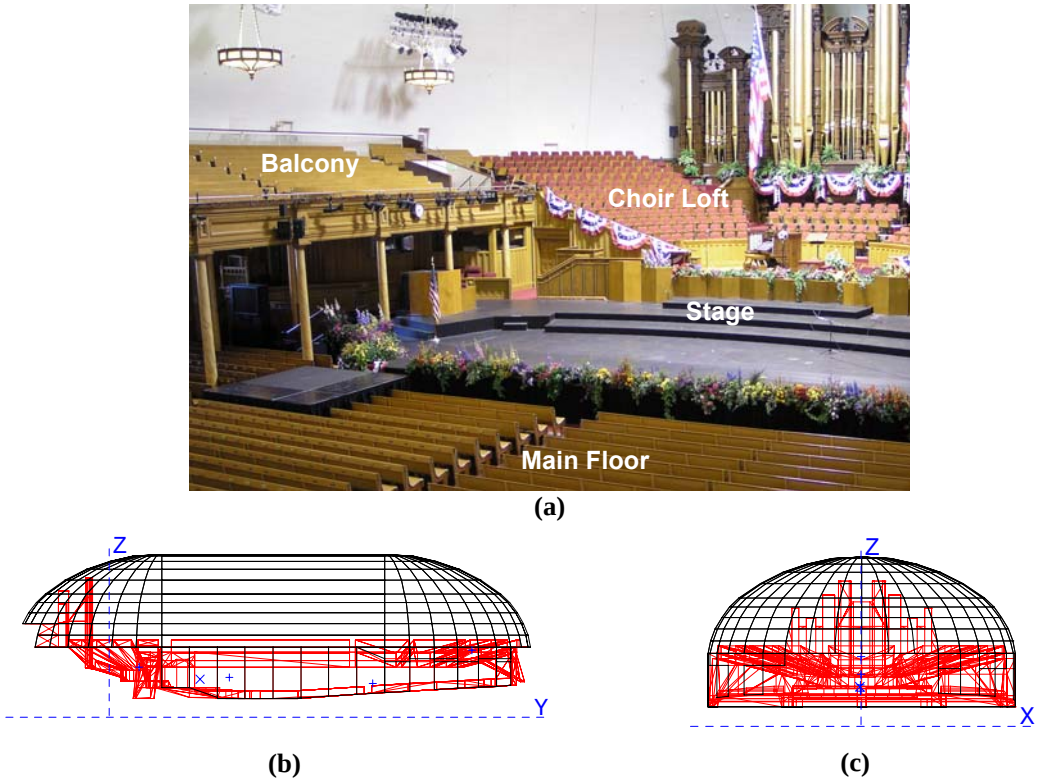

FIG. 1.1. Several different views of the Tabernacle. (a) Different seating areas in the Tabernacle. (b) Side view drawing of the Tabernacle. (c) Rear view drawing of the Tabernacle. These drawings show two different views of the curvature of the ceiling.

When architectural acoustics parameters are determined for halls, they are typically measured for only a few selected seating locations.[13,14] However, the parameter values are not necessarily uniform over the entire seating area of a hall. In some cases, they differ significantly, depending on both source and receiver locations. Therefore, in

this project, several seating locations in the hall were measured in order to investigate the spatial variation of the sound field by looking at the spatial variation of the different objective parameters. Pelorson, Vian and Polack studied the spatial variation of room acoustic parameters as part of their study on the variability of room acoustical parameters. In one case, they found that large spatial variability corresponded to low acoustical quality. They also observed that reverberation time and lateral efficiency did not show significant spatial variation in the halls they studied. On the other hand, the clarity factor for music produced such a large range of values that many positions would need to be measured in the hall in order for the mean to accurately represent that hall when comparing it to others.[15] They calculated the reverberation time (RT), the early decay time (EDT), clarity factor for music (C80), definition (D50), signal to noise ratio (S/N), center time (T_c) and strength index (G), but they did not calculate the lateral fraction (LF), binaural quality index (BQI), speech transmission index (STI), or any echo criteria (ECM, ECS). They studied smaller halls and only reported the standard deviation and range of the parameter values.

The unique shape and resultant acoustics of the Tabernacle provide an especially interesting environment for investigating the spatial variation of such parameters. Furthermore, through the use of several receiver positions, the hall enabled the study of convergence of parameter values as a function of increasing the number of receiver positions. This allowed a determination of the minimum number of receiver positions necessary to characterize the hall. A comparison between values measured in the Tabernacle and those published for the Boston Symphony Hall (a hall known for its

outstanding acoustics) was also made, in order to show how characterizing a hall by measuring only a few seats can be misleading.

To further analyze the sound in halls, computer software packages have been developed to model room acoustics. These packages allow the user to draw a room in three dimensions, place sources and receivers in different locations, and auralize the environment. An auralization is a binaural recording of what speech or music would sound like in the room at a specific receiver position for a given source position.[16,17,18] To create an auralization, the binaural impulse response is convolved with music or speech that has been recorded in an anechoic environment. The impulse response is typically simulated using the image source and ray-tracing methods.[19] These methods also lead to the prediction of the acoustical parameters mentioned previously. The impulse responses and parameter predictions are very important to assess how changes in the hall might affect its acoustics.

The goals of this research effort were to thoroughly characterize the acoustics of the Tabernacle and to investigate the spatial variation of its architectural acoustics parameters. Another objective was to determine the minimum number of receiver locations necessary to characterize the hall. A third goal was to study the acoustics of previous configurations of the hall in conjunction with historical comments.

The scope of the research project was limited to impulse response measurements for five different source positions and three different types of receivers in an unoccupied hall. While there are many architectural acoustics parameters, only nine were derived from the impulse responses. Computer modeling was performed almost exclusively in

CATT-Acoustic™ v. 8.0c (build 3). Ray-tracing viewing was performed in EASE® v. 4.1.0.2.

The following chapter explores the impulse response measurement procedure. Chapter 3 discusses the architectural acoustics parameters used in the investigation. The actual values of the parameters in the Tabernacle are then shown in Chapter 4. Statistical and subjective analyses of the parameters are presented in Chapter 5. Chapter 6 presents details and analysis of the computer model of the current configuration of the Tabernacle. Chapter 7 discusses the measurements required for historical computer models and relates the results of these models to historical comments about the hall acoustics. Chapter 8 draws conclusions and suggests topics for further exploration.

2 Impulse Response Measurements

2.1 Maximum-Length Sequence Technique

To characterize the acoustics of the Tabernacle, several impulse response measurements were taken in the unoccupied hall using the MLS technique.[20] A maximum-length sequence is a periodic sequence of integers that is generated by an n-step shift register to produce a period length of $N = 2^n-1$. Since the Fourier transform of this sequence has essentially the same magnitude for all frequencies of interest, it is frequency independent and has the same spectrum as a single impulse. To obtain the impulse response of the room using the signal, the measured room response is cross correlated with the original signal generated by the analyzer.[21]

When taking room response measurements using the MLS method, it is important to use a sequence with a period long enough to capture the full response of the room. For this to be the case, the time period of the sequence should be longer than the reverberation time of the room. In the Tabernacle, this meant using a sequence of length N = 262,143 or 5.196 seconds, since the next lowest sequence length was only 2.6 seconds and the reverberation time was measured to be above 3 seconds during preliminary measurements.

2.2 Measurement Setup

A TEF 20 analyzer was used to generate and process the 262,143-point sequence using 10 averages and one pre-excite sequence, for a measurement time of approximately one minute for each impulse response. Each response was saved in both the MLS binary format and the Matlab® float format for post processing. For data storage and stability to

the connection between the laptop and the TEF analyzer, an external ZIP® drive was connected between the two, as shown in Fig. 2.1. This figure also shows the connections used for the source and receivers.

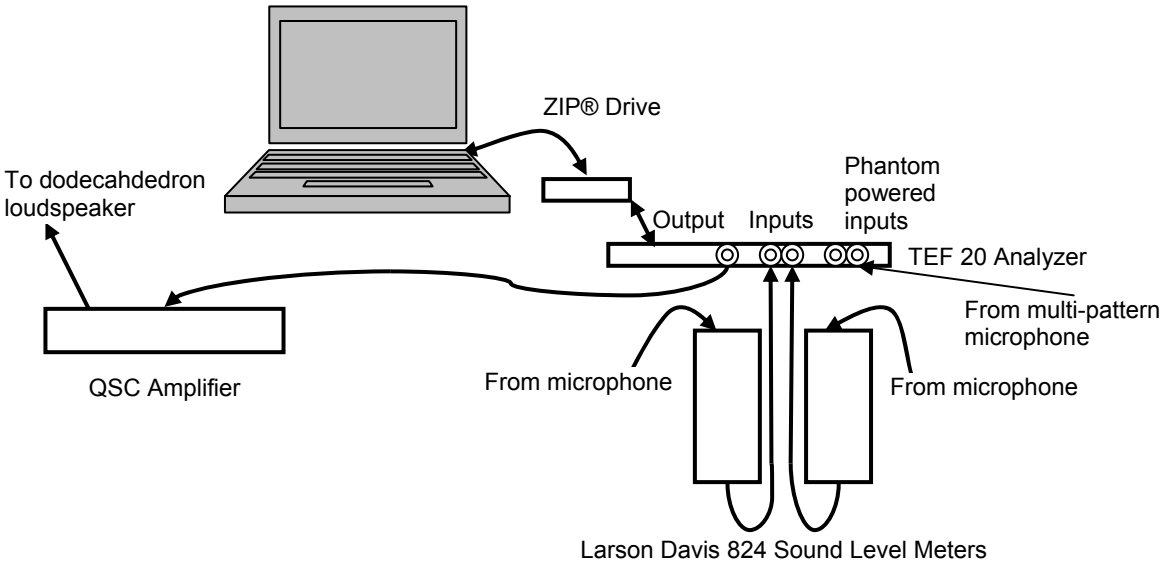

FIG. 2.1. Measurement setup, excluding the microphones and dodecahedron loudspeaker, showing the connections used for two omnidirectional microphones. The phantom power connections on the right of the TEF were used for a multi-pattern microphone.

The TEF was connected to a custom-built dodecahedron loudspeaker through a QSC CX702 amplifier and to two Larson Davis 2650 random-incidence microphones and PRM902 preamplifiers through two Larson Davis 824 sound level meters used as power supplies. Figure 2.2(a) shows the Larson Davis omnidirectional microphone arrangement used to measure impulse responses throughout the hall. An Audio Technica AT4050 multi-pattern microphone [Fig. 2.2(b)] and a KEMAR (Knowles Electronic Manikin for Acoustic Research) manikin [Fig. 2.2(c)] were also used to measure impulse responses for several relevant source-receiver configurations. The phantom power on the TEF was

only used to power the multi-pattern microphone. The omnidirectional microphones and their electronics were used with right-angle adapters in the left and right ears of the KEMAR manikin. The gains for the output driving the dodecahedron loudspeaker and the input from the multi-pattern microphone were adjusted in the TEF Sound Lab software and the gains for the omnidirectional microphones were adjusted through the sound level meters. All of the equipment, except the loudspeaker and microphones, was located on a table in the middle of the far right section on the main floor in the Tabernacle.

(a) **(b)** **(c)**

FIG. 2.2. Receivers that measured several impulse responses in the Tabernacle. (a) Omnidirectional, random-incidence microphone. (b) Multi-pattern microphone. (c) KEMAR manikin.

2.3 Source Positions

Several source positions were used, as shown in Fig. 2.3 and Table 2.1. The MLS signal was sent through the dodecahedron loudspeaker with all drivers active for the first three source positions: orchestra center stage, choir soprano section, and choir alto section. For the orchestra center stage position shown in Figs. 2.3 and 2.4, the height of

the center of the dodecahedron loudspeaker was about 1.4 m. This position was chosen in order to approximate the response of the hall for the orchestra on the stage. This is a rough approximation since the dodecahedron loudspeaker was essentially a point source at center stage, while the orchestra is a distributed source, covering the entire stage. The MLS signal coming from the dodecahedron loudspeaker also produced sound for a broad portion of the audio spectrum while an orchestra has frequency dependence depending on where the different instruments are positioned on the stage. Nevertheless, this central source location was used to provide relevant information about the hall.

Figures 2.3 and 2.5 show the second source position in the middle of the soprano section of the choir loft, and the third position in the alto section. These positions were chosen to approximate the response of the hall to the choir. To measure the response of the hall to the installed sound system, the next scheme was to have the dodecahedron loudspeaker back at center stage, but this time with only one driver active. The driver was directed toward a microphone about 0.5 m away that was connected to the house sound system, as shown in Fig. 2.6(a). Figure 2.6(b) shows the fifth source position with the dodecahedron loudspeaker at a former pulpit location, approximately where the acoustical demonstration table now stands. This source position was chosen to compare with results of the historical model. Again, this is a rough approximation since the historical model includes the rostrum, a smaller choir loft, and a smaller organ case instead of the current larger choir loft, larger organ case, and the orchestra stage.

(a)

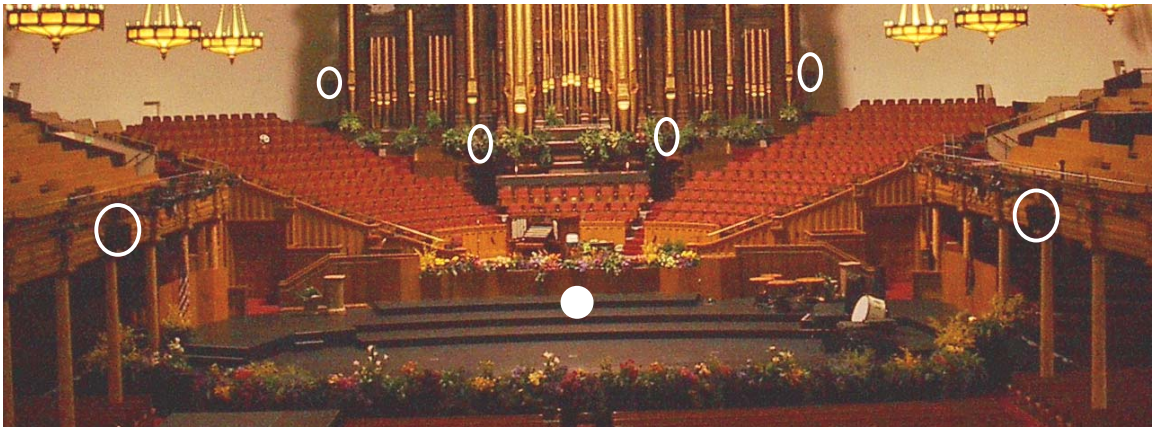

(b)

FIG. 2.3. Locations for the dodecahedron loudspeaker in the Tabernacle. (a) Soprano, alto, pulpit, and center stage positions. The filled circles show the former positions, while the open circle shows the source in the last position. (b) Locations of the loudspeakers for the sound system measurements. The filled circle shows the location of the dodecahedron loudspeaker and the open circles show the locations of the loudspeakers that are visible in this picture. Two additional loudspeakers, one in front of the left and right sections under the balcony, are not shown.

Table 2.1. Table of information about each source position used to measure impulse responses and characterize the acoustics of the Salt Lake Tabernacle.

Source Number	Source Position	Source Height
1	Center Stage	1.4 m
2	Choir Soprano Section	1.5 m
3	Choir Alto Section	1.5 m
4	Stage – Sound System	1.5 m
5	Old Pulpit Position	1.5 m

FIG. 2.4. Dodecahedron loudspeaker at center stage, behind the stage conductor's stand.

(a) **(b)**

FIG. 2.5. Second and third dodecahedron loudspeaker locations. (a) Soprano section. (b) Alto section.

(a) (b)

FIG. 2.6. Fourth and fifth dodecahedron loudspeaker locations. (a) On stage, through the sound system. (b) Pulpit position. Fig. 2.3(b) shows the sound system loudspeaker locations.

2.4 Receiver Positions and Types

Several receiver positions were chosen to measure the response of the hall in different seating areas. For the orchestra center stage source position, 133 receiver positions were utilized, as shown in Fig. 2.7. A reduced number of receiver positions were used for the rest of the source positions in order to conserve time. Figure 2.8(a) shows the receiver positions used for the source in the choir sections and through the sound system. For the source at the old pulpit position, we assumed complete symmetry of the sound field in the hall and only placed the omnidirectional receivers in the north half of the hall, as shown in Fig. 2.8(b). Measurements with KEMAR were only made at a few of these same locations, marked by the + symbols in Fig. 2.8(b).

All receivers were placed approximately at seated ear height for all receiver positions except the choir positions, which were adjusted to standing ear height to assess the response of the room for standing choir members. To speed up the omnidirectional receiver measurements, two microphones were alternately used in the process. While one was in use, the other was moved to the next measurement position. For the

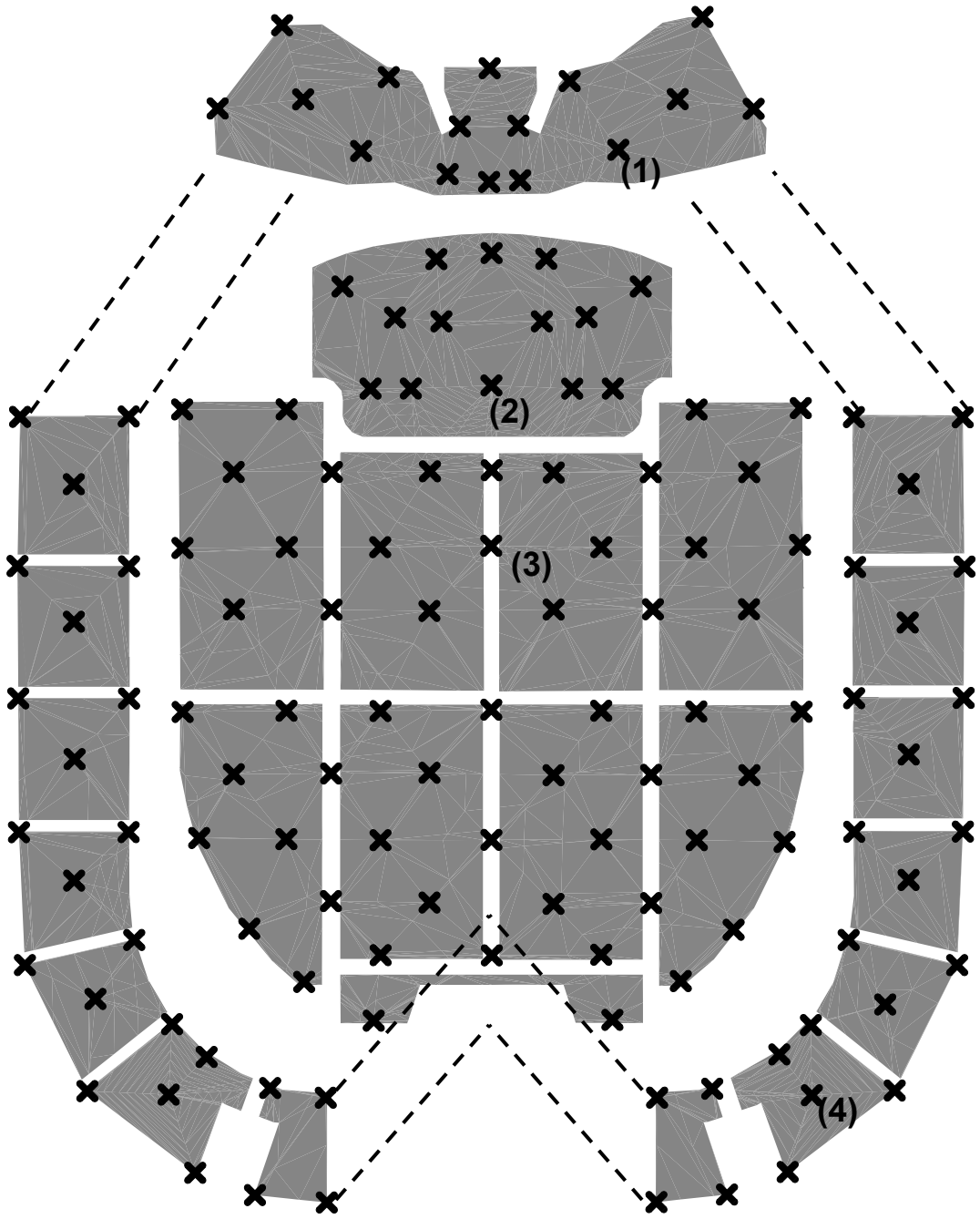

FIG. 2.7. Receiver locations for the source at center stage. The numbers 1 through 4 show the receiver locations for the impulse responses shown later in Fig. 3.3. The dashed lines show how the balcony is split and shifted so all of the receiver positions on the main floor and balcony can be seen in a single plan view.

measurements made with the multi-pattern microphone, the null of the microphone for the bipolar setting was oriented toward the choir conductor position, except for the stage receiver positions, where it was oriented toward the orchestra conductor position. The KEMAR manikin was also oriented toward these same positions, even when this meant turning it at an angle relative to the benches.

Most of the measurements were taken from February through April 2004, with a few more sets taken in July 2004. Due to the quantity of measurements, many measurements were taken during the day, when there were still a few people in the hall. The rest of the measurements were taken later at night, including ambient noise measurements. Taking most of the measurements earlier in the year was beneficial because this meant that humidity and temperature in the building, as well as the number of people in the building, did not vary much throughout the day. The exterior doors were also kept shut more during this time of year than in the warmer summer months.

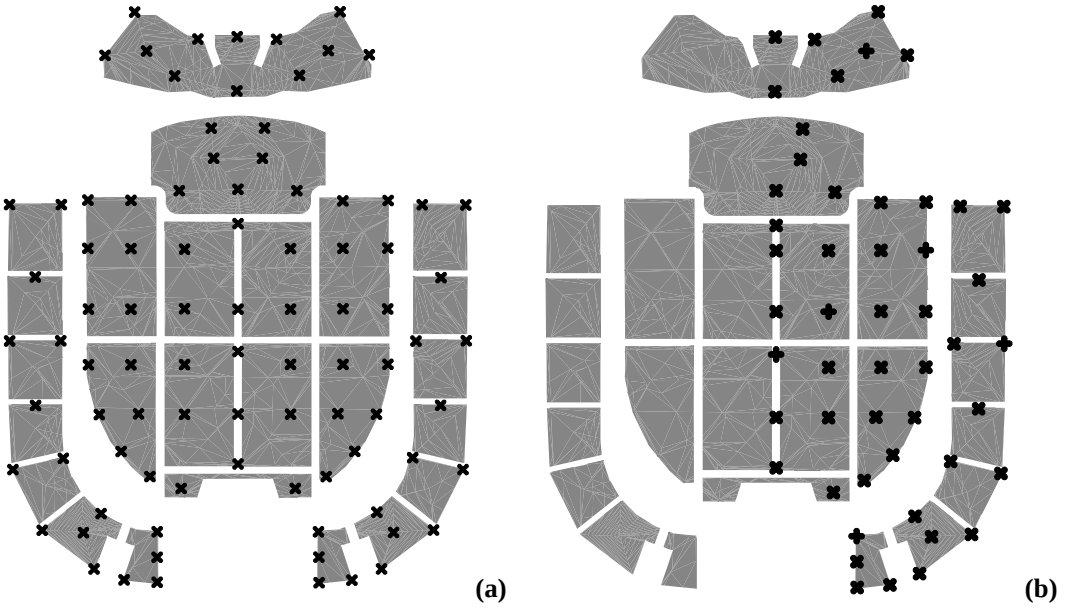

FIG. 2.8. Receiver locations. (a) Source in the choir locations and through the sound system. (b) Source at the old pulpit position. The few KEMAR locations used for the source at the pulpit position are marked by the + symbols.

3 Acoustics in the Tabernacle

To quantify the quality of an auditorium or concert hall, it is necessary to use objective parameters. However, these parameters must also be related to subjective preferences in order to make them useful when communicating ideas about the hall to people who make decisions about the space, such as owners and performers. In architectural acoustics research, many objective parameters have been developed to correlate with these subjective preferences. In this study, nine objective parameters were calculated, in order to cover several different auditory aspects of the hall.

3.1 Balanced Noise Criterion

The balanced noise criterion (NCB) was developed to quantify how much background noise is allowable in various listening environments. It is calculated from frequency-dependent NCB curves based on the American National Standard for speech-interference level (SIL) for occupied spaces.[22] For this project, the required sound pressure level (SPL) measurements were taken late at night in an unoccupied Tabernacle. Levels during events might actually be higher than those found. To calculate the NCB value for a specific location, the octave-band SPLs for several locations in the Tabernacle were plotted against the NCB curves, as shown in Fig. 3.1. The overall NCB rating was determined by the highest SPL value relative to the NCB curves, shown by the red circle in Fig. 3.1. Typically, a value of NCB-20 or lower is desired for concert halls,[23] but with such thin floor and exterior wall constructions, this is not attained in the Tabernacle.

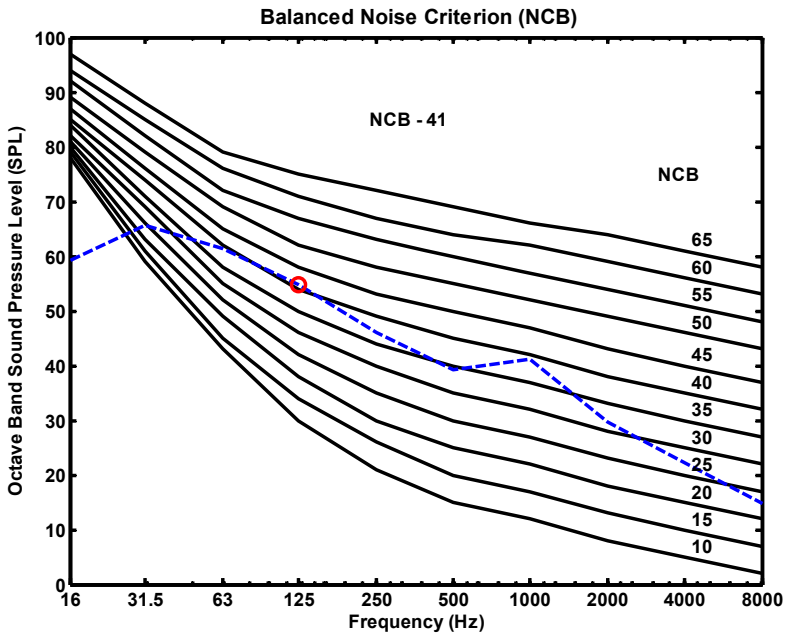

FIG. 3.1. Balanced Noise Criterion (NCB) curves used for calculating the NCB for position 3 in Fig. 2.7. The dashed blue line shows the octave band SPL measured at this location. The red circle shows the point on the dashed line that falls above the highest NCB curve to get the value of NCB-41.

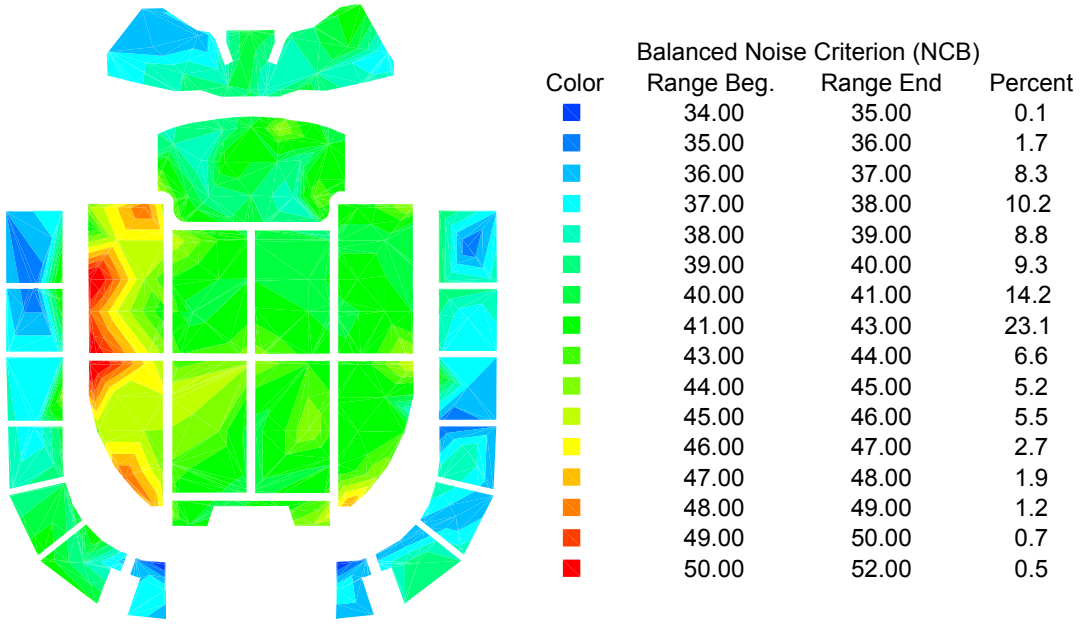

FIG. 3.2. Color map of the measured values for the balanced noise criterion (NCB).

Figure 3.2 shows the NCB mapped over the seating areas of the Tabernacle. The measurements of background noise were taken after the Tabernacle was closed to the public. However, that was when traffic was moving nearby and the cleaning crew started cleaning the sidewalks outside, so it was not completely quiet. If there was a noticeably loud noise during a measurement, the measurement was taken again when the noise subsided. The higher values shown by the red on the left of the main floor are caused by an equipment room below the floor which produces noticeable low frequency vibrations. These vibrations could be felt through the pews in this area.

3.2 Impulse Response Plots

The log-squared impulse response is useful in plots because the decay of reverberant sound in a room is typically exponential. When the squared impulse response is plotted on a log scale, it takes on a linear decay, as shown over a large portion of Fig. 3.3(a). This makes it easier to see the general decay of the room and check impulse response irregularities. In the case of the Tabernacle, clusters of focused reflections could often be seen protruding from the linear slope. This is especially apparent in impulse response shown in Figs. 3.3(b) and 3.3(c) for the receiver positions on the stage and the main floor (2 and 3 in Fig. 2.7). Figure 4.7 shows focusing of the sound for the seat on the main floor in a ray-tracing diagram from EASE®. These reflections produced the first cluster of reflections after the direct sound. Higher order reflections from the side walls and other areas of the ceiling produced the later clusters of reflections.

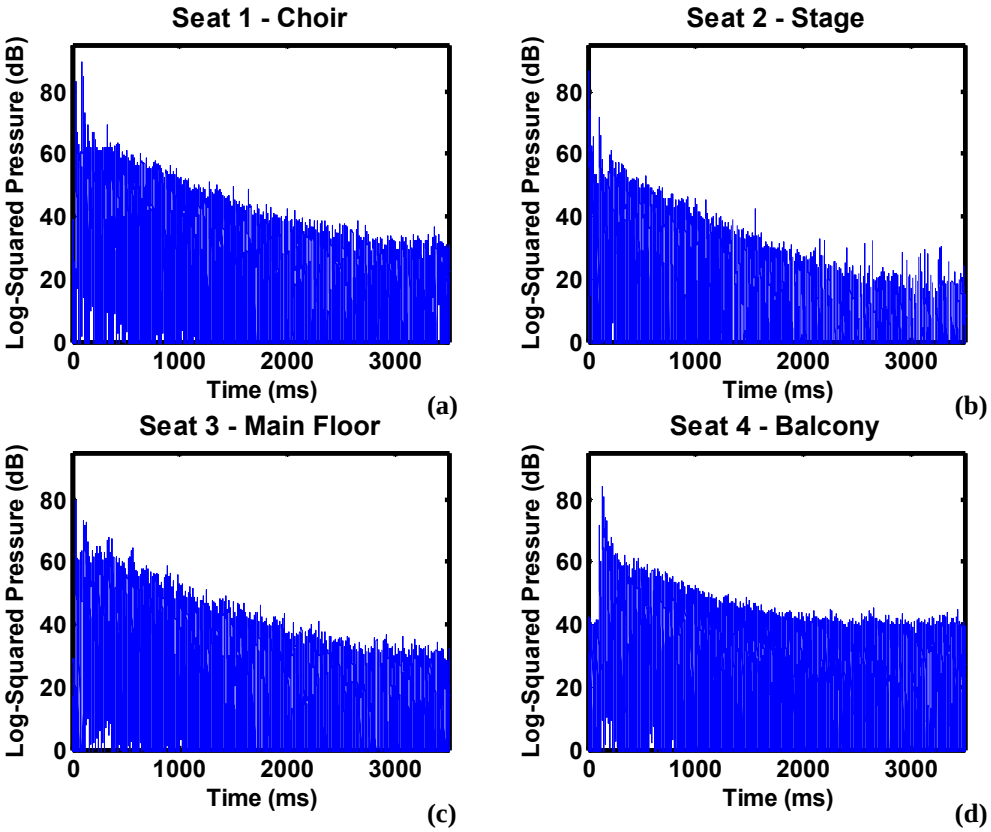

FIG. 3.3. Plots of the log-squared impulse responses for the four receiver locations marked in Fig. 2.7, with the source at center stage. (a) Response measured at seat 1, in the choir loft. (b) Response measured at seat 2, on the stage. (c) Response measured at seat 3, on the main floor. (d) Response measured at seat 4, in the balcony. The focusing effects of the curved ceiling are shown by clusters of high-level reflections. In graph (b), the spikes that protrude from the decay after 1000 ms are a result of measurement noise.

3.3 Architectural Acoustics Parameters

Reverberation time (RT) is a measure of the reverberation in the room. It is defined as the time it takes for the sound level to decrease by 60 dB and is a function of the volume of the room and the amount of sound absorption in the room. Typically, reverberation time is derived and extrapolated from the decay between 5 dB down and 35 or 25 dB down the Schroeder curve, before the response decays into the noise floor.[24] The Schroeder curve is calculated by reverse integration of the squared impulse response,

$$S = \int_{\infty}^{0} p^2(t)dt\,, \tag{3.1}$$

which produces an envelope of the response (see Fig. 4.1). Since the sound absorption of most materials is frequency dependent, the reverberation time is also. Too much low frequency reverberation in a room is described as a rumble of sorts, and too much high frequency absorption is often described as a hiss. Reverberation also affects intelligibility of speech and blend of music. A shorter RT provides better intelligibility, but for better blending of the instruments and different notes, a longer RT is preferred. Therefore, the ideal reverberation time for a specific hall depends on the purpose of the hall, whether it is for speech or music, and what kind of music.[25] This will be discussed more when the Tabernacle reverberation times are presented.

The early decay time (EDT) is similar to the reverberation time, but it is derived from the first 10 dB of decay then multiplied by 6 to produce values comparable to RT values. This 10 dB is also calculated from the Schroeder curve, from 0 dB down to 10 dB down. The EDT is a better representation of the perceived reverberance.[24]

A parameter that is important for measuring the perception of music is the clarity factor for music (C_{80}). The C_{80} compares the energy in the first 80 ms of the impulse response to the energy in the rest of the response,[26]

$$C_{80} = 10\log\frac{\int_{0}^{.08} p^2(t)dt}{\int_{.08}^{\infty} p^2(t)dt}\,, \tag{3.2}$$

where the limits are in terms of seconds. Negative C_{80} values correspond to perception of more blend between instruments and positive values represent perception of more clarity of the different instruments.

An important perceptual factor for musicians is how well they can hear each other. This quality is calculated from the impulse response using the stage support factor (ST1).[27] The impulse responses measured for this parameter are determined by moving the dodecahedron loudspeaker to a few different locations on the stage while consistently placing the receiver one meter away from it. The amount of energy in the first 10 ms is then compared to the amount of energy between 20 ms and 100 ms after the direct sound, since the energy in the first 10 ms is important for the musicians to feel supported by the hall. This is represented mathematically as,

$$ST1 = 10\log\frac{\int_{.02}^{0.1} p^2(t)dt}{\int_0^{.01} p^2(t)dt}. \tag{3.3}$$

To correlate well with music perception, some parameters require receivers other than the omnidirectional microphone used for the parameters discussed above. The lateral fraction (LF) is a measure of the relative amount of side reflections at a given position in a hall and is measured using a multi-pattern microphone.[28] This microphone measures the sound field with its omnidirectional pattern, then the impulse response is measured again using the microphone's figure-8 pattern, to pick up only the reflections that come from either side of the listener, rejecting everything from in front of and behind the receiver. Higher amounts of side reflections correspond to a larger apparent source width, which is especially desirable for orchestras and large choirs. The definition for this parameter is,

$$LF = \frac{\int_{.005}^{.08} p_8^2(t)dt}{\int_0^{.08} p^2(t)dt}, \tag{3.4}$$

where p_8 is the pressure signal measured by the figure-8 pattern of the microphone.

Another parameter that requires a specific type of receiver is the binaural quality index (BQI).[29] This index is derived from binaural impulse responses measured using a manikin with microphones in its ears. KEMAR is a manikin with a polyester-fiberglass head and torso, a removable skullcap, and rubber ears. It was designed to represent an average human listener. The BQI measures the differences in the sound field measured at each ear, due to the spacing between the ears and the diffraction around the head. It is calculated from the early interaural cross-correlation coefficient ($IACC_E$). The IACC is a measure of the similarities measured at the two ears, so higher values correspond to more similarity between the two ears. It is derived from the interaural cross-correlation function,

$$IACF_t(\tau) = \frac{\int_{t_1}^{t_2} p_L(t) p_R(t+\tau)}{\left(\int_{t_1}^{t_2} p_L^2(t) dt \int_{t_1}^{t_2} p_R^2(t) dt \right)^{1/2}}, \tag{3.5}$$

where the subscripts *L* and *R* refer to the signals measured at the left and right ears, respectively. The $IACC_E$ is then derived from the IACF by taking the maximum value of this function when τ varies from -1 to +1 ms and setting t_1 equal to 0 ms and t_2 equal to 80 ms,

$$IACC_E = \max\left(IACF_E(\tau)\right). \tag{3.6}$$

The BQI is then calculated by taking the average of the $IACC_E$ for three octave bands (500 Hz, 1000 Hz, 2000 Hz) and subtracting this from one:

$$BQI = 1 - IACC_{E3}. \tag{3.7}$$

Therefore, higher values for the BQI correspond to greater differences between the ears and greater perception of spaciousness in a hall. A value of zero represents the situation of no differences in the sound field measured at each ear.

For speech, a few more parameters have been developed. The speech transmission index (STI) measures the intelligibility of speech in a hall. To simulate the amplitude modulations in average speaking, a modulation transfer function is applied to the impulse response. The STI shows how much of this modulation is lost between the source and the receiver, due to the reflection effects of the room. On a scale from 0 to 1, 1 is equivalent to perfect intelligibility.[30] The clarity factor for speech (C_{50}) is also used to measure intelligibility in a hall. This parameter compares the amount of energy in the first 50 ms of the impulse response to the rest of the response and is measured in decibels. It is defined by the following equation

$$C_{50} = 10\log\frac{\int_0^{.05} p^2(t)dt}{\int_{.05}^{\infty} p^2(t)dt}, \tag{3.8}$$

where the limits are in terms of seconds. Higher values are better for speech.[31]

Echoes are detrimental to both music and speech. The echo criterion developed by Dietsch and Kraak was used in this project to predict the perception of echoes in the Tabernacle. This criterion measures how much reflections protrude above the exponential decay of sound in the room. To compute it, the following ratio is first calculated:

$$t_S(\tau) = \frac{\int_0^{\tau} |p(t)|^n t dt}{\int_0^{\tau} |p(t)|^n dt} \tag{3.9}$$

where $n = 2/3$ for speech and the pressure signal is band-limited to 700-1400 Hz. For music, $n = 1$ and the pressure signal is limited to 700-2800 Hz. The echo criterion is defined as,

$$EC = \max\left(\frac{\Delta t_S(\tau)}{\Delta \tau}\right), \tag{3.10}$$

where $\Delta\tau = 9$ ms for speech, $\Delta\tau = 14$ ms for music, and $\Delta t_S(\tau)$ is the difference in $t_S(\tau)$ corresponding to the $\Delta\tau$.[32,33] Since the ratio has a constant slope for a constant sound decay, large changes in the slope indicate reflections that protrude from the decay of the response.

3.4 Converting Continuous Equations to the Discrete-time Domain

Due to the vast number of impulse responses that needed to be processed, it was necessary to automate the architectural acoustics parameter derivations. This was done through Matlab® algorithms that approximately truncated the impulse responses and calculated the various parameters (see Appendix A).

As shown above, many published acoustic parameter equations are expressed in terms of an integral of continuous squared pressure associated with an impulse response.[34] This can be approximated in the discrete-time domain by squaring the discrete pressure sequence term by term.[35] The relationship between the continuous pressure, $p_c(t)$, and the discrete measured pressure $p[n]$ is

$$p[n] = p_c(nT), \tag{3.11}$$

where T is the sampling period of the analog-to-digital converter used to measure and store the impulse response on the computer and n is the index of the sample. This discrete pressure is the sampled version of the continuous pressure. Approximating the

integrals in the formulas is then implemented through a Riemann sum.[36] This is shown by the following equations. According to the Riemann sum, the integral is approximated by a sum as

$$\int_{t_1}^{t_2} p_c^2(t)dt = \lim_{\|P\|\to 0} \sum_{n=n_1}^{n_2} p_c^2(t_n)\Delta t_n \,, \tag{3.12}$$

where Δt_n is the width of the partition associated with t_n, n_1 is the sample number corresponding to t_1, n_2 is the sample number corresponding to t_2, and $\|P\|$ is the maximum width of all partitions, Δt_n. Since the sampled signal is only defined at each sample, which are intervals of the sample period, T, this sum becomes

$$\int_{t_1}^{t_2} p_c^2(t)dt = \sum_{n=n_1}^{n_2} p_c^2(nT)T \,. \tag{3.13}$$

Another proof of this conversion starts with the equation for recovering a continuous signal from its samples:[37]

$$p_c(t) = \sum_{n=-\infty}^{\infty} p_c(nT)\frac{\sin[(\pi/T)(t-nT)]}{(\pi/T)(t-nT)}, \tag{3.18}$$

where T is the sampling period and n is the index of the sample. This equation can be rewritten as

$$p_c(t) = T\sum_{n=-\infty}^{\infty} p_c(nT)\frac{\sin 2\pi f_c(t-nT)}{\pi(t-nT)}, \tag{3.19}$$

where f_c is the cutoff frequency of the signal, or the Nyquist frequency, to avoid aliasing. Assuming a sampled squared signal is the same as a squared sampled signal, we can write

$$p_c^2(t) = T\sum_{n=-\infty}^{\infty} p_c^2(nT)\frac{\sin 2\pi f_c(t-nT)}{\pi(t-nT)} \tag{3.20}$$

$$= 2Tf_c \sum_{n=-\infty}^{\infty} p_c^2(nT) \frac{\sin 2\pi f_c(t-nT)}{2\pi f_c(t-nT)}. \tag{3.21}$$

To integrate this squared pressure signal, it is possible to integrate over one sampling period then add up all the samples. Integrating over one period is written as,

$$\int_{mT}^{(m+1)T} p_c^2(t)dt = 2Tf_c \sum_{n=-\infty}^{\infty} p_c^2(nT) \int_{mT}^{(m+1)T} \frac{\sin 2\pi f_c(t-nT)}{2\pi f_c(t-nT)} dt. \tag{3.22}$$

By substituting x for $2\pi f_c(t - nT)$, the integral becomes

$$\int_{mT}^{(m+1)T} p_c^2(t)dt = 2Tf_c \sum_{n=-\infty}^{\infty} p_c^2(nT) \int_{2\pi f_c(m-n)T}^{2\pi f_c(m+1-n)T} \frac{\sin x}{x} \frac{dx}{2\pi f_c} \tag{3.23}$$

$$= \frac{T}{\pi} \sum_{n=-\infty}^{\infty} p_c^2(nT) \int_{2\pi f_c(m-n)T}^{2\pi f_c(m+1-n)T} \frac{\sin x}{x} dx. \tag{3.24}$$

Since $T = \frac{1}{2f_c}$ if we use the Nyquist rate,

$$\int_{mT}^{(m+1)T} p_c^2(t)dt = \frac{T}{\pi} \sum_{n=-\infty}^{\infty} p_c^2(nT) \int_{(m-n)\pi}^{(m+1-n)\pi} \frac{\sin x}{x} dx. \tag{3.25}$$

The major contribution of the sinc function occurs at $m = n$, so that

$$\int_{mT}^{(m+1)T} p_c^2(t)dt \approx \frac{T}{\pi} p_c^2(mT) \sum_{n=-\infty}^{\infty} \int_{(m-n)\pi}^{(m+1-n)\pi} \frac{\sin x}{x} dx \tag{3.26}$$

$$\approx \frac{T}{\pi} p_c^2(mT) \int_{-\infty}^{\infty} \frac{\sin x}{x} dx. \tag{3.27}$$

Since the integral of the sinc function over the infinite interval is equal to π,

$$\int_{mT}^{(m+1)T} p_c^2(t)dt \approx Tp_c^2(mT). \tag{3.28}$$

Therefore, by summing all of these integrals together for all samples of interest,

$$\int_{t_1}^{t_2} p_c^2(t)dt \approx T \sum_{m=m_{t_1}}^{m_{t_2}} p_c^2(mT), \tag{3.29}$$

which is the same result obtained through a Riemann sum.

The limits of integration must also be converted for discrete-time processing. The lower integration limit for many of the parameters is time $t = 0$, corresponding to the time of arrival of the direct sound.[38] To find this arrival, an algorithm was developed to start at the beginning of the measured impulse response and find the point when the data exceeded a certain threshold. The other limit of integration is sometimes written in the continuous-time equations as integrating to infinity. This corresponds to the end of the valid part of the measured impulse response, before the response decays into the noise floor of the measurement. The algorithm used for this project found the maximum value of the last quarter of the measured response to establish the value for the measurement noise floor. Then the algorithm started 500 ms into the response and found the envelope of the response by finding the maximum value for each 50 ms section of the response. A moving average of this envelope was used to find the data point when the impulse response fell below the established noise floor. This point was used as the truncation point of the response, or the point that corresponded to infinity in the continuous equations shown above.

4 Data Maps of Parameters

To visualize the spatial variation of the parameters, their values were mapped over drawings of the Tabernacle seating areas. As in Fig. 2.7, the balcony seating areas have been split and displaced from the main floor seating areas to make it possible to see the values for all seating areas on one plot. To make these data maps easier to compare, the red values consistently correspond to poor listening conditions. The percent column in the legend on each map indicates the percentage of the map that is covered by each color.

4.1 Maps of Parameters for the Dodecahedron Loudspeaker at Center Stage

4.1.1 Reverberation Time

To derive the reverberation time from a measured impulse response, Schroeder developed a method using reverse integration of the squared impulse response. He showed that the integral of the squared impulse response was equivalent to the ensemble average of an infinite number of noise-decay curves.[39] Therefore, the reverse integration of the squared impulse response, also known as the Schroeder curve, provides an envelope of the decay of sound in the room. This integration was implemented numerically in Matlab® using the cumsum function according to following equation:

$$S[m_n] = \left(\sum_{n=N}^{m_n} p^2[n] \right) T \,, \tag{4.1}$$

where N is the index of the last sample in the truncated response and m_n is index used to store the sum for each point along the curve.

According to ISO 3382, the T30 RT is found by applying a least-squares regression to the integration curve between the 5 dB and 35 dB down points on the curve to find the time for the sound to decay 30 dB, then multiplying this by 2 to get the time for sound to decay 60 dB.[24] However, when reflections appeared that were as loud as or louder than the direct sound, it became necessary to start farther down the curve to ensure the decay was determined on the diffuse tail of the response, as shown in Fig. 4.1. This figure shows the log-squared impulse response for position 2 in Fig. 2.7, with the Schroeder integration curve and the linear least-squares regression used for extrapolation down to 60 dB for the range specified by ISO 3382 and three other ranges.

The various RT values were calculated for all receiver positions and mapped over the seating area to see which range produced the most uniform values. In principle, the reverberation time should be somewhat independent of spatial position. The most uniform map was produced by calculating the RT from 10 dB to 20 dB down ($T10_{10\text{-}20}$) then extrapolating to 60 dB down with this slope, although this was only slightly more uniform than that of the ISO method, once the correct truncation algorithm was implemented. The $T10_{10\text{-}20}$ method is more resistant to inaccuracies in truncation point since it does not include the later part of the Schroeder curve in the calculation.

It was therefore used to calculate the reverberation times for the rest of the source positions. Figure 4.2 shows the spatial variation of the reverberation time by mapping the values for the ISO method and the $T10_{10\text{-}20}$ method for the various receiver positions. Figure 4.3 show the maps of the reverberation time calculated from the Schroeder curve in the ranges of 10 dB to 15 dB down and 15 dB to 35 dB down. The range of the legend in each color map is larger than the range of the actual data in a given map because it

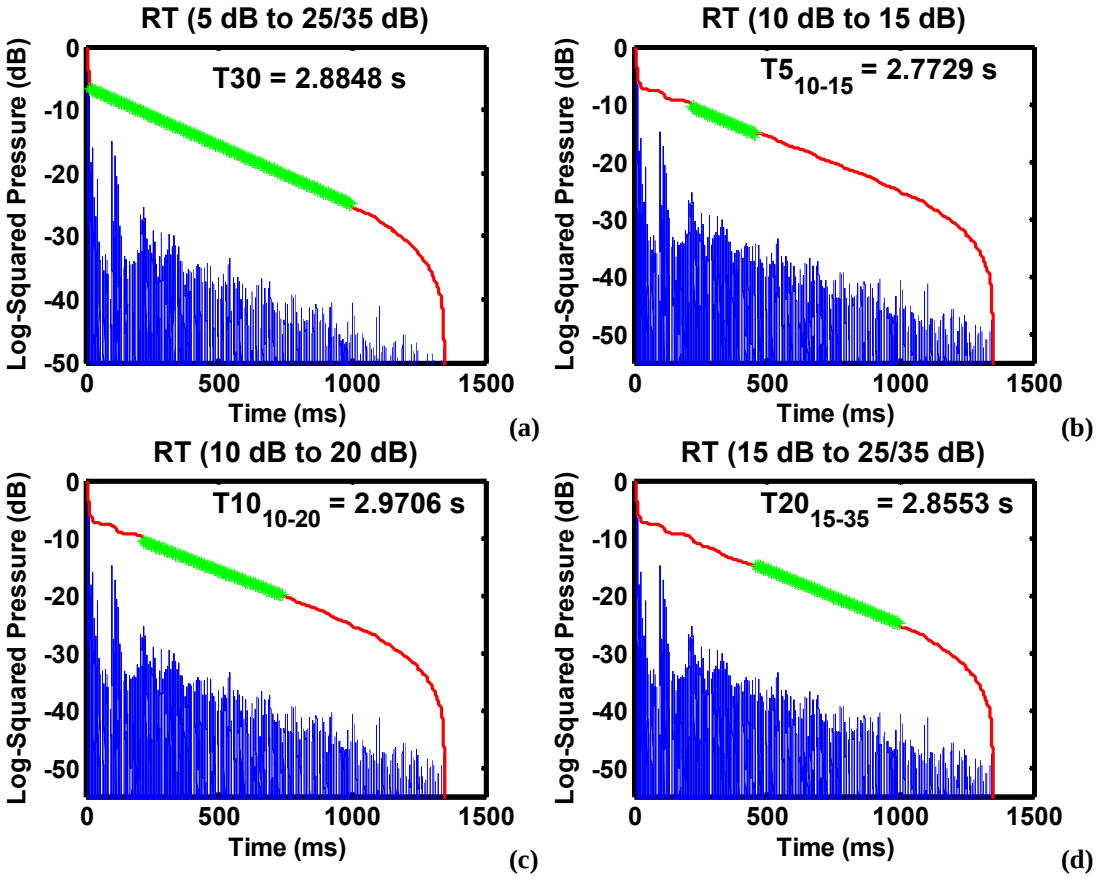

FIG. 4.1. Plots of the log-squared impulse response for seat 2 in Fig. 2.7, showing the Schroeder integration curve and four different lines used for calculating the reverberation time. (a) Reverberation time calculated according to the guidelines given by ISO 3382. (b) Reverberation time calculated from the slope of the Schroeder integration curve from 10 dB to 15 dB down ($T5_{10\text{-}15}$). (c) Reverberation time calculation similar to graph (b), except the range is from 10 dB down to 20 dB down ($T10_{10\text{-}20}$). (d) Calculation similar to ISO 3382, except starting at 15 dB down instead of 5 dB down ($T20_{15\text{-}35}$). The reverberation time calculated by the ISO method is shorter than the time calculated by looking at 10 to 20 dB down because the early focused reflections force the beginning of the line to start higher.

covers the range of all the various reverberation time values for the source at center stage.

While all reverberation time values shown in Fig. 4.2 and the corresponding mean values, $\overline{P}$, in Table 4.1 (s is the standard deviation) are longer than the ideal range for orchestral music of (1.8 – 2.1 s[40]), they are suitable for organ and choral music, which were often written for reverberant cathedrals. Therefore, the unoccupied T30 and $T10_{10\text{-}20}$ values for the hall, falling mostly between 3.5 and 4.5 seconds, are reasonable.

While this is too long according to many standards, it is acceptable as part of the sound one expects to hear while listening to the Mormon Tabernacle Choir or the Tabernacle organ. The occupied reverberation time of about 3 seconds (see Fig. C.2) is better for the orchestra, but still a little longer than the preferred values.

Table 4.1. Statistics for the various reverberation time calculations.

	$T30_{5\text{-}35}$	$T10_{10\text{-}20}$	$T5_{10\text{-}15}$	$T20_{15\text{-}35}$
Min	2.24	2.38	2.60	1.19
Max	4.57	4.78	5.02	4.55
$\overline{P}$	3.83	3.95	4.02	3.48
s	0.34	0.33	0.35	0.67

4.1.2 Early Decay Time

Early decay times (EDT) were also calculated from the impulse responses through reverse Schroeder integration. For this parameter, the time for the first 10 dB of decay on the integration curve was measured then multiplied by 6 to be on the same scale as the reverberation time.[41] In Fig. 4.4, the map of EDT shows significantly more spatial variation than the RT, including a much larger range between the minimum and maximum values. This variation in values is due in part to the focusing effects of the curved ceiling. The focused reflections from the ceiling came very soon after the direct sound in the rear balcony and choir seats so they were essentially combined with the direct sound in the Schroeder integration to produce shorter EDT values. Shorter values around the source at center stage were caused by the relatively strong direct sound measured by nearby receivers. These lower values were shown by the blue areas in Fig. 4.4.

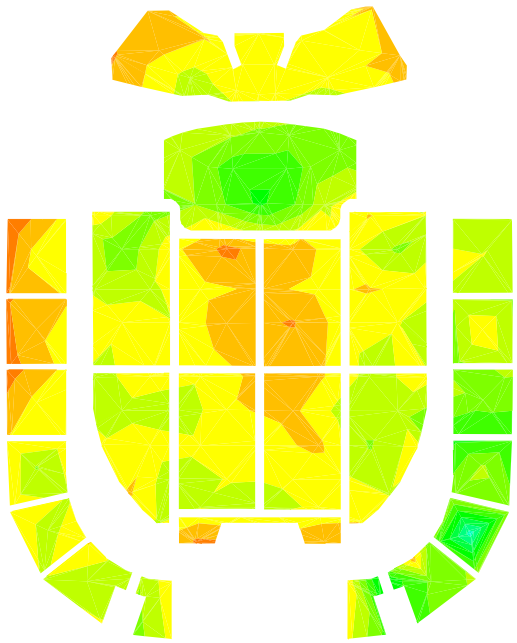

T30 for Source at Center Stage

Color	Range Beg.	Range End	Percent
	1.10	1.35	0.0
	1.35	1.60	0.0
	1.60	1.85	0.0
	1.85	2.10	0.0
	2.10	2.35	0.0
	2.35	2.60	0.1
	2.60	2.85	0.3
	2.85	3.10	0.8
	3.10	3.35	4.9
	3.35	3.60	10.5
	3.60	3.85	27.0
	3.85	4.10	38.7
	4.10	4.35	16.6
	4.35	4.60	1.1
	4.60	4.85	0.0
	4.85	5.10	0.0

(a)

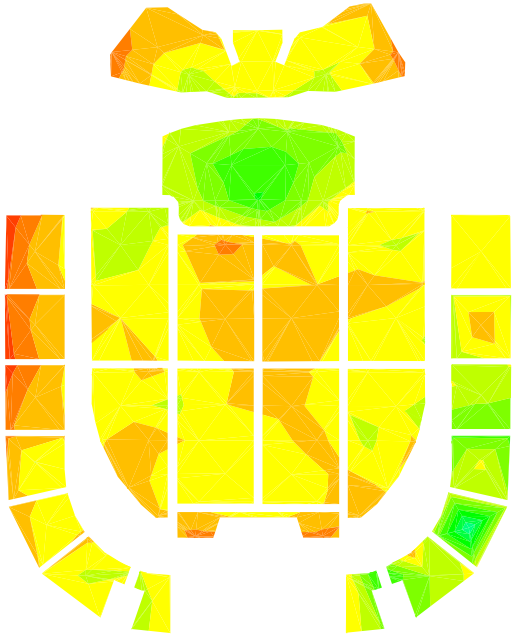

T10 for Source at Center Stage

Color	Range Beg.	Range End	Percent
	1.10	1.35	0.0
	1.35	1.60	0.0
	1.60	1.85	0.0
	1.85	2.10	0.0
	2.10	2.35	0.0
	2.35	2.60	0.1
	2.60	2.85	0.2
	2.85	3.10	0.4
	3.10	3.35	3.0
	3.35	3.60	6.7
	3.60	3.85	13.3
	3.85	4.10	46.6
	4.10	4.35	25.7
	4.35	4.60	3.4
	4.60	4.85	0.6
	4.85	5.10	0.0

(b)

FIG. 4.2. Color map of the measured values of the reverberation time for the source at center stage. (a) ISO 3382 method, $T30_{5\text{-}35}$. (b) $T10_{10\text{-}20}$. The range of the map is larger than the range of the mapped values because mapped range encompasses the minimum and maximum values for all the various reverberation times.

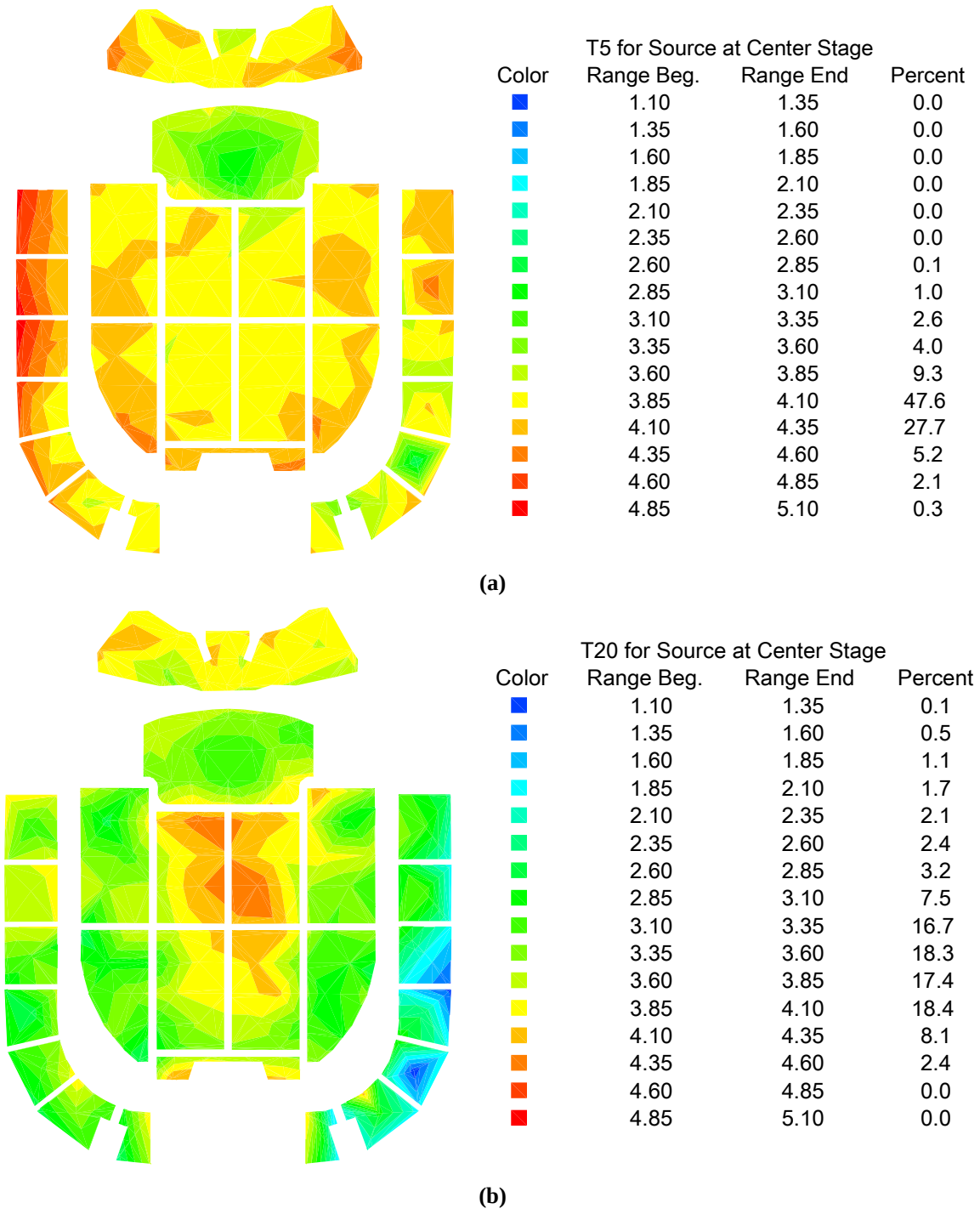

FIG. 4.3. Color map of the measured values for the reverberation time for the source at center stage. (a) $T5_{10\text{-}15}$. (b) $T20_{15\text{-}35}$.

The very long EDT values in the side balcony are also due to focused reflections, but because they arrive later relative to the direct sound, they shift the later portions of

the Schroeder integration curve up close in level to the direct sound, which produces a longer EDT. For concert halls with upholstered seats, the preferred range of EDT values is approximately 1.5 to 2.6 seconds.[40] Naturally, the EDT values in the Tabernacle are longer, since the hall is larger than many concert halls and none of the audience seats are upholstered.

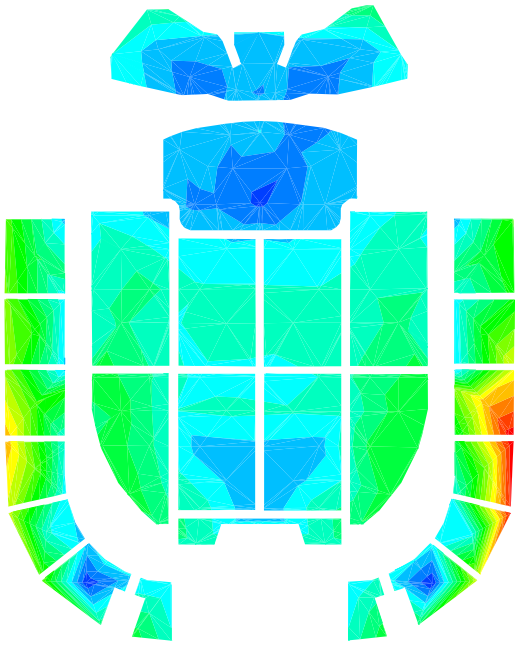

EDT for Source at Center Stage

Color	Range Beg.	Range End	Percent
	1.60	2.25	0.4
	2.25	2.90	6.7
	2.90	3.55	17.4
	3.55	4.20	18.6
	4.20	4.85	24.8
	4.85	5.50	11.7
	5.50	6.15	8.6
	6.15	6.80	3.5
	6.80	7.45	2.6
	7.45	8.10	2.0
	8.10	8.75	1.3
	8.75	9.40	0.9
	9.40	10.05	0.7
	10.05	10.70	0.5
	10.70	11.35	0.3
	11.35	12.00	0.1

FIG. 4.4. Color map of the early decay time (EDT) for the source at center stage.

4.1.3 Clarity Factor for Music

As mentioned previously, the C_{80} is a measure of the perceived clarity of music in a hall. It was calculated from the measured impulse responses using the relationship

$$C_{80} = 10 \log \frac{\sum_{n=n_0}^{n_{80}} p^2[n]}{\sum_{n=n_{80}}^{N} p^2[n]}, \tag{4.2}$$

where $p^2[n]$ is the squared sampled impulse response, n_0 is the sample number of the direct sound, and n_{80} is the sample number 80 ms after the direct sound. This is the

discrete-time equivalent of the continuous equation given in Eq. 3.2. Since this parameter is calculated by dividing a sum of one part of the impulse response by a sum of another part, the sampling period divides out, so it was not included in the Matlab® code.

Typically, listeners prefer C_{80} values between -3 dB and +3 dB, although it depends on the genre of music being played.[40] Conductors prefer the C_{80} of a hall to be positive for rehearsals so they can hear subtle mistakes more clearly. During performances, they prefer a negative C_{80} value so the instruments blend together better and mistakes become much less noticeable.

Several focusing effects of the ceiling are easy to see in the map of C_{80} values in Fig. 4.4. The values that fall into the ideal range for symphonic music are shown by the green and light blue areas. Specifically, there are some areas of very high clarity found in the balcony areas toward the back of the hall. This is caused by the concave ceiling toward back of the hall focusing sound down to these areas of the balcony, as shown in Fig. 4.6. Again, since these areas are close to the ceiling, the focused clusters of reflections come within 80 ms after the direct sound, thus increasing clarity. On the other hand, Fig. 4.7 shows how focused reflections from the curved ceiling reach the front of the main floor later in time (well after the first 80 ms) to produce lower clarity. The reflections arriving in the first 80 ms are shown in red. Some of those causing the cluster of reflections right after 80 ms are shown in blue.

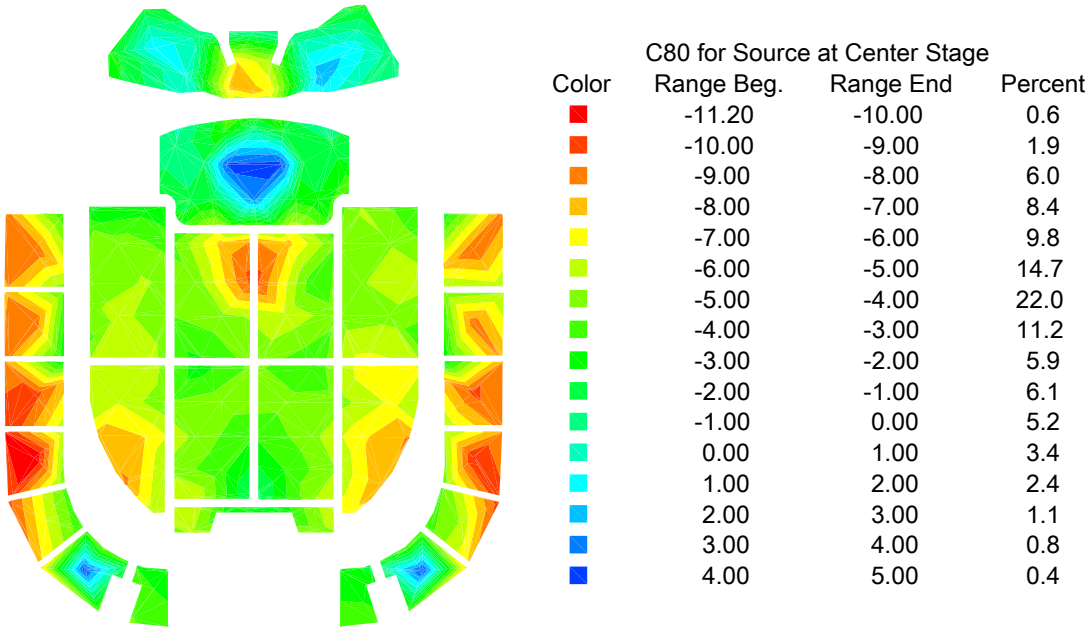

FIG. 4.5. Color map of the clarity factor for music (C_{80}) for the source at center stage.

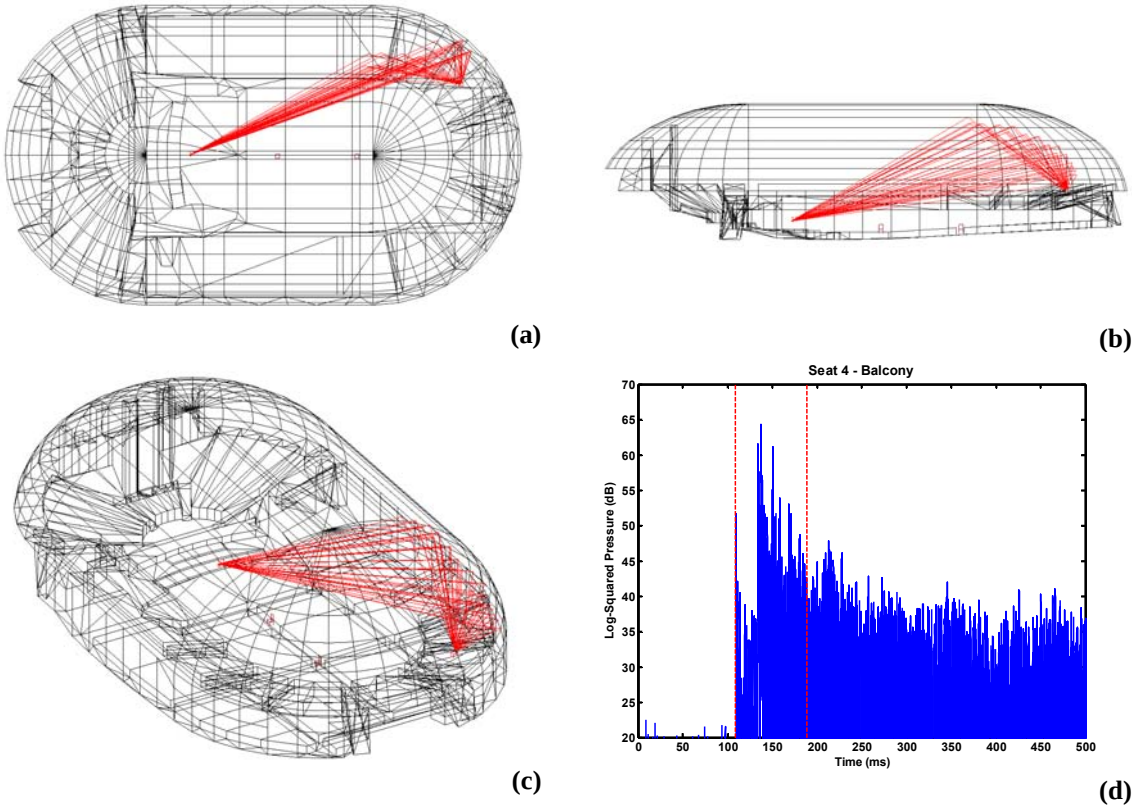

FIG. 4.6. Ray-tracing diagrams and measured impulse response for seat 3 shown in Fig. 2.7, in the balcony. (a) Top view of the ray-tracing in the EASE model. (b) Side view of the ray-tracing in the EASE model. All of the rays shown arrive in the first 80 ms. (c) Isometric view of the ray-tracing in the EASE model. (d) First 500 ms of the measured log-squared impulse response, with red dashed lines to show the first 80 ms.

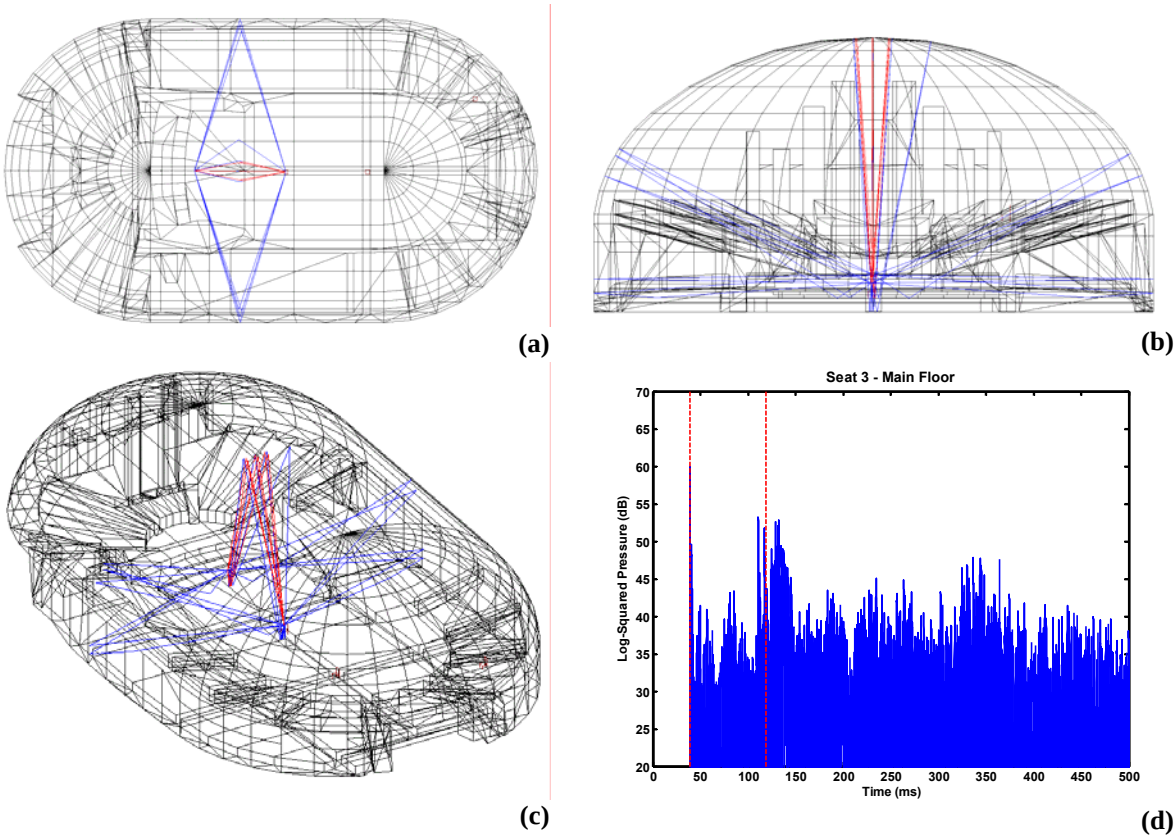

FIG. 4.7. Ray-tracing diagrams and measured impulse response for seat 3 shown in Fig. 2.7, on the main floor. (a) Top view of the ray-tracing in the EASE model. (b) Rear view of the ray-tracing in the EASE model. (c) Isometric view of the ray-tracing in the EASE model. (d) First 500 ms of the log-squared impulse response, with red dashed lines to show the first 80 ms. The red rays show the reflections that arrived in the first 80 ms and the blue rays show the ceiling and side wall reflections that contributed to the cluster of reflections right after 80 ms. This later clusters of reflections shown in the impulse response decreased the clarity.

4.1.4 Stage Support Factor

The stage support factor (ST1) measures how well the stage and the hall support the musicians on stage, predicting how well they can hear each other. The impulse responses for this parameter are measured between the source and the receiver 1 meter away, at a few different areas on the stage. As suggested by Beranek, the ST1 is then calculated using the formula

$$ST1 = 10\log\frac{\sum_{n=n_{20}}^{n_{100}} p^2[n]}{\sum_{n=n_0}^{n_{10}} p^2[n]}, \tag{4.3}$$

where again, n_x is the index for the sample at x milliseconds after the direct sound. The preferred range for this parameter is -14.5 to -12 dB.[40,42] As Fig. 4.7 shows, the ST1 values for the Tabernacle are well below this range. This is due to the lack of close reflecting surfaces. The high ceiling above the stage, the width of the stage, and the fact that the rear wall for the stage is only a few feet above the performers, are all detrimental to acoustic ensemble. The higher values show that the orchestra members that are best supported by the hall are those towards the edges of the stage, especially toward the rear stage right, where the front of the broadcast booth provides a reflecting surface.

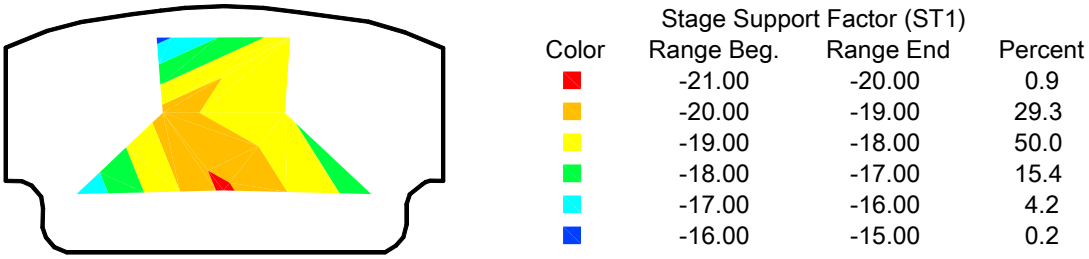

FIG. 4.8. Color map for the stage support factor (ST1).

4.1.5 Lateral Fraction

To quantify the proportion of lateral reflections present in the hall, impulse response measurements were made using the multi-pattern microphone, in both the omnidirectional and bidirectional (figure-8) settings. For this study, the null of the bidirectional microphone was aimed at the choir conductor position as a compromise between the performance positions of the orchestra on the stage and the choir in the choir loft. Therefore, the microphone measured the side reflections that would be heard by a

listener facing the choir conductor. The measurements were combined to compute the lateral fraction (LF) values using the relationship

$$LF = \frac{\sum_{n=n_5}^{n_{80}} p_8^2[n]}{\sum_{n=n_0}^{n_{80}} p^2[n]}, \tag{4.4}$$

where $p_8[n]$is the impulse response measured by the figure-8 pattern of the microphone and $p[n]$ is the omnidirectional impulse response measurement. The map of the LF in Fig. 4.9 shows a distinct lack of side reflections down the center of the hall, in the choir loft, and in the balcony sections towards the front of the hall. In the choir loft, the low LF values show that while some side reflections arrive from the ceiling, the direct sound from the source on the stage and reflections from behind the receiver are stronger than any lateral reflections, including those from the ceiling. Overall, the hall has a lack of lateral energy at most seats. However, the orange and yellow areas show several positions with LF values within the ideal range between 0.10 and 0.25.[28]

4.1.6 Binaural Quality Index

After the omnidirectional and multi-pattern microphones were used, the KEMAR manikin was also used to measure the impulse responses of the room at the same receiver locations. The BQI was calculated from these measurements according to the following procedure. First, the early interaural cross-correlation function was calculated according to the relationship

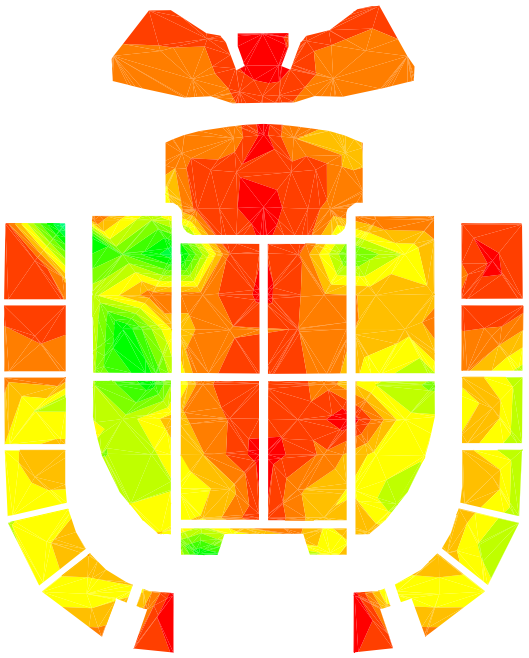

LF for Source at Center Stage

Color	Range Beg.	Range End	Percent
	0.00	0.06	4.2
	0.06	0.12	25.7
	0.12	0.18	21.4
	0.18	0.24	16.7
	0.24	0.30	17.2
	0.30	0.36	8.6
	0.36	0.42	2.8
	0.42	0.48	2.0
	0.48	0.54	1.2
	0.54	0.60	0.1
	0.60	0.66	0.0
	0.66	0.72	0.0
	0.72	0.78	0.0
	0.78	0.84	0.0
	0.84	0.90	0.0
	0.90	1.00	0.0

FIG. 4.9. Color map for the lateral energy fraction (LF) for the source at center stage.

$$IACF_E[n_\tau] = \frac{\sum_{n=n_0}^{n_{80}} p_L[n]\,p_R[n+n_\tau]}{\left(\sum_{n=n_0}^{n_{80}} p_L^2[n] \sum_{n=n_0}^{n_{80}} p_R^2[n]\right)^{1/2}}, \tag{4.5}$$

where the subscript E on the function indicates the early energy, n_τ is the index of the sample corresponding to the value of τ which varies from -1 to +1 ms, $p_L[n]$ is the impulse response measured from the left ear of KEMAR, and $p_R[n]$ is the impulse response measured at the right ear. The early interaural cross-correlation function was calculated because the BQI is based on the early IACC ($IACC_E$). Furthermore, the BQI is based on the $IACC_E$ for the 500 Hz, 1 kHz and 2 kHz octave bands. The $IACF_E$ was therefore calculated for the impulse response filtered by these octave band filters. Next, the interaural cross-correlation coefficient was calculated by taking the maximum value of the interaural cross-correlation function:

$$IACC_E = \left| IACF_E \left[n_\tau \right] \right|_{\max}. \tag{4.6}$$

The binaural quality index (BQI) was then calculated from the average of the $IACC_E$ values for the three octave bands mentioned previously:

$$BQI = 1 - IACC_{E3}. \tag{4.7}$$

Figure 4.10 shows how the early lateral energy is distributed through the hall as measured by the binaural quality index (BQI). When KEMAR was anywhere along the center line of the hall, the impulse responses measured at each ear were very similar, due to the symmetry of the hall. Therefore, the lowest BQI values (shown by the orange and yellow areas) are down the center line of the hall. The lower BQI values in the center of the main floor are also caused by the large width of the hall and the narrow balcony fascia which provide few useful lateral reflections. The green and blue areas show the highest values of BQI, which show the many early lateral reflections provided by the nearby walls. Lower values in the balcony sections toward the front of the hall are due to the distance of these receivers from any side walls. Since KEMAR faced the choir conductor position, these front sections are where the effective side walls were toward the front and rear of the hall. The green areas have measured values that are acceptable, since they are in the same range as a satisfactory hall. For orchestra music in halls with over 1,400 seats, the ideal range for BQI is 0.65 to 0.71.[40] These values are shown in the areas that are light blue, which are closer to the side walls on the main floor and the stage.

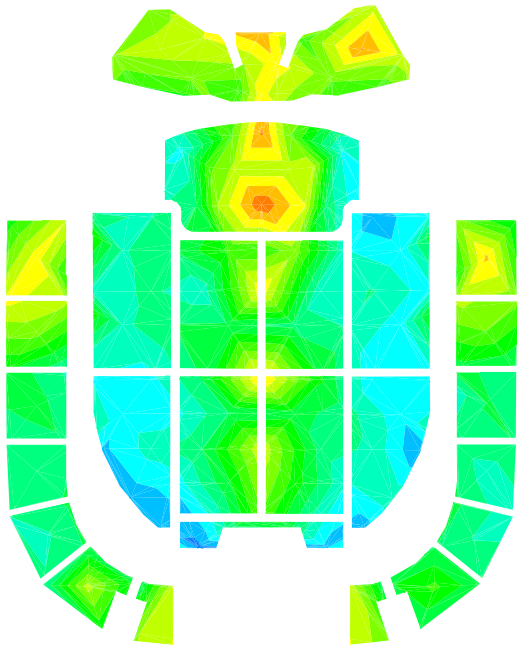

BQI for Source at Center Stage

Color	Range Beg.	Range End	Percent
	0.00	0.06	0.0
	0.06	0.12	0.0
	0.12	0.18	0.2
	0.18	0.24	1.3
	0.24	0.30	4.5
	0.30	0.36	10.1
	0.36	0.42	10.4
	0.42	0.48	8.0
	0.48	0.54	7.2
	0.54	0.60	11.0
	0.60	0.66	19.1
	0.66	0.72	15.1
	0.72	0.78	10.6
	0.78	0.84	2.4
	0.84	0.90	0.1
	0.90	1.00	0.0

FIG. 4.10. Color map of the binaural quality index (BQI) for the source at center stage.

4.1.7 Echo Criteria

To measure the perception of echoes in the Tabernacle, the echo criteria developed by Dietsch and Kraak were used.[32,33] To calculate these criteria, a specific energy ratio was first calculated:

$$t_S[n_\tau] = \frac{\sum_{n=n_0}^{n_\tau} |p_{L+R}[n]|^x n}{\sum_{n=n_0}^{n_\tau} |p_{L+R}[n]|^x}, \tag{4.8}$$

where x is equal to 2/3 for the speech criterion, x is equal to 1 for the music criterion and $p_{L+R}[n]$ is the sum of the impulse responses measured at the left and right ears of KEMAR. The criteria are calculated from this ratio using

$$EC = \max\left(\frac{\Delta t_S[n_\tau]}{\Delta n_\tau}\right), \tag{4.9}$$

where Δn_τ is 9 ms for the speech criterion, 14 ms for the music criterion, and $\Delta t_S[n_\tau]$ is the difference in t_S values that were Δn_τ apart. These values were converted to numbers of samples by dividing through by 1000 to convert the units to seconds then multiplying by the 48 kHz sample rate of the measurement.

The estimated threshold for 10% of listeners to hear an echo for music is 1.5. The positions exceeding this value are shown in yellow in Fig. 4.11. The value at which 50% of listeners would hear an echo in music is 1.8. The positions exceeding this value are shown in red. The echoes in the choir are caused by the return reflections from the ceiling at the rear of the hall.

For speech, the threshold is lower than the threshold for music because echoes are more easily perceived in speech than in music. The threshold above which 10% of listeners will hear an echo for speech is 0.9 and the threshold for 50% of listeners hearing an echo is 1.0. The areas in Fig. 4.12 that meet or exceed the 10% threshold are shown in yellow and orange and the areas that meet or exceed the 50% threshold are shown in red. This map shows more likely perception of echoes down the center of the hall and in the balcony in addition to the higher perception of echoes that were measured for music in the choir loft. Interestingly, the red and orange areas in the choir loft and toward the front and center of the main floor in both echo criteria maps are also areas with low clarity, as shown in Fig 4.5 and Fig. 4.14.

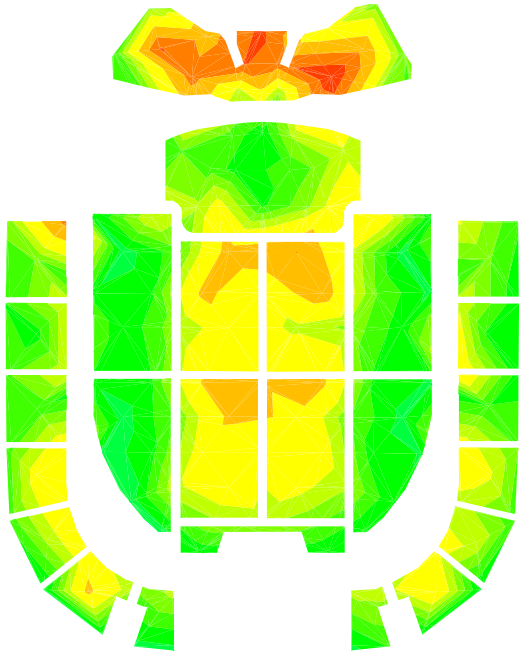

ECM for Source at Center Stage

Color	Range Beg.	Range End	Percent
	0.00	0.09	0.0
	0.09	0.18	0.0
	0.18	0.27	0.0
	0.27	0.36	0.0
	0.36	0.45	0.0
	0.45	0.54	0.0
	0.54	0.63	2.9
	0.63	0.72	16.4
	0.72	0.81	17.4
	0.81	0.90	13.8
	0.90	1.00	13.6
	1.00	1.20	24.6
	1.20	1.40	7.4
	1.40	1.60	3.2
	1.60	1.80	0.6
	1.80	2.00	0.0

FIG. 4.11. Color map of the Dietsch echo criterion values for music (ECM) for the source at center stage. The areas where 10-50% of the listeners would perceive an echo for music are shown in yellow, and areas where at least 50% of listeners would perceive an echo for music are shown in red.

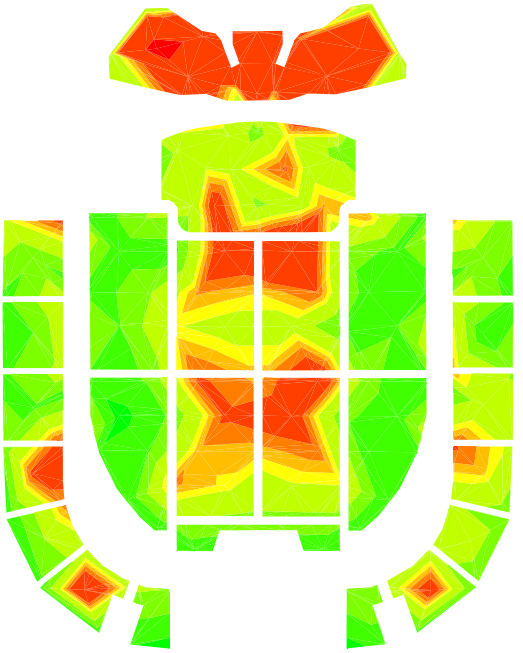

ECS for Source at Center Stage

Color	Range Beg.	Range End	Percent
	0.00	0.08	0.0
	0.08	0.16	0.0
	0.16	0.24	0.0
	0.24	0.32	0.0
	0.32	0.40	0.0
	0.40	0.48	0.0
	0.48	0.56	0.0
	0.56	0.64	0.5
	0.64	0.72	18.7
	0.72	0.80	19.3
	0.80	0.90	25.5
	0.90	0.93	7.6
	0.93	0.96	7.1
	0.96	1.00	6.0
	1.00	1.50	15.0
	1.50	2.00	0.3

FIG. 4.12. Color map of the Dietsch echo criterion values for speech (ECS) for the source at center stage. The areas where 10-50% of the listeners would perceive an echo for speech are shown in yellow, and areas where at least 50% of listeners would perceive an echo for speech are shown in red.

4.1.8 Speech Transmission Index

Another important parameter for quantifying the quality of a hall for speech is the speech transmission index (STI).[43,44,45] First, the valid part of the impulse response was squared to make it an energy quantity. This squared response was then summed to attain the total energy

$$e_p = \sum_{n=1}^{N} p^2[n]. \tag{4.10}$$

The next step was to produce the Fourier transform of the squared impulse response, (e.g., using the Matlab® 'fft.m' script):

$$P[k] = \sum_{j=1}^{N} p^2[j]\left(e^{-2i\pi(j-1)(k-1)/N}\right). \tag{4.11}$$

This spectrum was then normalized by the total energy calculated previously,

$$P_N[k] = \frac{P[k]}{e_p}, \tag{4.12}$$

to produce the complex modulation transfer function (CMTF). The next step was to take the magnitude of the CMTF to get the modulation transfer function (MTF). Since the STI is calculated from the MTF for each of the octave bands from 125 Hz to 8 kHz, the broadband impulse response was filtered with corresponding octave band filters and the previous steps were carried out for these filtered responses. From these 7 MTFs, the amplitude was determined at 14 modulation frequencies, from 0.63 Hz to 12.5 Hz, at 1/3 octave intervals. The 98 amplitudes, or *m*-values, were then converted to apparent signal-to-noise ratios using the relationship

$$\left(\frac{S}{N}\right) = 10\log\left(\frac{m}{1-m}\right). \tag{4.13}$$

For the STI, these apparent signal-to-noise ratios must be limited between -15 dB and +15 dB, so this was implemented using an if-statement in Matlab®. The next step was to calculate the mean apparent signal-to-noise ratio (neglecting the ambient noise) for each octave band from the 14 values, to get a total of 7 values, one for each octave band then combine these numbers into one number, $(S/N)_{av}$, using a weighted average. These weights are assigned according to the importance of each octave band for speech communication, so the 2 kHz band had the highest weight. Finally, the average value was converted to an STI value using the relationship

$$STI = \frac{\left(\frac{S}{N}\right)_{av} + 15}{30}. \tag{4.14}$$

The map of STI in Fig. 4.12 shows the speech intelligibility for the omnidirectional source at center stage. Values between 0.30 and 0.45 correspond to poor speech intelligibility, values between 0.45 and 0.60 correspond to fair intelligibility, and values above 0.60 correspond to good or excellent intelligibility.[46,47] The lower values in the balcony and towards the back of the main floor are not necessarily concerns, because when a talker needs to be heard by everyone in the Tabernacle, he or she typically does not speak from the stage without a microphone for sound reinforcement. The intelligibility in these areas and under the balcony is higher for the sound system as the source (see Fig. 4.20). The red areas in the back of the balcony sections are due to the distance between the source and the receiver as well as the lack of early energy at these locations. The higher values in the balcony are due to the focusing effects mentioned earlier for the C_{80}, and shown in Figs. 4.5 and 4.6.

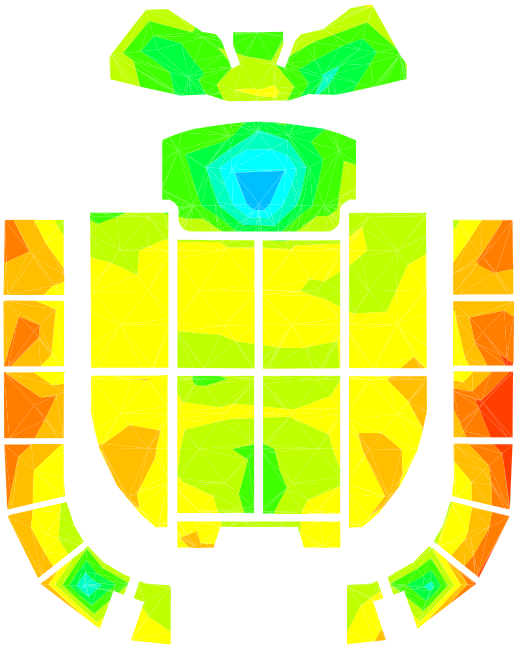

STI for Source at Center Stage

Color	Range Beg.	Range End	Percent
	0.20	0.25	0.0
	0.25	0.30	1.2
	0.30	0.35	6.5
	0.35	0.40	13.4
	0.40	0.45	34.0
	0.45	0.50	23.6
	0.50	0.55	11.1
	0.55	0.60	5.9
	0.60	0.65	2.0
	0.65	0.70	1.5
	0.70	0.75	0.7
	0.75	0.80	0.0

FIG. 4.13. Color map of the speech transmission index (STI) for the source at center stage.

4.1.9 Clarity Factor for Speech

The clarity factor for speech (C_{50}) is also a useful measure of speech quality in a hall. Good speech intelligibility correlates to values of $C_{50} > 0$.[46] To calculate the C_{50}, the impulse response was squared and summed like the C_{80}, but comparing the first 50 ms to the rest of the response instead of the first 80 ms:

$$C_{50} = 10 \log \frac{\sum_{n=n_0}^{n_{50}} p^2[n]}{\sum_{n=n_{50}}^{N} p^2[n]}. \qquad (4.15)$$

Figure 4.14 shows the color map of the C_{50}. This parameter also shows the interesting focusing effects in the rear balcony sections, like the C_{80} in Fig. 4.5. The blue values show the seating areas that would have good speech intelligibility, according to this parameter. Focused reflections also produced decreased clarity toward the middle of the main floor, since the reflections in only the first 50 ms were included in the

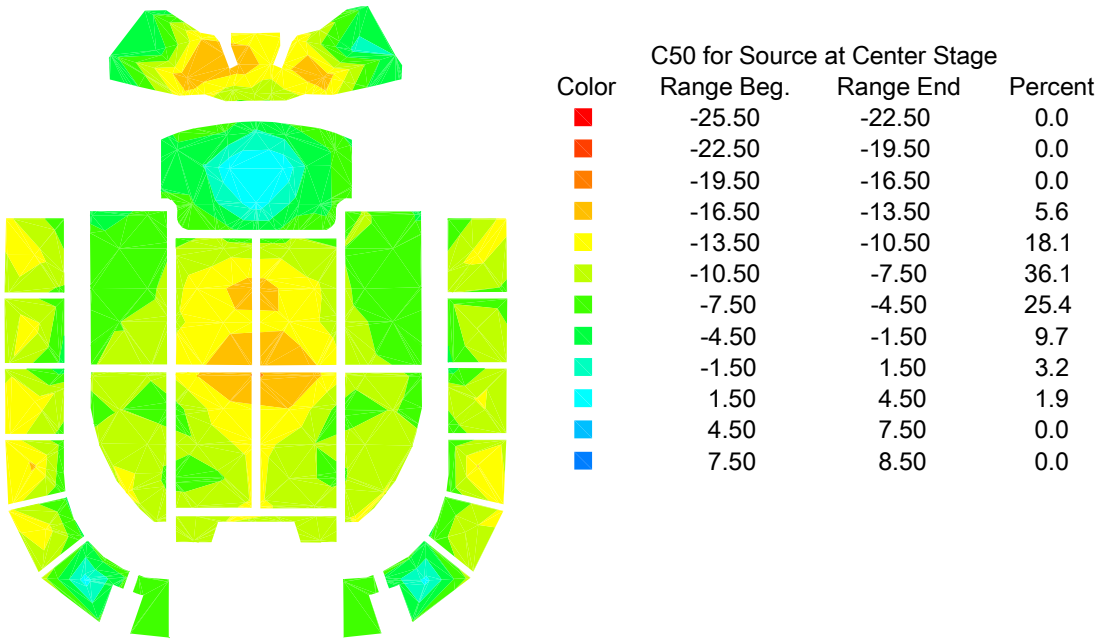

FIG. 4.14. Color map of the clarity factor for speech (C_{50}) for the source at center stage.

numerator. The reflections from the ceiling similar to those shown in Fig. 4.7 would arrive at this location after the first 50 ms, causing decreased clarity.

4.2 Maps of Parameters for the Source in the Choir Soprano and Alto Sections

Since the Mormon Tabernacle Choir is the principal performing group in the Tabernacle, impulse responses of the room were measured again with the dodecahedron loudspeaker in the choir loft, in both the soprano and alto choir sections. Behaviors in the tenor and bass sections were assumed to be symmetrical. Figure 4.15 shows the measured RT and EDT values for the source in the soprano section. As in the map of EDT for the source at center stage (Fig. 4.4), there is an area around the source with lower EDT values, since the nearby receivers measure shorter times for the first 10 dB of

T10 for Source in Choir Soprano Section

Color	Range Beg.	Range End	Percent
	1.10	1.35	0.0
	1.35	1.30	0.0
	1.60	1.85	0.0
	1.85	2.10	0.0
	2.10	2.35	0.0
	2.35	2.60	0.0
	2.60	2.85	0.0
	2.85	3.10	0.0
	3.10	3.35	0.0
	3.35	3.60	1.7
	3.60	3.85	4.0
	3.85	4.10	13.7
	4.10	4.35	41.3
	4.35	4.60	32.5
	4.60	4.85	6.7
	4.85	5.10	0.1

(a)

EDT for Source in the Choir Soprano Section

Color	Range Beg.	Range End	Percent
	0.00	0.75	1.9
	0.75	1.50	2.0
	1.50	2.25	0.9
	2.25	3.00	3.5
	3.00	3.75	27.5
	3.75	4.50	56.5
	4.50	5.25	7.8
	5.25	6.00	0.0
	6.00	6.75	0.0
	6.75	7.50	0.0
	7.50	8.25	0.0
	8.25	9.00	0.0
	9.00	9.75	0.0
	9.75	10.50	0.0
	10.50	11.25	0.0
	11.25	12.00	0.0

(b)

FIG. 4.15. Color maps for the source in the soprano section of the choir loft. (a) $T10_{10\text{-}20}$ map. (b) EDT map.

decay due to the high level of the direct sound. The color maps for the RT and EDT with the source in the alto section are shown in Fig. 4.16. Again, the EDT map shows the lower values around the source.

Figure 4.17 shows the maps of C_{80} for the source in these same choir section positions. Since both of these positions are not near the focal point of the curved ceiling, the lower C_{80} values that were seen in the balcony for the source at center stage (Fig. 4.5) are no longer present in these maps. Furthermore, the lower values shown by the yellow area on the left in the map for the source in the soprano section show the shadow effect of the balcony. There was no direct line of sight or sound between these receiver positions and the source.

Maps of the ECM for the source in both the soprano and alto sections are shown in Fig. 4.18. The higher values on the stage and under the balcony are results of focusing effects of the curved ceiling, which produce focused, delayed reflections from the front and rear portions of the ceiling. The color maps for the rest of the parameters measured for the source in the choir soprano and alto sections are found in Appendix B.

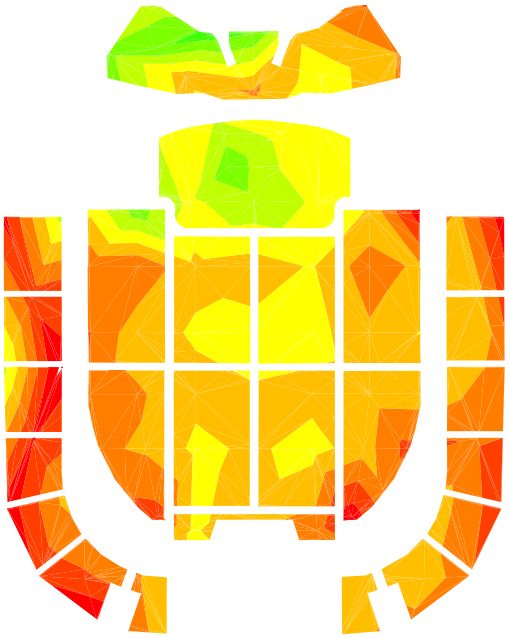

T10 for Source in Choir Alto Section

Color	Range Beg.	Range End	Percent
	1.10	1.35	0.0
	1.35	1.30	0.0
	1.60	1.85	0.0
	1.85	2.10	0.0
	2.10	2.35	0.0
	2.35	2.60	0.0
	2.60	2.85	0.0
	2.85	3.10	0.0
	3.10	3.35	0.2
	3.35	3.60	2.7
	3.60	3.85	6.7
	3.85	4.10	20.2
	4.10	4.35	38.0
	4.35	4.60	21.9
	4.60	4.85	8.2
	4.85	5.10	2.1

(a)

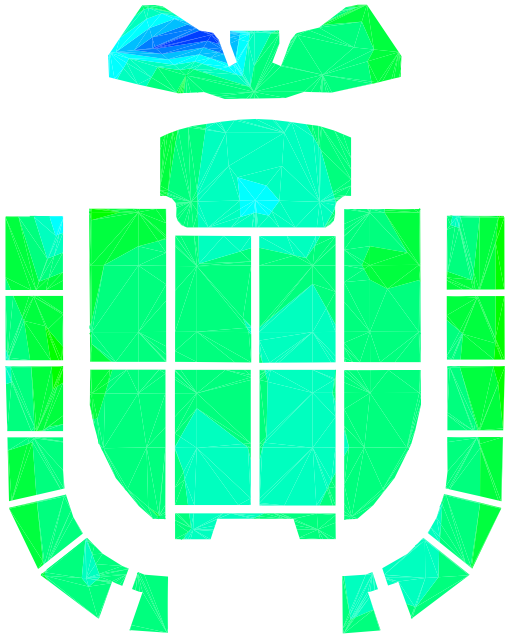

EDT for Source in the Choir Alto Section

Color	Range Beg.	Range End	Percent
	0.00	0.75	0.3
	0.75	1.50	0.6
	1.50	2.25	0.8
	2.25	3.00	2.1
	3.00	3.75	24.9
	3.75	4.50	53.4
	4.50	5.25	16.5
	5.25	6.00	1.4
	6.00	6.75	0.0
	6.75	7.50	0.0
	7.50	8.25	0.0
	8.25	9.00	0.0
	9.00	9.75	0.0
	9.75	10.50	0.0
	10.50	11.25	0.0
	11.25	12.00	0.0

(b)

FIG. 4.16. Color maps for the source in the alto section of the choir loft. (a) $T10_{10\text{-}20}$ map. (b) EDT map.

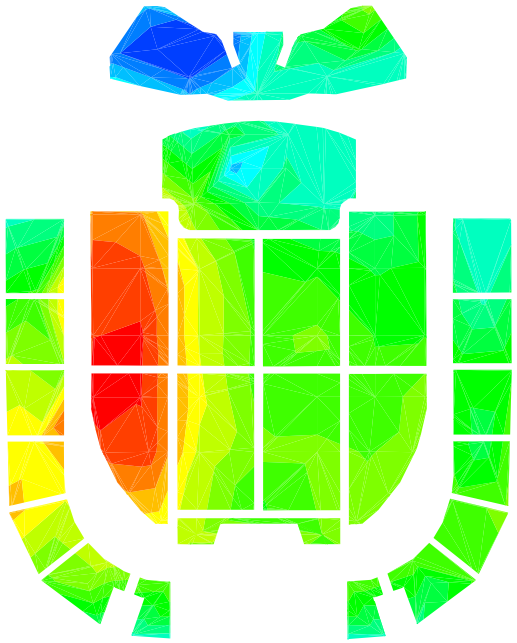

C80 for Source in Choir Soprano Section

Color	Range Beg.	Range End	Percent
	-16.50	-14.90	2.4
	-14.90	-13.30	5.2
	-13.30	-11.70	3.5
	-11.70	-10.10	2.4
	-10.10	-8.50	5.1
	-8.50	-6.90	7.4
	-6.90	-5.30	13.2
	-5.30	-3.70	19.2
	-3.70	-2.10	12.0
	-2.10	-0.50	7.6
	-0.50	1.10	6.7
	1.10	2.70	9.2
	2.70	4.30	1.2
	4.30	5.90	1.2
	5.90	7.50	1.6
	7.50	9.90	2.2

(a)

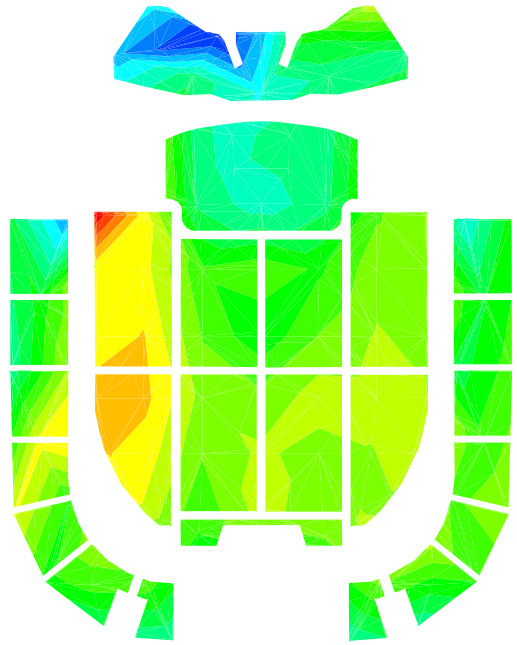

C80 for Source in Choir Alto Section

Color	Range Beg.	Range End	Percent
	-16.50	-14.90	0.0
	-14.90	-13.30	0.1
	-13.30	-11.70	0.2
	-11.70	-10.10	2.8
	-10.10	-8.50	7.5
	-8.50	-6.90	12.0
	-6.90	-5.30	22.4
	-5.30	-3.70	15.7
	-3.70	-2.10	11.5
	-2.10	-0.50	7.9
	-0.50	1.10	10.3
	1.10	2.70	4.9
	2.70	4.30	1.5
	4.30	5.90	1.5
	5.90	7.50	1.1
	7.50	9.90	0.6

(b)

FIG. 4.17. Color maps for the C_{80} for the source in the choir loft. (a) Source in the soprano section. (b) Source in the alto section.

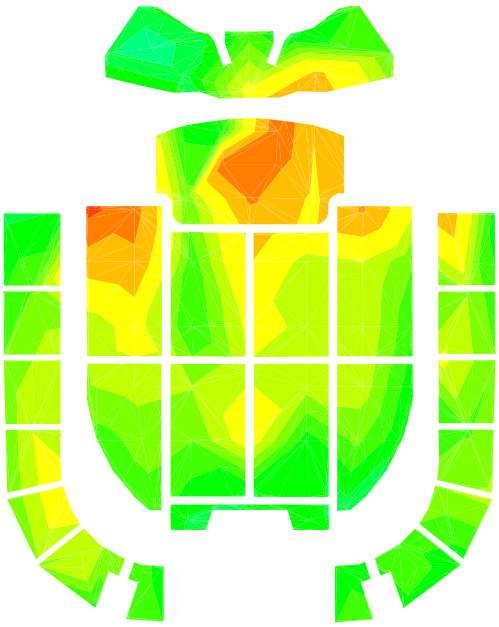

ECM for Source in the Choir Soprano Section

Color	Range Beg.	Range End	Percent
	0.00	0.09	0.0
	0.09	0.18	0.0
	0.18	0.27	0.0
	0.27	0.36	0.0
	0.36	0.45	0.0
	0.45	0.54	0.8
	0.54	0.63	3.5
	0.63	0.72	11.1
	0.72	0.81	15.6
	0.81	0.90	20.1
	0.90	1.00	23.9
	1.00	1.20	13.5
	1.20	1.40	8.2
	1.40	1.60	3.2
	1.60	1.80	0.1
	1.80	2.00	0.0

(a)

ECM for Source in the Choir Alto Section

Color	Range Beg.	Range End	Percent
	0.00	0.09	0.0
	0.09	0.18	0.0
	0.18	0.27	0.0
	0.27	0.36	0.0
	0.36	0.45	0.0
	0.45	0.54	0.0
	0.54	0.63	0.1
	0.63	0.72	1.1
	0.72	0.81	15.1
	0.81	0.90	18.8
	0.90	1.00	21.9
	1.00	1.20	28.2
	1.20	1.40	6.7
	1.40	1.60	4.3
	1.60	1.80	2.5
	1.80	2.00	1.4

(b)

FIG. 4.18. Color maps for the ECM for the source in the choir loft. (a) Source in the soprano section. (b) Source in the alto section.

4.3 Maps of Parameters for the Sound System

Figure 4.19 shows the maps of the $T10_{10\text{-}20}$ and EDT for the response of the Tabernacle to the sound system. They are the most uniform maps of these parameters since the source is distributed across the width of the hall, including under the balcony. The quietest primary source (dodecahedron loudspeaker with one driver active) is the only one near the focal point of the curved ceiling. This arrangement provided a more uniform coverage over the seating areas for the direct sound and since most of the sources were far from a focal point of the ceiling, these reflections were more diffuse instead of being focused to one location. Furthermore, since only one driver on the dodecahedron loudspeaker was active, the ceiling was not as fully excited, as it was for the other tests. The spatial symmetry of the values is caused by the symmetry in both the sound system and the shape of the hall itself. There are no higher values in these maps because the sound system directs most of the sound into the seating areas, and not onto the ceiling or walls.

Figure 4.20 shows the map of STI for the Tabernacle sound system as the source. The green areas under the balcony show an increase in STI for these receiver locations compared to the STI values for the source at center stage shown in Fig. 4.13. Intelligibility also improved in the balcony toward the front and rear of the hall. The color maps for the rest of the parameters measured for the source through the sound system are found in Appendix B.

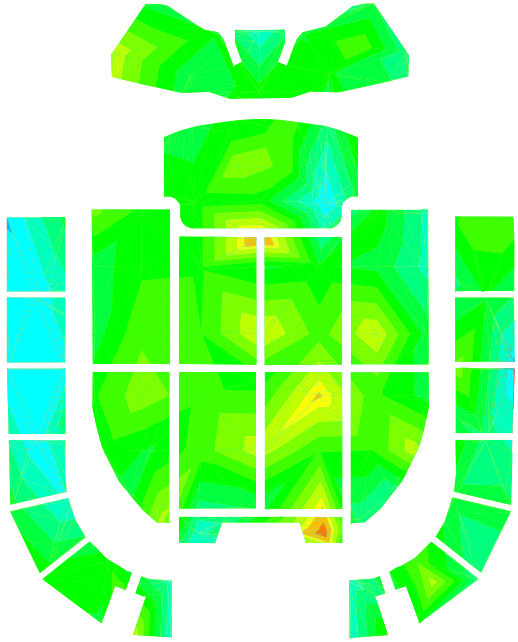

T10 for Source through the Sound System

Color	Range Beg.	Range End	Percent
	1.80	2.08	0.0
	2.08	2.36	0.0
	2.36	2.64	0.0
	2.64	2.92	6.2
	2.92	3.20	5.4
	3.20	3.48	9.2
	3.48	3.76	15.8
	3.76	4.04	26.5
	4.04	4.32	22.0
	4.32	4.60	9.9
	4.60	4.88	3.8
	4.88	5.06	0.8
	5.06	5.34	0.3
	5.34	5.62	0.1
	5.62	5.90	0.0
	5.90	6.20	0.0

(a)

EDT for Source through the Sound System

Color	Range Beg.	Range End	Percent
	0.00	0.75	0.0
	0.75	1.50	0.7
	1.50	2.25	5.1
	2.25	3.00	25.3
	3.00	3.75	50.6
	3.75	4.50	17.6
	4.50	5.25	0.6
	5.25	6.00	0.0
	6.00	6.75	0.0
	6.75	7.50	0.0
	7.50	8.25	0.0
	8.25	9.00	0.0
	9.00	9.75	0.0
	9.75	10.50	0.0
	10.50	11.25	0.0
	11.25	12.00	0.0

(b)

FIG. 4.19. Color maps for the sound system in the Tabernacle. (a) $T10_{10\text{-}20}$ map. (b) EDT map.

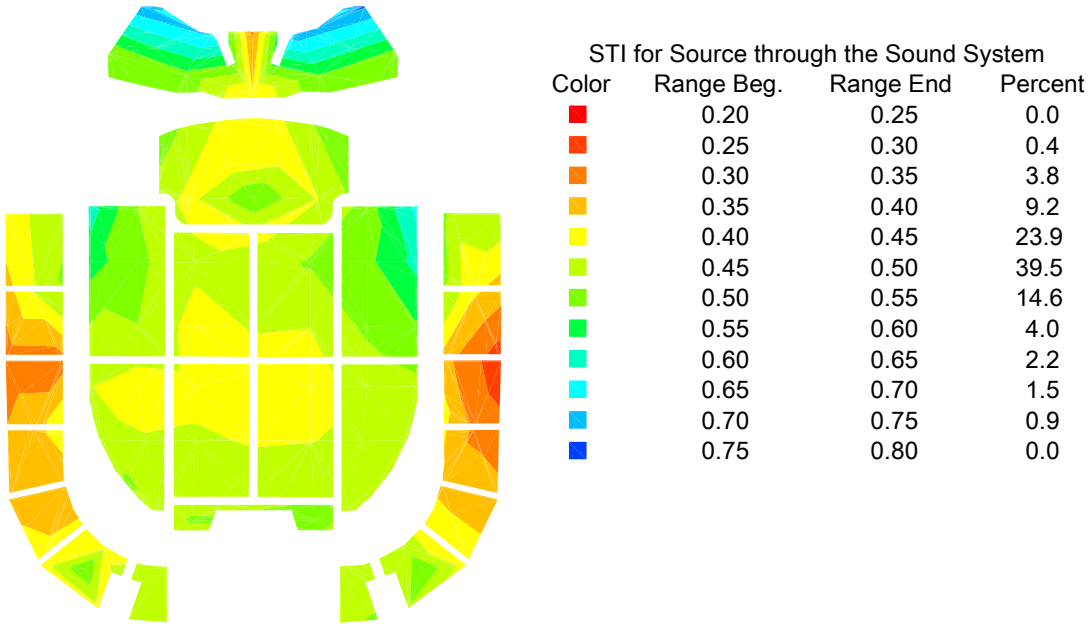

FIG. 4.20. Color map of STI for the sound system in the Tabernacle.

4.4 Maps of Parameters for the Source at the Old Pulpit Position

For comparison with the historical computer models, a few impulse response measurements were made with the dodecahedron loudspeaker at the old pulpit position, with one driver active, aimed down the center line of the hall. The resulting color maps shown in this section were created because these specific parameters corresponded to the historical comments that are discussed in Chapter 7. The map of EDT for the source at the pulpit is shown in Fig. 4.19(a) because EDT correlates well with perceived reverberance. Figure 4.19(b) shows the map of STI because the pulpit was used for speech. These maps show perfect symmetry because the impulse responses were only measured on the right side of the hall and the measured values were copied to the left side under a symmetry assumption.

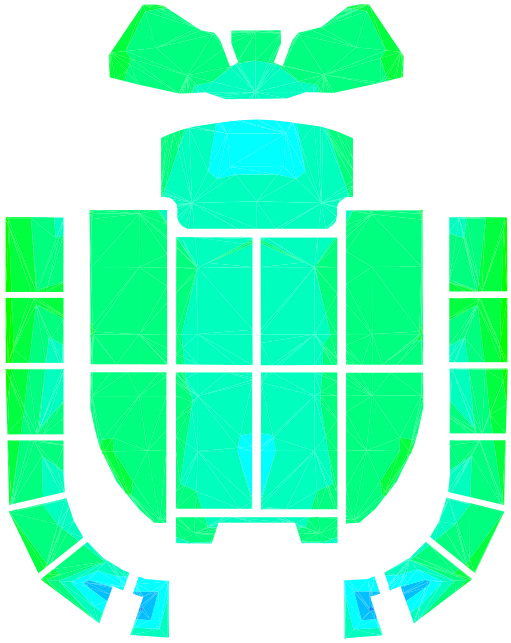

EDT for Source at the Pulpit

Color	Range Beg.	Range End	Percent
	0.00	0.75	0.0
	0.75	1.50	0.0
	1.50	2.25	0.9
	2.25	3.00	5.7
	3.00	3.75	33.9
	3.75	4.50	49.8
	4.50	5.25	8.7
	5.25	6.00	1.1
	6.00	6.75	0.0
	6.75	7.50	0.0
	7.50	8.25	0.0
	8.25	9.00	0.0
	9.00	9.75	0.0
	9.75	10.50	0.0
	10.50	11.25	0.0
	11.25	12.00	0.0

(a)

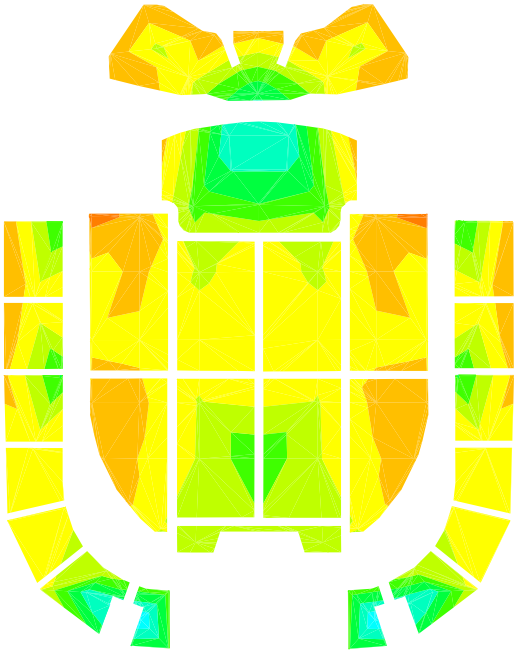

STI for Source at Pulpit

Color	Range Beg.	Range End	Percent
	0.20	0.25	0.0
	0.25	0.30	0.0
	0.30	0.35	0.3
	0.35	0.40	19.0
	0.40	0.45	45.4
	0.45	0.50	19.7
	0.50	0.55	7.2
	0.55	0.60	4.8
	0.60	0.65	3.4
	0.65	0.70	0.2
	0.70	0.75	0.0
	0.75	0.80	0.0

(b)

FIG. 4.21. Color maps for the source at the location of the old pulpit. (a) EDT map. (b) STI map. These maps show perfect symmetry because measurements were only taken on the right half of the hall and the values from these measurements were copied to the left half.

The map of EDT shows the problems with reverberance underneath the balcony and in the back of some of the balcony sections. Overall, the STI values are uniform over the seating areas, but they are only in the fair range. Additional absorption in the room due to the presence of audience members would tend to decrease EDT and increase STI. On the other hand, audience noise would decrease the signal-to-noise ratio and thereby reduce STI once again. The color maps for the rest of the parameters measured for the source through the sound system are found in Appendix B.

5 Statistical and Subjective Evaluations of the Acoustic Parameters

With so many impulse response measurements and parameter values to keep track of, statistical analysis of the data was required to better understand the average characteristics and variation of the sound field in the hall. The means and standard deviations of the parameters were calculated under the assumption that the values in the sample were normally distributed. Pelorson studied five halls and found that EDT was normally distributed, but C_{80} and RT were not.[48] Based on this finding, the mean and standard deviation values used in this study for the EDT are the true statistical values, while those for C_{80} and RT are not. Nevertheless, they are still useful indicators of the overall average value and amount of variation of each parameter over the seating areas in the Tabernacle.

5.1 Ordinary and Area-Weighted Statistics

We started by computing the means, $\overline{P}$, and the standard deviations, s, of the parameter values for each set of receiver positions. The receiver positions were spaced fairly evenly within each seating area, but this spacing was not exactly uniform over the entire hall (see Figs. 2.7 and 2.8). The statistics are shown for all source positions in Tables 5.1 through 5.5. They weight all parameter values equally and do not account for the fact that some measurement positions were more closely spaced than others — effectively covering less of the seating area than receivers that were spaced farther apart. To compensate for this, the area-weighted means and area-weighted standard deviations were then calculated. The equation for the area-weighted mean is

$$\overline{P_A} = \frac{\sum_{n=1}^{N} A_n P_n}{\sum_{n=1}^{N} A_n}, \tag{5.1}$$

where A_n is the effective area covered by each measurement position, P_n is the parameter value in question at the same measurement position, and N is the total number of receiver positions in the hall. The equation for the area-weighted standard deviation is

$$s_A = \sqrt{\frac{\sum_{n=1}^{N} A_n \left(P_n - \overline{P_A}\right)^2}{\sum_{n=1}^{N} A_n}}. \tag{5.2}$$

The effective area for each measurement position was determined using an AutoCAD® drawing of the floor plan and manual segmentation of the seating areas around each position, as shown in Fig. 5.1. This process of segmenting the seats areas around each receiver position and calculating the area-weighted statistics was repeated for each set of receiver positions.

The area-weighted statistics for the various parameters are also shown for the different source positions in Tables 5.1 through 5.5. For the results shown in these tables, the ordinary mean was within one difference limen[49] of the area-weighted mean for all of the parameters. Therefore, the area-weighted mean produces results that are not noticeably different from the ordinary mean when calculated for all 133 positions.

Table 5.1. Statistics for parameter values from impulse responses for the source at center stage.

	RT	EDT	C80	LF	BQI	ECM	ECS	STI	C50
Min	2.38	1.70	-11.1	0.02	0.00	0.54	0.60	0.26	-16.8
Max	4.77	12.0	4.5	0.65	0.85	1.79	1.70	0.74	4.1
$\overline{P}$	3.95	4.75	-4.4	0.17	0.54	0.92	0.87	0.45	-7.6
$\overline{P_A}$	3.96	4.77	-4.4	0.17	0.55	0.93	0.87	0.45	-8.1
s	0.33	2.15	3.2	0.10	0.18	0.27	0.24	0.08	4.2
$\mathbf{s_A}$	0.39	1.52	2.5	0.08	0.14	0.21	0.13	0.08	2.6

Table 5.2. Statistics for parameter values from impulse responses for the source in the soprano section of the choir loft.

	RT	EDT	C80	LF	BQI	ECM	ECS	STI	C50
Min	3.39	0.36	-16.3	0.06	0.17	0.47	0.59	0.37	-20.4
Max	6.17	4.83	9.9	0.41	0.88	1.66	1.51	0.63	8.2
$\overline{P}$	4.33	3.75	-3.9	0.22	0.55	0.90	0.84	0.45	-6.3
$\overline{P_A}$	4.31	3.77	-4.3	0.21	0.53	0.92	0.85	0.45	-6.6
s	0.44	0.90	5.7	0.08	0.17	0.26	0.19	0.05	6.0
$\mathbf{s_A}$	0.37	0.79	3.5	0.08	0.13	0.38	0.14	0.05	7.9

Table 5.3. Statistics for parameter values from impulse responses measured with the source in the alto section of the choir loft.

	RT	EDT	C80	LF	BQI	ECM	ECS	STI	C50
Min	3.25	0.18	-15.8	0.06	0.19	0.66	0.57	0.30	-25.5
Max	5.64	5.61	9.9	0.38	0.85	1.52	2.00	0.89	7.4
$\overline{P}$	4.27	4.01	-3.8	0.19	0.53	0.97	0.99	0.46	-7.3
$\overline{P_A}$	4.24	3.98	-3.9	0.18	0.51	1.00	1.03	0.46	-7.8
s	0.41	0.84	4.7	0.08	0.16	0.19	0.28	0.10	5.4
$\mathbf{s_A}$	0.32	0.74	2.9	0.09	0.12	0.14	0.41	0.08	7.4

Table 5.4. Statistics for parameter values measured from impulse responses measured with the sound system as the source. The subscript O on the EC labels indicates that these values were derived from impulse responses measured with an omnidirectional microphone instead of summing the responses measured by the microphones in the left and right ears of KEMAR.

	RT	EDT	C80	$\mathbf{ECM_O}$	$\mathbf{ECS_O}$	STI	C50
Min	1.90	0.88	-6.6	0.38	0.53	0.27	-16.4
Max	5.54	4.76	5.6	1.70	1.55	0.76	4.1
$\overline{P}$	3.84	3.21	-0.4	0.88	0.87	0.48	-3.0
$\overline{P_A}$	3.85	3.29	-0.7	0.91	0.89	0.47	-3.3
s	0.66	0.78	2.5	0.28	0.23	0.09	3.9
$\mathbf{s_A}$	0.41	0.69	2.2	0.20	0.27	0.07	5.1

Table 5.5. Statistics for parameter values from impulse responses measured with the source at the location of the original pulpit position.

	RT	EDT	C80	BQI	ECM	ECS	STI	C50
Min	2.62	1.39	-7.5	0.12	0.69	0.83	0.33	-11.6
Max	5.86	5.50	7.9	0.59	1.72	1.65	0.69	5.1
$\overline{P}$	4.09	3.91	-2.1	0.38	1.05	1.08	0.45	-4.2
$\overline{P_A}$	4.12	3.86	-2.6	0.37	1.10	1.12	0.45	-4.7
s	0.6	0.74	2.7	0.21	0.40	0.32	0.08	3.2
s_A	0.53	0.82	3.4	0.19	0.35	0.25	0.09	3.4

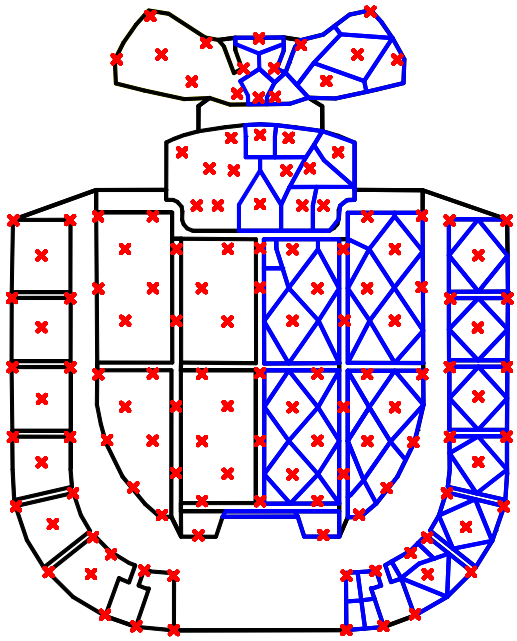

FIG. 5.1. This floor plan shows how the seating areas were divided among the various receiver positions for the source at center stage. The blue lines outlining the individual receiver areas were only drawn on one half, since the receiver areas were symmetric.

5.2 Convergence of Statistics for the Source at Center Stage

While measuring 133 positions provides extensive coverage of the sound field in the Tabernacle, such a large measurement set is impractical for most studies. In fact, most hall measurements for acoustical characterization typically include only a few receiver positions. To find a compromise between these two extremes, an algorithm was developed to determine the minimum number of receiver positions that were needed to characterize the Tabernacle. To ascertain this minimum number of receiver positions, the

ordinary and area-weighted statistics were calculated for increasing numbers of positions, starting with two positions and increasing one position at a time until all 133 positions were included.

The stratified sample technique was used to choose the order of including the measurement positions. The seating areas were divided up into four strata: central main floor and stage positions, main floor positions under the balcony, choir and opposite balcony positions, and the side balcony positions. The choir and opposite balcony seats were grouped into the same stratum because both of these sections of seats are directly under the hemispherical sections of the ceiling. Receiver positions were randomly chosen from each stratum until all 133 positions had been included. These random choices were made by hand since the different strata were not the same size. This ensured that receiver locations from the smallest stratum could be chosen among the last locations selected.

For the area-weighted statistics, a large matrix was generated to store different effective receiver areas that depended on how many measurements were being included in the average. Starting with values based on the complete set of receiver areas, one receiver position was removed at a time. The removed receiver area was divided evenly among the surrounding receivers that were still included in the set. This process was repeated until there was only one receiver left, having the total seating area assigned to it. When the area-weighted statistics were computed for the various parameter values, the matrix was applied in reverse order, starting with one receiver and increasing one receiver at a time until all 133 positions were included.

Figure 5.2 shows the results of this calculation for T10 as a function of increasing the number of receiver positions from 2 up to 133. Figures 5.3 through 5.8 show the same types of convergence plots for the rest of the parameters. The dashed horizontal lines on the graphs on the left are drawn at values corresponding to one difference limen above and below the overall mean. Accordingly, there is no perceptible difference between the overall mean and any value that falls within these lines. The circles on the graphs on the left show the minimum number of receiver positions required for the progressive mean to consistently remain within the window. For the graphs on the right, the dashed lines are drawn at values corresponding to one difference limen above and below the overall standard deviation. As with the graphs on the left, the red circles in the graphs on the right indicate the minimum number of receiver positions required for the standard deviation to consistently remain between the dashed lines. The means appear to have converged, but the standard deviation values could continue to increase, and converge to higher values than the overall value for all 133 receiver locations.

While the difference limens are typically used for comparing between just two different conditions and not between average or standard deviation values, they are useful as a first attempt to obtain an estimate of how many receiver locations would be required to characterize the acoustics of a hall. The red circles in the plots indicate where there would be no audible difference between the statistic for that number of seats and the statistical value for all 133 receiver locations. For the standard deviation values, it is not completely clear what this approach would correspond to physically. A more useful approach would be to establish preferred standard deviation values that correspond to subjective preferences for uniformity in a hall. This could be established by taking high-

density measurements in a few excellent shoebox-shaped halls, since the best halls in the world typically have this geometry. If this geometry produces a fairly uniform sound field, it would be particularly useful for establishing preferred variation values.

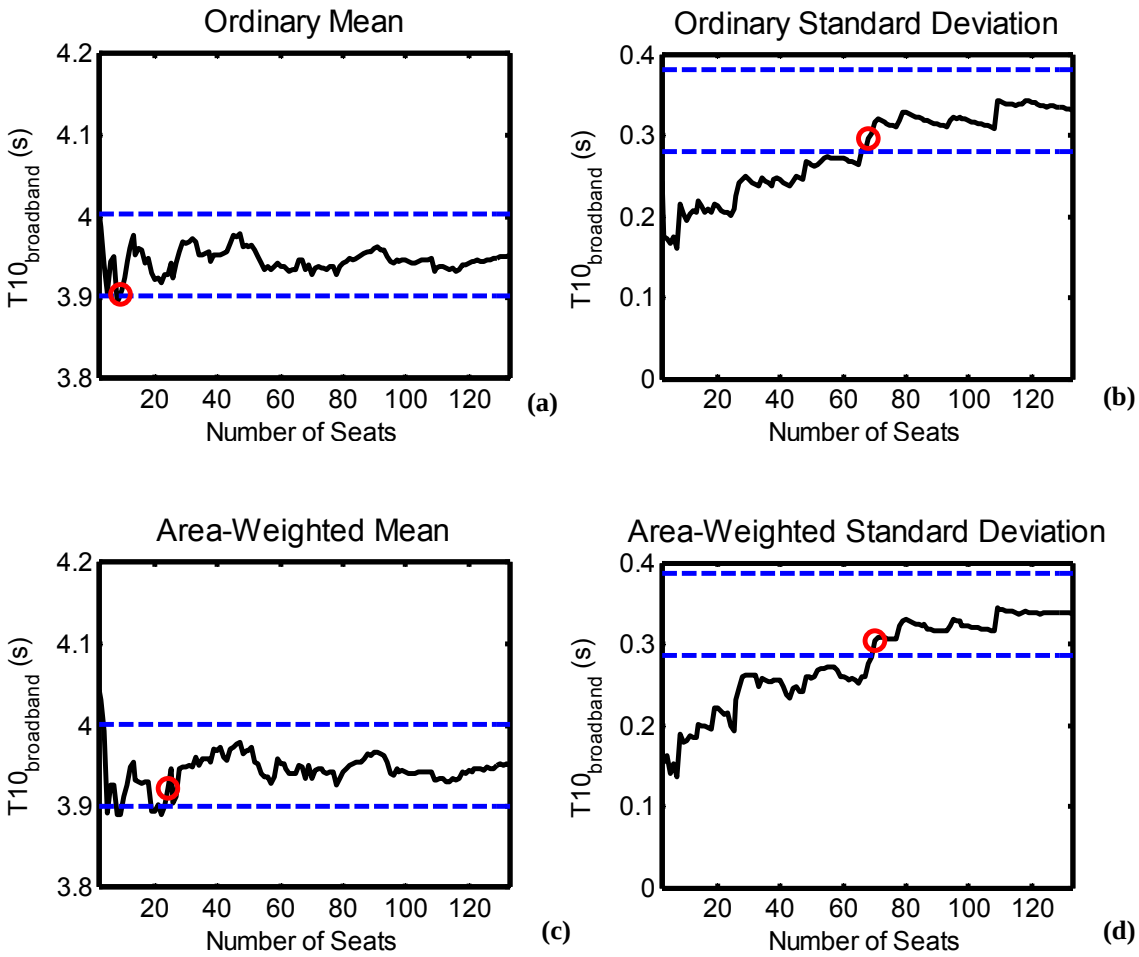

FIG. 5.2. Graphs showing the convergence of the statistics as a function of increasing receiver locations for the broadband RT ($T10_{10\text{-}20}$). (a) Ordinary mean. (b) Ordinary standard deviation. (c) Area-weighted mean. (d) Area-weighted standard deviation. The dashed lines are drawn at values that are one difference limen above or below the final mean or standard deviation value for all 133 receiver positions and the red circles show the points after which the black lines consistently stay between the dashed lines.

Following this approach, Table 5.6 shows the minimum number of measurement positions required for all parameters, based on both the ordinary and area-weighted means and standard deviations. Except for the EDT parameter, the ordinary mean

requires fewer receiver positions than the area-weighted mean in order to measure a mean value not noticeably different from the mean value calculated for all 133 receiver positions. Values for the echo criteria were not included in this table because no published difference limens were available for them. According to ISO 3382, only 14 receiver positions would be required for halls the size of the Tabernacle.[24] This number is fitting to the convergence results for some of the parameters, but definitely not for the EDT and C_{80}. In general, 14 receiver positions would not be enough to characterize the Tabernacle. This number may be adequate for a hall that has a more uniform sound field, since the EDT and C_{80} are the parameters that are most sensitive to the focusing effects of the ceiling in the Tabernacle (see Figs. 4.4 and 4.5).

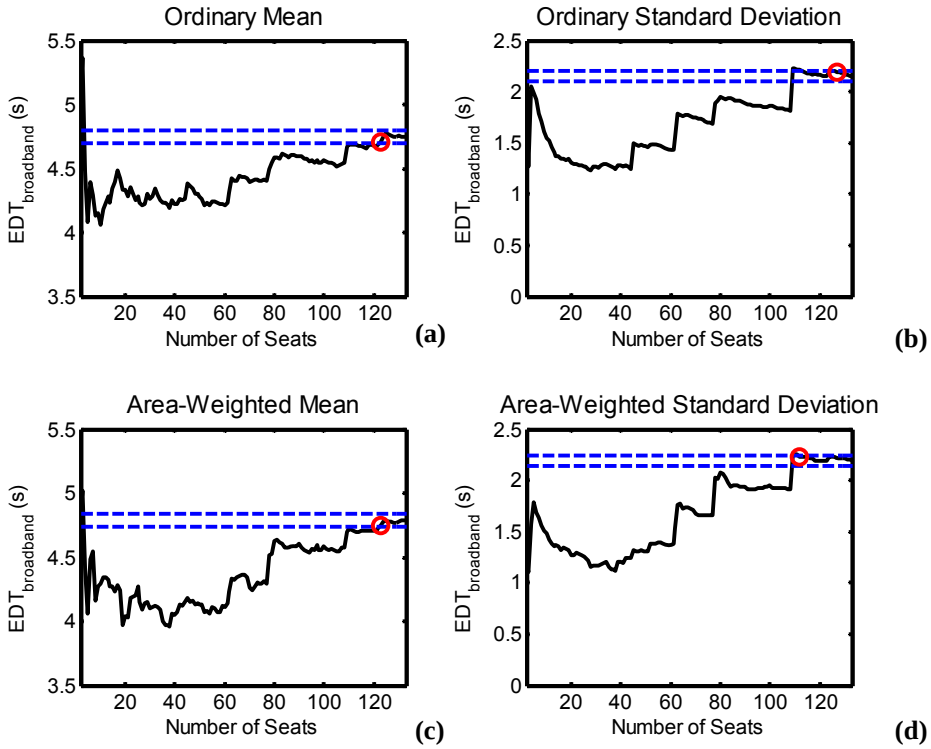

FIG. 5.3. Graphs showing the convergence of the statistics as a function of increasing receiver locations for the EDT. (a) Ordinary mean. (b) Ordinary standard deviation. (c) Area-weighted mean. (d) Area-weighted standard deviation.

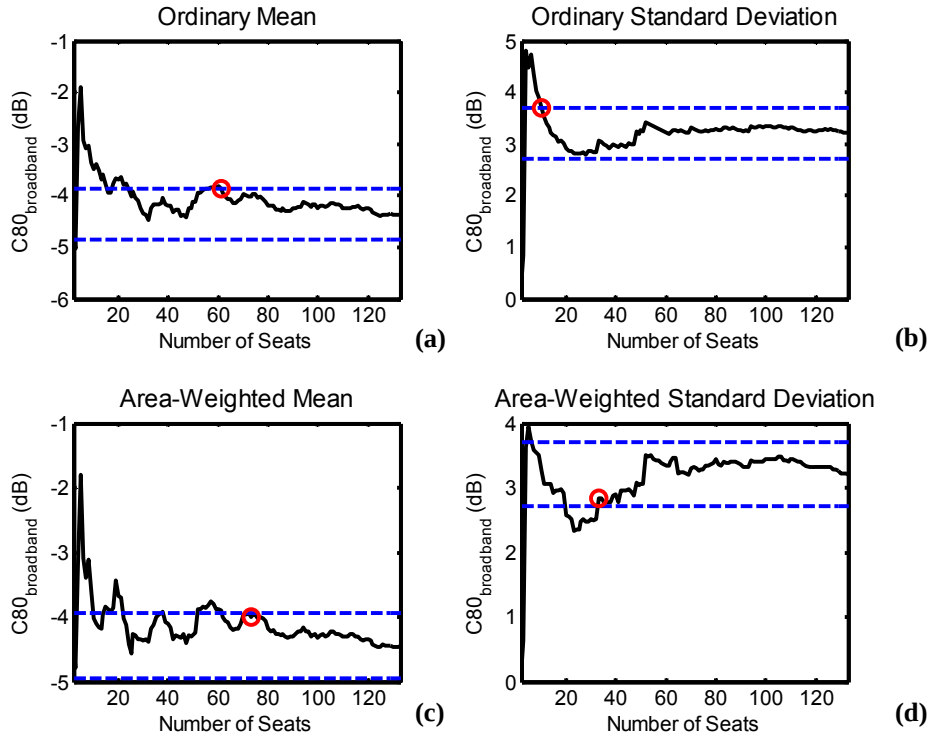

FIG. 5.4. Graphs showing the convergence of the statistics as a function of increasing receiver locations for the C80. (a) Ordinary mean. (b) Ordinary standard deviation. (c) Area-weighted mean. (d) Area-weighted standard deviation.

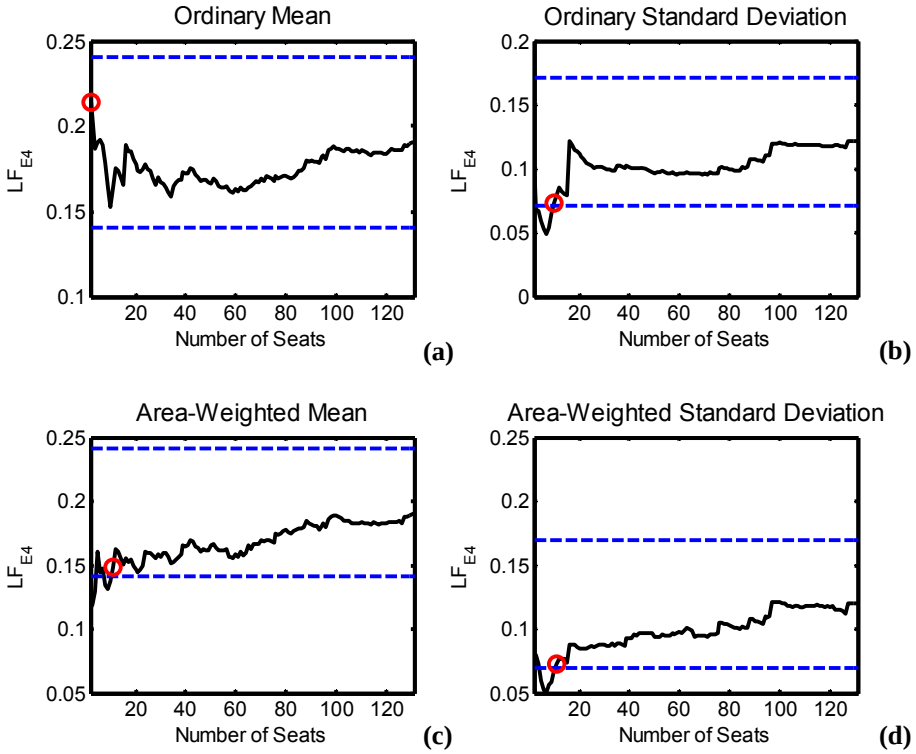

FIG. 5.5. Graphs showing the convergence of the statistics as a function of increasing receiver locations for the LF. (a) Ordinary mean. (b) Ordinary standard deviation. (c) Area-weighted mean. (d) Area-weighted standard deviation.

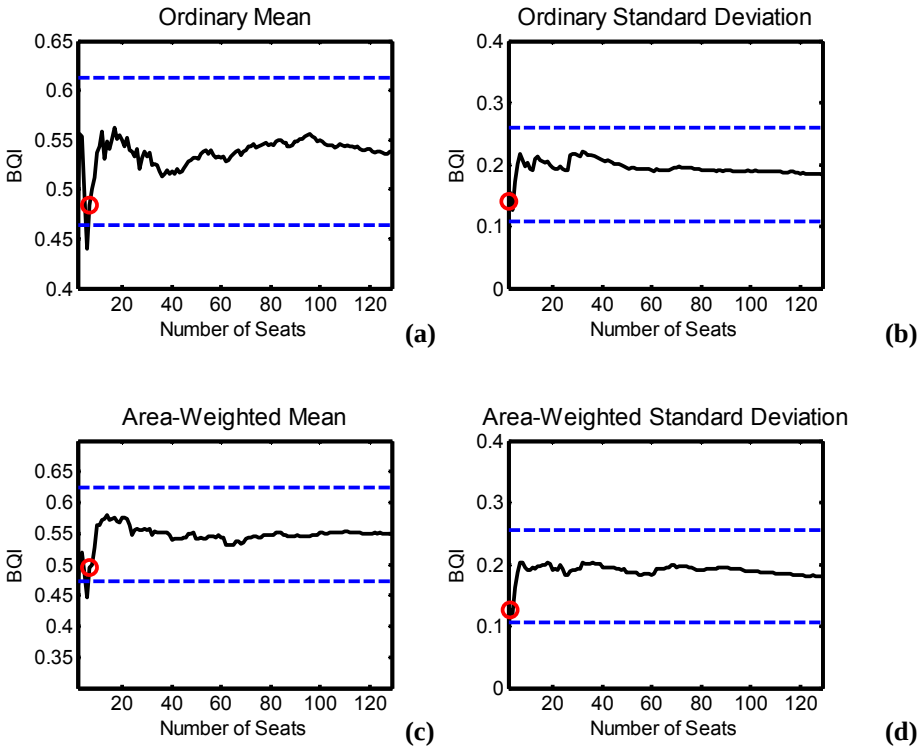

FIG. 5.6. Graphs showing the convergence of the statistics as a function of increasing receiver locations for the BQI. (a) Ordinary mean. (b) Ordinary standard deviation. (c) Area-weighted mean. (d) Area-weighted standard deviation.

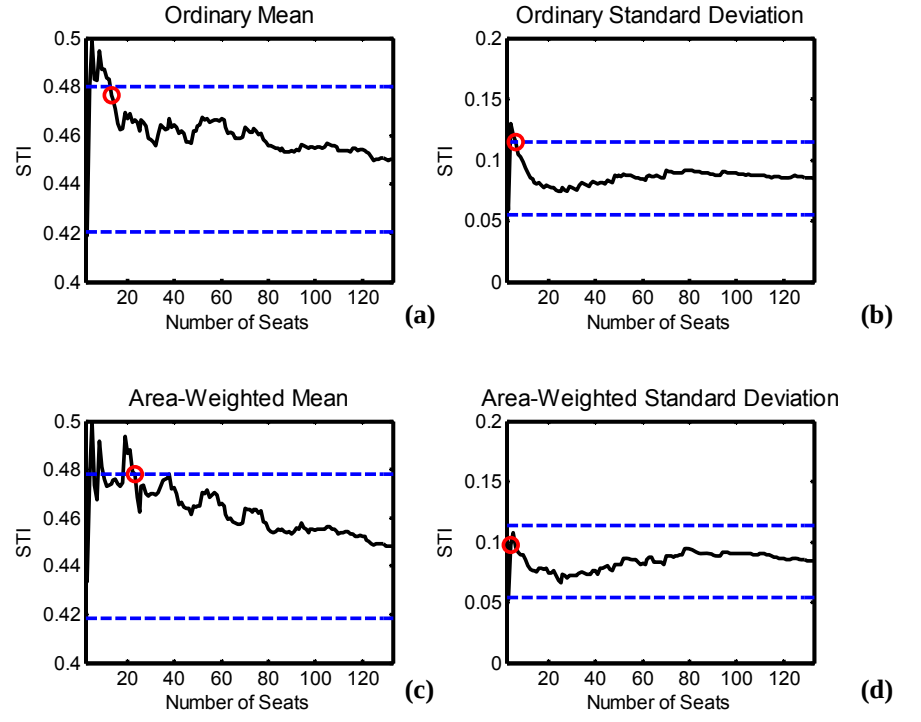

FIG. 5.7. Graphs showing the convergence of the statistics as a function of increasing receiver locations for the STI. (a) Ordinary mean. (b) Ordinary standard deviation. (c) Area-weighted mean. (d) Area-weighted standard deviation.

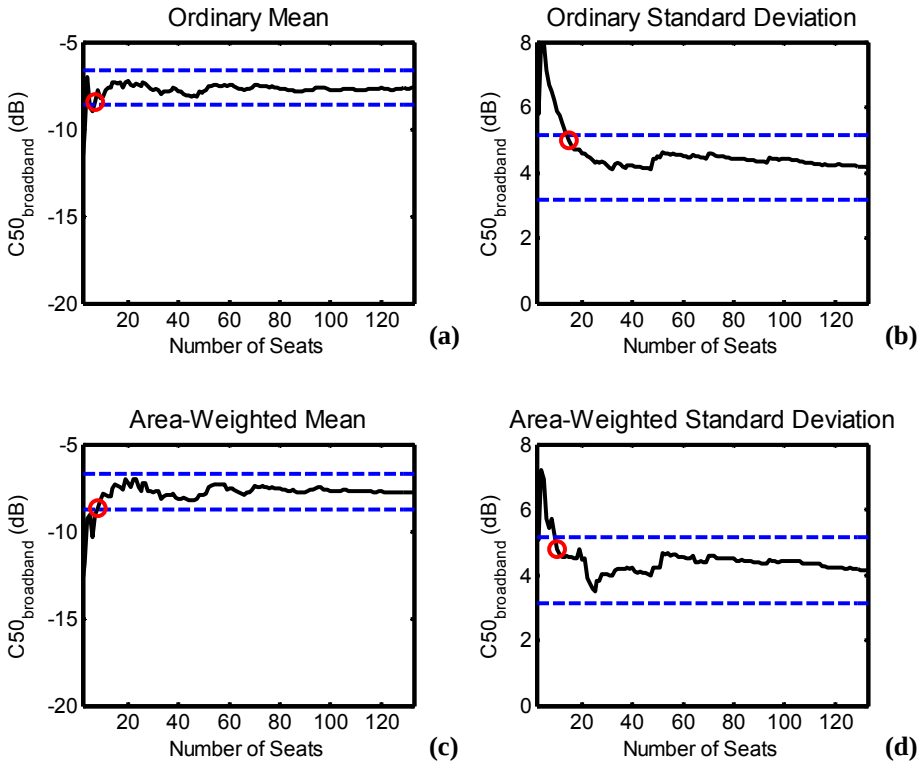

FIG. 5.8. Graphs showing the convergence of the statistics as a function of increasing receiver locations for the C50. (a) Ordinary mean. (b) Ordinary standard deviation. (c) Area-weighted mean. (d) Area-weighted standard deviation.

Table 5.6. Table of results from the convergence algorithm, for the dodecahedron loudspeaker at center stage. Each number is the minimum number of measurement positions required to calculate the progressive statistic within one difference limen of the overall statistical value determined from all 133 receiver positions. These results correspond to the red circles on the graphs in Figs. 5.2 through 5.8.

	RT	EDT	C80	LF	BQI	STI	C50
$\overline{P}$	9	123	61	2	7	13	7
$\overline{P_A}$	24	123	73	11	7	23	8
s	68	127	10	10	2	6	15
$\mathbf{s_A}$	70	112	33	11	3	4	10

5.3 Comparison with Boston Symphony Hall

To see how this characterization of the acoustics of the Tabernacle compares with other halls, a few parameter values from the Tabernacle were compared to published unoccupied values for Boston Symphony Hall. The values from Boston Symphony Hall

are averages of values measured by a few different people in the early 1990s.[50] Boston Symphony Hall was chosen for this comparison because it is well known as one of the great concert halls of the world and many published values are available for it. To show how the measured Tabernacle parameter values compare to these published values, the former were again mapped over the seating areas. However, in this case, the limits for the different colors were set by the number of difference limens between the Tabernacle values and the Boston Symphony Hall values. Notably, the RT and EDT values are significantly longer than those given for Boston Symphony Hall, since the Tabernacle is much larger (6,500 seats), seating more than twice as many as Boston Symphony Hall (2,625 seats).[51] The comparison of other parameters, such as C_{80} and BQI, was more equitable. Furthermore, as seen in Table 4.1 and Fig. 4.4, the C_{80} varies significantly over the seating areas of the Tabernacle, making it a more interesting parameter for investigation.

To see the comparison between the two halls on a data map, the ranges that are used for orange, yellow, and green in Fig. 5.9 correspond to C_{80} values for the 2000 Hz octave band that are within specific numbers of difference limens from the average values given for Boston Symphony Hall, for an unknown number of receiver positions. The 2000 Hz octave band was used because the published values for Boston Symphony Hall were only given in octave bands. This band is one of the more significant in human perception and is the band for which the average C_{80} value for the Tabernacle is closest to that for Boston Symphony Hall. The red areas on the data map are more than two difference limens below the average value for Boston Symphony Hall (-2.97 dB), and the blue areas are more than two difference limens above. The yellow regions are within one

difference limen. As shown in the figure, some seats in the Tabernacle sound as clear as the average value given for Boston Symphony Hall, even though the acoustics in these halls are very different. For the octave bands below 2000 Hz, all of the average values for the Tabernacle are noticeably lower than those for Boston Symphony Hall (see Table 5.7). Figure 5.10 shows a similar map for the BQI values.

Since there is no data available on the spatial variation of parameters in Boston Symphony Hall, it is not possible to compare its overall variation with that of the Tabernacle. However, it is reasonable to assume that the sound field is more uniform in Boston Symphony Hall (due to the lack of focusing surfaces) and therefore better represented by average values based on a small number of measurement positions than the Tabernacle would be. If the receiver positions chosen for a study of the Tabernacle were located mostly in the yellow areas shown in the data map, the Tabernacle could be portrayed as having acoustics with clarity comparable to that of Boston Symphony Hall. Such an assertion would be misleading if the entire seating area were to be taken into account. Of course, the same could be said of any other hall. As a result, there is clearly a need for a new architectural acoustics parameter that appropriately represents the uniformity of sound fields in halls. The parameter would describe the spatial uniformity of the various parameters and indicate how many uniformly spaced measurement positions would be required to accurately characterize a hall and compare it to other halls.

Another data map was created to show how many receiver locations in the Tabernacle that were within one difference limen of the Boston Symphony Hall for a cross section of both C_{80} and BQI values. For this map, an average of the C_{80} values for the 500 Hz, 1000 Hz, and 2000 Hz octave bands was used since these are the bands used

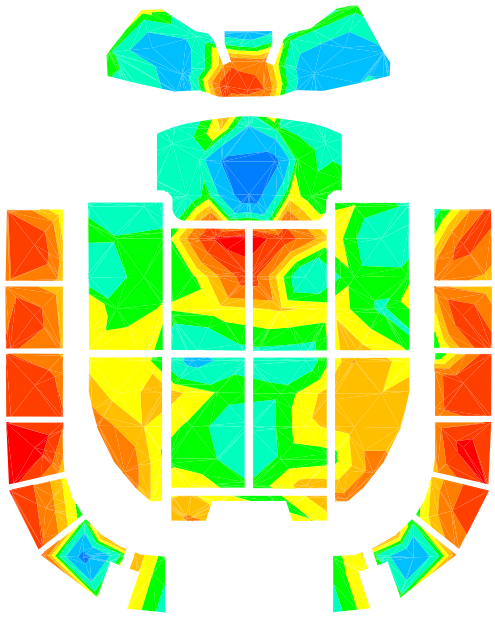

C80 compared to Boston Symphony Hall, 2000 Hz

Color	Range Beg.	Range End	Percent
	-10.00	-8.00	1.8
	-8.00	-6.00	11.8
	-6.00	-4.47	11.3
	-4.47	-3.47	11.6
	-3.47	-2.47	15.6
	-2.47	-1.47	19.9
	-1.47	0.53	19.3
	0.53	4.00	7.3
	4.00	7.50	1.4

FIG. 5.9. Color map of the measured C_{80} values for the source at center stage for the 2000 Hz octave band, colored according to how close the values are to the published value for C_{80} at 2000 Hz for Boston Symphony Hall (-2.97 dB). The yellow shows values that are within one difference limen.

for the BQI. The map in Fig. 5.11 shows the locations where both, either, or neither parameter values are within one difference limen of the combined values for Boston Symphony Hall. Overall, there are 12 positions in the Tabernacle that have values within one difference limen of both parameters. While only based on a cross section of two parameters, these might be considered better seats in the hall than those matching only one or none of the Boston Symphony Hall values.

Table 5.7 compares additional octave-band values for the Boston Symphony Hall with corresponding area-weighted mean values calculated for the Tabernacle. Specifically, the values are represented as the Tabernacle values minus the Boston Symphony Hall values. The positive values in the first two rows show the differences in size and absorption between the two halls which produce longer decay times. The Tabernacle has a larger volume (30,250 m^3) and lack of seat cushions as opposed to Boston Symphony Hall's smaller volume (18,750 m^3) and lightly upholstered seats.

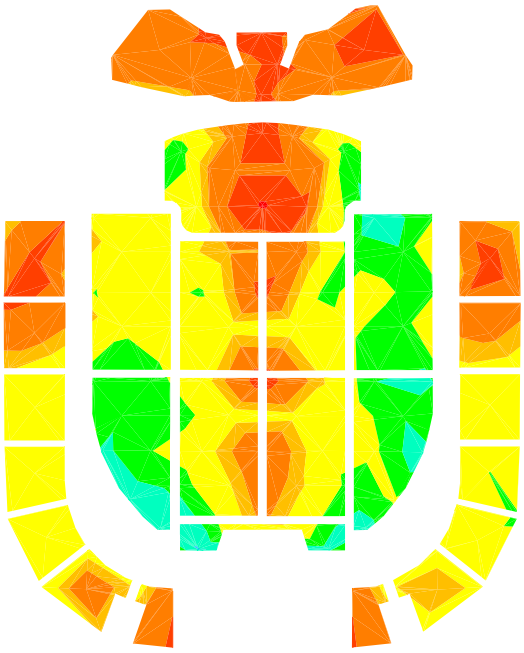

BQI compared to Boston Symphony Hall

Color	Range Beg.	Range End	Percent
	0.00	0.15	0.0
	0.15	0.31	7.3
	0.31	0.46	24.7
	0.46	0.54	9.6
	0.54	0.69	39.0
	0.69	0.77	15.7
	0.77	0.85	3.6
	0.85	0.95	0.0
	0.95	1.00	0.0

Figure 5.10. Color map of the measured BQI values for the source at center stage, colored according to how close the values are to the calculated value for BQI for Boston Symphony Hall (0.61). The yellow show values that are within one difference limen.

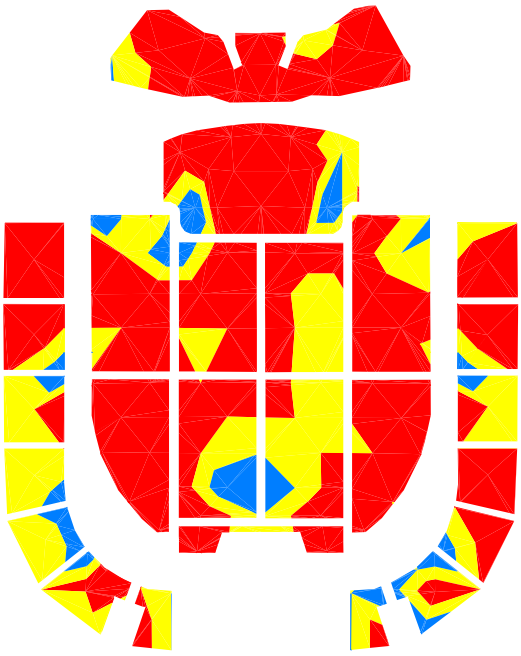

BQI and C80 compared to Boston Symphony Hall

Color		Percent
	Neither	65.5
	One	28.8
	Both	5.7

FIG. 5.11. Color map of comparison between the Tabernacle and Boston Symphony Hall for both C80 and BQI. The blue areas show where both the C80 and BQI Tabernacle values are within a difference limen of the Boston Symphony Hall values.

The lower values in the 4000 Hz octave band are a result of the high-frequency absorption apparently provided by the extensive Tabernacle ceiling and increased losses due to air absorption. This high-frequency absorption can be seen in a plot of the measured reverberation time as a function of frequency, in Appendix D, Fig. D.1. The negative values in the C_{80} row show how the reverberation in the Tabernacle produces more blend at many seats than would be heard in Boston Symphony Hall at lower frequencies. Again, the effect of the high-frequency absorption can be seen in the 4000 Hz octave band, where the area-weighted mean C_{80} value for the Tabernacle is higher than the average value for Boston Symphony Hall. The 2000 Hz values are similar. The BQI value for Boston Symphony Hall was calculated from the published octave band values for $IACC_E$, and was only slightly lower than the average measured value for the Tabernacle.

Table 5.7. Difference between area-weighted mean parameter values from the Tabernacle and the mean parameter values for Boston Symphony Hall.

Difference	125 Hz	250 Hz	500 Hz	1000 Hz	2000 Hz	4000 Hz
RT (s)	1.384	1.580	1.737	1.353	0.471	-0.315
EDT (s)	2.138	3.739	3.835	2.754	0.887	-0.107
C_{80} (dB)	-0.9	-2.4	-2.5	-2.2	0.2	1.7
BQI	-0.065					

Table 5.8 provides a slightly different comparison between the two halls by showing how many seats in the Tabernacle fall within one difference limen of the values measured in Boston Symphony Hall for each parameter. As discussed previously, the overall reverberation in the Tabernacle is noticeably longer than in Boston Symphony Hall, so the zeroes in the first two rows of this table are not surprising. However, there are receiver positions in the Tabernacle that are not noticeably different than Boston Symphony Hall when measuring C_{80} as shown by the yellow areas in Fig. 5.9. There are

more similarities between the values for the two halls in this case because the C_{80} covers such a large range of values, and this range does not completely shift when one hall is larger than another. For the BQI, the high number of similar seats is due to the fact that the range of the BQI as a parameter is limited from 0 to 1, but the difference limen is larger than that of RT or EDT, which have much larger overall ranges.

Table 5.8. Number of receiver positions (out of all 133 positions) in the Salt Lake Tabernacle that have measured values for each parameter within one difference limen of the published values for Boston Symphony Hall.

Receiver Positions	Difference Limen[49]	125 Hz	250 Hz	500 Hz	1000 Hz	2000 Hz	4000 Hz
RT	0.05 s	0	1	1	0	0	6
EDT	0.05 s	0	0	1	0	5	11
C_{80}	0.5 dB	31	25	20	21	45	29
BQI	.075	46					

5.4 Subjective Evaluation of the Acoustics

The objective parameters mentioned above are relevant in characterizing the acoustics of a hall because they have been shown to correlate to subjective impressions. Another method of looking at the subjective impressions of a hall is to perform a subjective survey of those who use the hall, either performers, patrons, or both. This kind of survey is very valuable in understanding how these people perceive the hall and can give insight into which characteristics of a specific hall are well liked.

In February of 2004, Jon Holloman conducted a survey of the subjective impressions of the acoustics of the Tabernacle of a few Mormon Tabernacle Choir members, listening in different areas of the hall.[52] Figure 5.12 shows the approximate listening positions evaluated during rehearsals for the Mormon Tabernacle Choir and the Orchestra at Temple Square. As this figure shows, most of the listening positions were on the main floor of the hall, a few were in the choir loft, and one was in the balcony. As

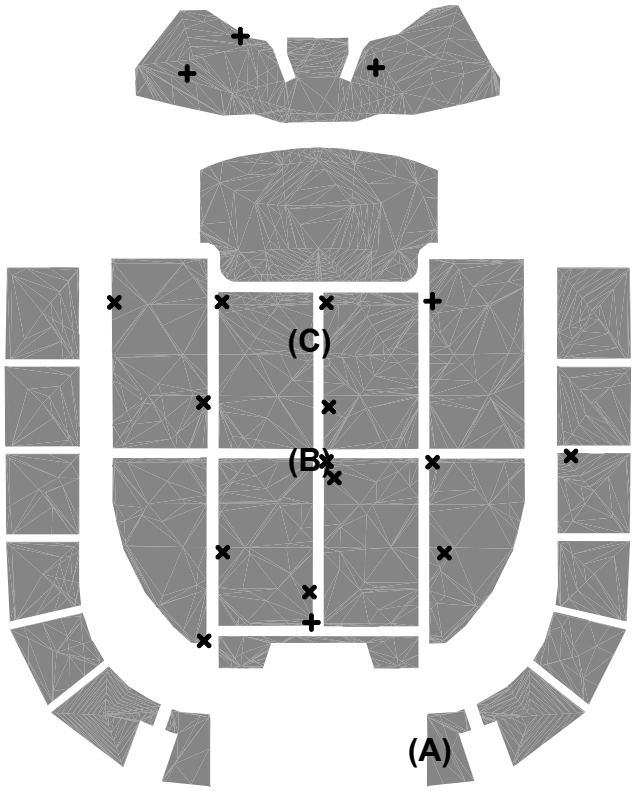

FIG. 5.12. Map of the Tabernacle seating areas to show the locations of various listener positions used in the subjective survey. Preferred listening positions are also shown. Each survey position for the unoccupied hall is marked with an x and each survey position for the occupied hall is shown with a +. Letters A and B show the positions where the two conductors preferred to listen to the choir. Letter C shows where Holloman preferred to listen to the choir.

shown in Appendix E, Holloman let the listeners rate various subjective parameters on a scale from 1 to 7, with his descriptions of what these numbers meant for each parameter. The parameters used in his survey were reverberation time, mid-frequency strength factor, low-frequency strength factor, first reflection, binaural quality factor, envelopment factor, bass ratio, clarity factor, ambient noise, and stage support factor. Lines to make additional comments about the clarity factor and the stage support factor were also included.

Table 5.9. Average values from the subjective survey results.

Parameter	Subjective (1)	Average Value unoccupied	Average Value occupied	Subjective (7)
Reverberation Time	**Too short**	4.8	4.0	**Too long**
Mid-frequency Strength Factor	**Too little**	4.0	3.8	**Too much**
Low-frequency Strength Factor	**Too little**	3.5	3.4	**Too much**
First Reflection	**Not noticeable**	4.2	5.0	**Too strong**
Binaural Quality Factor	**Not even**	5.7	3.6	**Even**
Envelopment Factor	**Too close**	4.2	4.8	**Too Distant**
Bass Ratio	**Not enough**	3.4	3.2	**Too much**
Clarity Factor	**Unclear**	4.2	3.4	**Clear**
Ambient Noise	**Not noticeable**	4.5	5.4	**Too much**
Stage Support Factor	**No support**	N/A	2.3	**Support**

Table 5.9 shows the average results of the subjective surveys. While not statistically complete, these averages still provide an interesting view of subjective impressions in the Tabernacle. Lower values correspond to the subjective preferences listed on the left and higher values correspond to the preferences listed on the right of the values in the table. Not surprisingly, the ambient noise was more noticeable with an audience present. The decrease in the binaural quality rating for the occupied hall was most likely due to the location of the listeners for the occupied hall. Overall, the mid-frequency strength factor and the bass ratio were the most uniformly rated over the hall. The subjective qualities that varied the most were the first reflection, binaural quality factor and ambient noise. The spatial variability of the perception of the first reflection and binaural quality factor were likely caused by the focusing effects of the curved ceiling and the width of the hall. Noise sources outside the hall and under the floor caused the ambient noise to vary noticeably throughout the hall.

One interesting comment made about the reverberation time in the hall was that the perceived reverberation time dropped by 60% when there was an audience in the balcony as compared to just having an audience on the main floor. Another comment was that the orchestra and choir sounded muddy at the front of the main floor. Also, the choir conductors preferred to sit in specific locations when they listened to the choir. One conductor usually sat in the rear section of the balcony, shown by the **A** in Fig. 5.11. The other conductor preferred to listen to the choir from the location shown by the **B** in and Holloman preferred to listen from position **C**.[53]

5.4.1 Comparison of Subjective Evaluations to Objective Results

To compare the measured results to the subjective evaluations, the maps of EDT, C_{80} and BQI for source on the stage, in the choir loft, and through the sound system were studied. Since the sound system is a distributed source, the maps for the source through the sound system might offer the most equivalent comparison to the choir, since it is also distributed across the width of the hall. In addition, since the EDT correlates to the perceived reverberation time for music, this parameter offers a more equivalent comparison to the subjective results for reverberation time. For the empty hall, the measured results agreed with the subjective results; the reverberation time is too long in the hall for almost all locations.

The measured results for the clarity factor also agree well with the subjective results. Overall, the clarity is low according to both sets of results, especially under the balcony. The lowest C_{80} values are in the front and center of the main floor, which correlates very well with Holloman's comment that the sound is muddy in these seats, which were right in front of the area where he preferred to listen to the choir and

orchestra. The main difference between the subjective clarity ratings and the objective values for the sound system measurements is that the clarity is much lower in the choir loft according to the subjective ratings. This difference may be due to the fact that for the subjective ratings, the choir is actually in the choir loft and the orchestra is on the stage, making a much more distributed source and adding to the background noise in these areas. The choir loft is where the choir is not accurately represented by the sound system.

For the source at center stage and in the choir soprano section, the BQI, C_{80} and LF values are similar for the two different choir conductor listening positions. The BQI was slightly lower for the second conductor listening position when the source was in the choir alto section. The RT, EDT, and C_{80} values are also similar for both positions with the source through the sound system. Why one conductor prefers the balcony and the other prefers the main floor is simply a matter of personal preference. However, it is not surprising that both locations are similar, since to some degree, both conductors would be listening for the same acoustical characteristics of the choir.

6 Contemporary Computer Model

To further characterize the acoustics of the Tabernacle, an acoustical computer model was created. Such models can be used to predict the parameters mentioned earlier and create auralizations. This chapter discusses the creation of the computer model in CATT-Acoustic™ and the results of this model. The parameter values from the model are compared to the measured results and auralizations created by the model are discussed.

6.1 Computer Modeling Methods

6.1.1 Ray-tracing Method

The ray-tracing method of simulating sound in a room is based on the assumptions of geometric acoustics. Sound is modeled as rays or cones that are emitted from the source in all directions. Each ray is traced as it reflects off different surfaces in the room until it loses enough energy due to the absorption of the room surfaces to become negligible. The intensity of the reflected ray at each surface is determined by the absorption coefficient of the surface, which is defined as the ratio between the absorbed sound energy and incident sound energy. The absorption coefficient can be interpreted in the software in two different ways. One is to assume that the surface absorbs a certain fraction (α) of energy of the ray. The other is to interpret the absorption coefficient as the probability that the ray will be absorbed completely.[54] When the incident ray hits a room surface, the angle of the reflected ray is determined by the scattering coefficient of the surface. If there is no scattering coefficient assigned, the angle of reflection is the same as the angle of incidence, as shown in Fig. 6.1(a). The scattering coefficient is defined as

the ratio between the non-specular or diffuse reflected sound energy and total reflected sound energy, as shown in Fig. 6.1(b).[55]

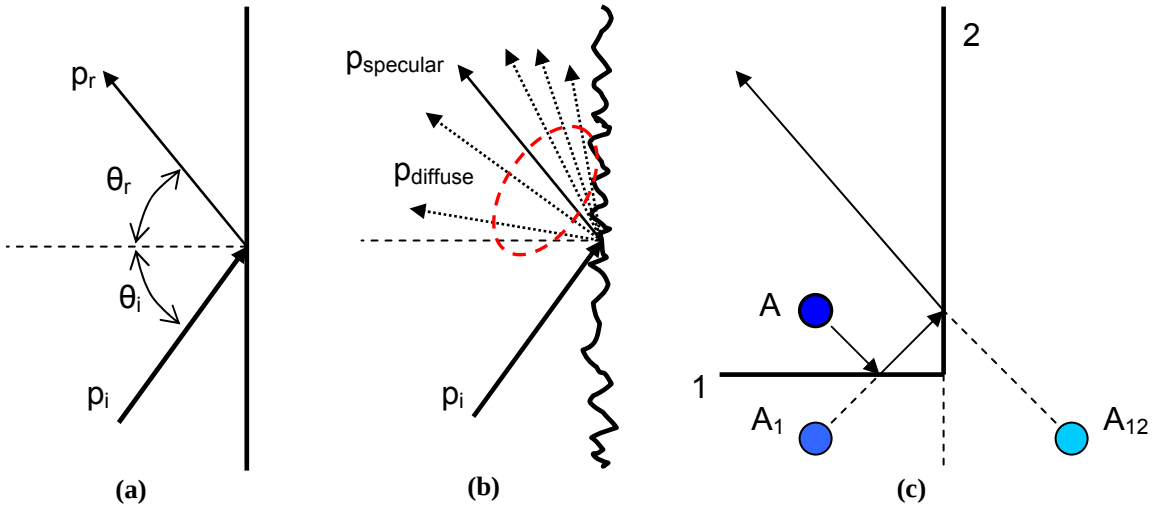

FIG. 6.1. Diagrams of ray tracing and image source methods. (a) Ray tracing for a specular reflection. (b) Ray tracing for diffuse reflections. (c) Image source method. The subscripts on the image sources in diagram (c) indicate the surface(s) used to create the image source.

6.1.2 Image Source Method

In the image source method, sound reflections are modeled by using image sources. An image source is created for each surface around the primary source, with its location symmetric about its respective surface, as shown in Fig. 6.1(c). The sound ray that is reflected from the surface is calculated as though it is produced by the image source. Second-order reflections are created by second-order image sources (image sources of first-order image sources), and so on. Therefore, the number of image sources, and hence the calculation time, increases very rapidly with increasing complexity in room geometries, since many different surfaces must be included in the model. In this computer modeling method, the absorption coefficients are applied to the image sources, and scattering coefficients are applied by dividing the surface into several radiating patches.[56]

6.1.3 CATT-Acoustic™ Method

To take advantage of the benefits of both the ray-tracing and image source methods, CATT-Acoustic™ (CATT™) uses a hybrid method that combines the two. This method is called Randomized Tail-Corrected Cone-tracing (RTC). The direct sound, first order specular and diffuse reflections, and second-order specular reflections are calculated using the image source method. For the rest of the early part of the response, the reflections are calculated by cone-tracing. In cone-tracing, cones are emitted from the source instead of rays to save computation time by covering the surface of the source with cone faces instead of small tips of rays. The late part of the response is calculated in one of two ways, depending on what it is used for. If it is used for numerical prediction, it is calculated using extrapolation. For post-processing used for auralizations and exported impulse responses, the late part of the response is calculated as a randomized tail based on the general geometry of the room, including the general shape and volume. This is used for binaural post-processing because it typically produces a more natural sounding auralization than extrapolation.[57,58]

6.2 CATT-Acoustic™ Model

To create the computer model in CATT™, the model was first drawn in AutoCAD® by converting floor plan and elevation drawings into a three-dimensional drawing. To make this three-dimensional drawing compatible with CATT™, it was created using the AutoCAD® interface provided by CATT™. The interface allowed for observing and changing the direction of the faces and created the GEO file of points and faces for CATT™ from the AutoCAD® drawing. The model incorporated a total of 1368 faces.

The source type for all positions was an omnidirectional source. To have this source further simulate the dodecahedron loudspeaker that was used for measurements, the octave-band frequency response of the dodecahedron loudspeaker was measured at one location in an anechoic chamber and applied to the source in the model. To compare the results of the model with the measured results, it was initially created for the unoccupied condition.

Drawings of the model are shown in Figs. 6.2 and 6.3. Figure 6.2 shows the locations of the source on the stage and in the choir loft, as well as a few receiver positions. For further comparison with the measured data, all 133 receiver positions were modeled. Since CATT™ only allows 99 receiver positions to be modeled at once, the 133 positions were divided into nine groups, according to seating area [main floor (4 groups), balcony (3 groups), choir, and stage]. This also made it easier to keep track of all receiver positions. Omnidirectional receivers were used for calculating the impulse responses that were exported for later computation of architectural acoustics parameters and comparison with measured results. The same Matlab® code (see Appendix A) used to calculate the parameters from the measured impulse responses was used to calculate the parameters from the exported CATT™ responses. This was done to produce greater uniformity in comparisons. For auralizations, binaural receivers were used at significantly fewer receiver locations.

The absorption and scattering coefficients for the model were first obtained by looking up similar materials in tables of coefficients.[59,60,61,62,63,64,65,66] Appendix C contains tables of the coefficients that were used in the model and the published coefficients with their references. For the 8 kHz and 16 kHz octave bands, the

coefficients were extrapolated in CATT™. Most of the published absorption coefficients were only modified slightly for inclusion in the model, after listening to a few auralizations. The most significant surfaces in the Tabernacle were the plaster ceiling and the seating areas, so these coefficients were studied in more detail.

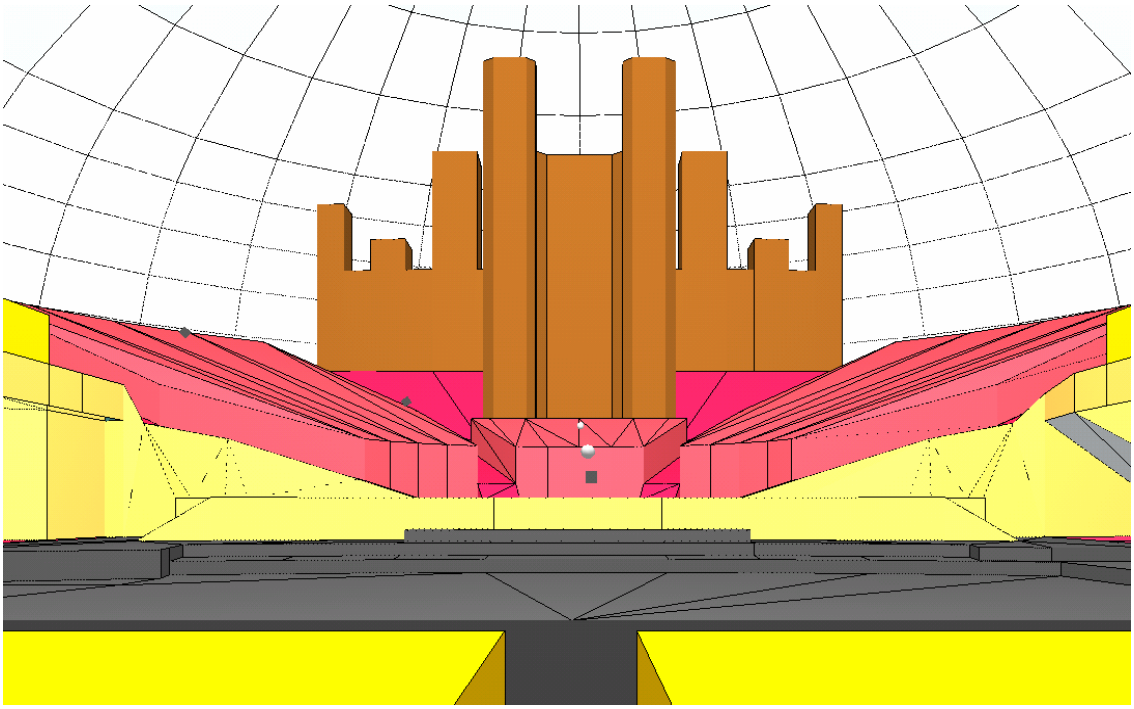

FIG. 6.2 View from inside the CATT-Acoustic computer model of the current Tabernacle interior. The small black squares above the stage and in the choir loft on the left are the source positions. Some of the receivers used for the impulse response plots in Fig. 6.5 can be seen as the white spheres.

Table 6.1 shows the absorption coefficients for these surfaces that were used in the model, as well as some other coefficients that were investigated. The first coefficients listed (plaster 1 and unoccupied 1) were used in the models and are modified from the second absorption coefficients (plaster 2 and unoccupied 2). The second and third coefficients are from different published values.[60,64,65] The second absorption coefficient for the unoccupied seating areas was actually for wood/metal seating, so the absorption coefficients for the pews in the Tabernacle in the first set of coefficients were

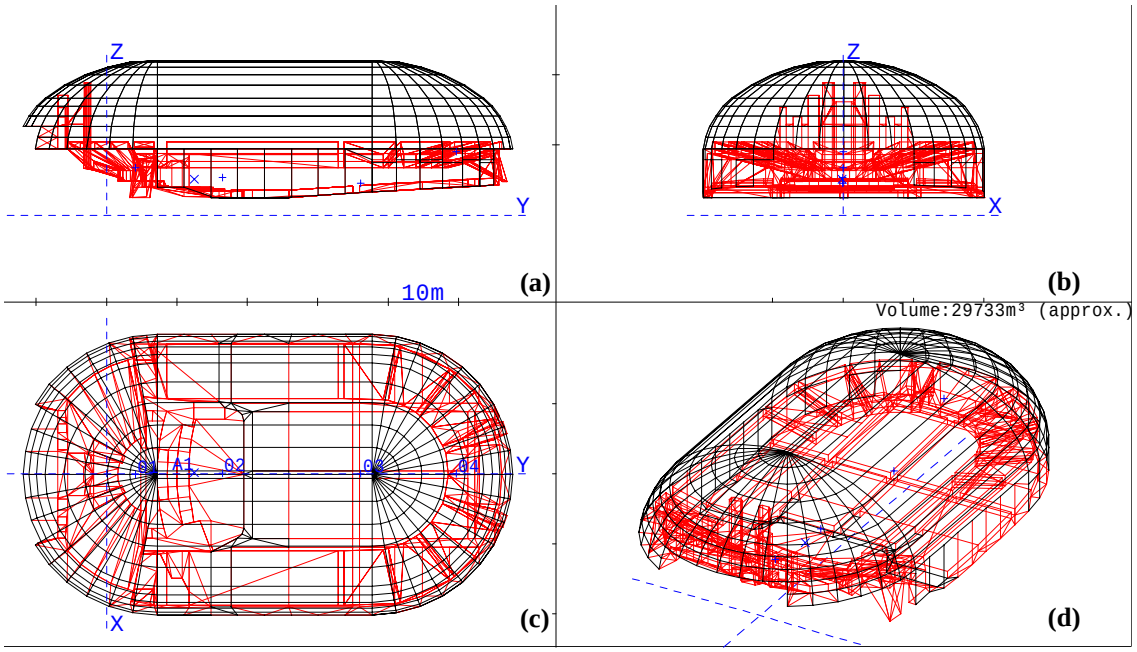

FIG. 6.3. Wire-frame drawings of the CATT-Acoustics™ computer model. (a) Side view. (b) Rear view. (c) Top view. (d) Isometric view.

increased slightly, since the pews are made entirely of wood. The third set of absorption coefficient values were also published values, but did not model the conditions of the Tabernacle very well. This plaster coefficient did not provide nearly enough absorption in the low frequencies (the Tabernacle ceiling has a large air space behind it). The unoccupied seating coefficient was modified from a coefficient for wooden pews that only listed a value for the 500 Hz octave band and the other octave band values were estimated by keeping value and following the same frequency dependence as a coefficient for wooden seats.[60] This provided too much absorption, as discussed later and as can be seen in the RT and clarity values in Table 6.2.

Table 6.1. Various absorption coefficients tried in the CATT™ model, for the plaster ceiling and the unoccupied pews. The first coefficients listed for each material are the coefficients that were actually used in the model for exporting impulse responses and creating auralizations.

	125 Hz	250 Hz	500 Hz	1000 Hz	2000 Hz	4000 Hz
α (plaster 1)	0.15	0.12	0.08	0.06	0.04	0.02
α (plaster 2)	0.30	0.10	0.10	0.05	0.04	0.05
α (plaster 3)	0.02	0.03	0.04	0.05	0.04	0.03
α (unoccupied 1)	0.043	0.063	0.07	0.08	0.14	0.15
α (unoccupied 2)	0.02	0.02	0.03	0.06	0.06	0.05
α (unoccupied 3)	0.30	0.36	0.41	0.46	0.66	0.66

To check the accuracy of the first model, a detailed calculation was performed to ensure the model was closed. The model was slightly modified to close the holes then the calculation was run again. This process was repeated until the percentage of rays leaking out of the model was well below 1%. Figure 6.4 shows the final CATT™ plot of the leaks in the model, in both time and space. The graph in the upper-left corner of the figure shows what percentage of rays leaked out of the model during the length of the calculated impulse response. The peaks in the grid around the three-dimensional model show where the rays leaked out of the model. The peak that is numbered shows the place where the most rays leaked out. In this case, even where the most rays leaked out, only 13 of approximately 360,000 total rays (set by the "auto number" feature in CATT™) leaked out of the model over 5200 ms.

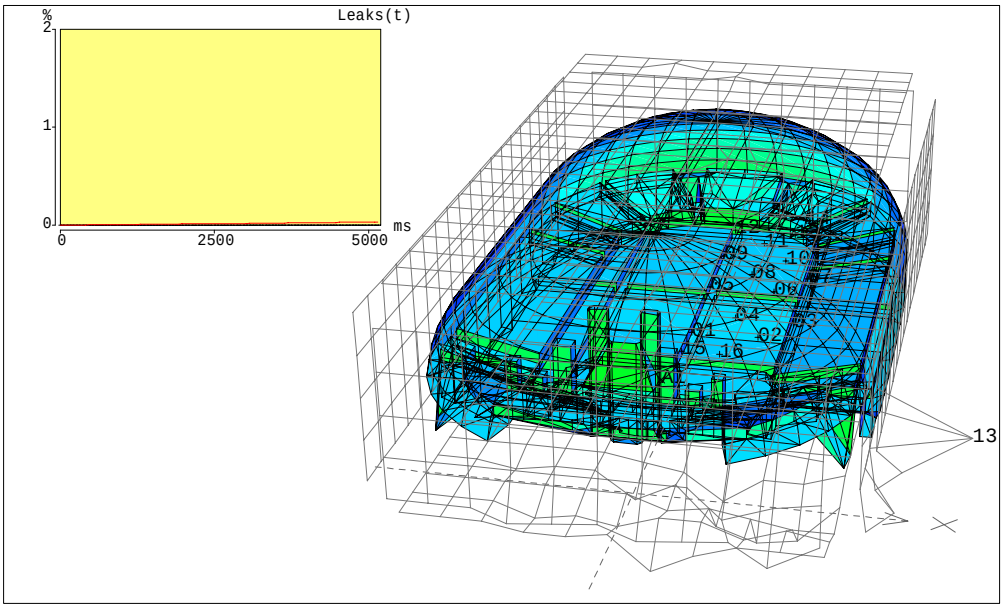

FIG. 6.4. Plots showing how many rays leak from the model. The graph on the right shows where the rays leaked out of the model. Only the spot where the most rays leak out shows the number of rays that leaked.

6.3 Analysis of Current Computer Model

6.3.1 Impulse Response Plots

To validate the computer model of the Tabernacle, the impulse responses were exported and plotted to compare with the measured responses. Figure 6.5 shows the comparison of four different responses from the source at center stage, with the CATT™ responses on the bottom for each pair of plots. Since the model was made from the AutoCAD® drawings of the hall, the time of arrival of the direct sound is pretty much the same for all of the receiver positions in both the measured and modeled responses. For the choir and stage impulse responses, the timing of the clusters of reflections after the direct sound for the CATT™ responses are similar to the reflections shown in the measured responses. However, the number and amplitude of the individual reflections in the clusters are different, due to the estimation of the scattering coefficients and the simplifications of the hall in the model.

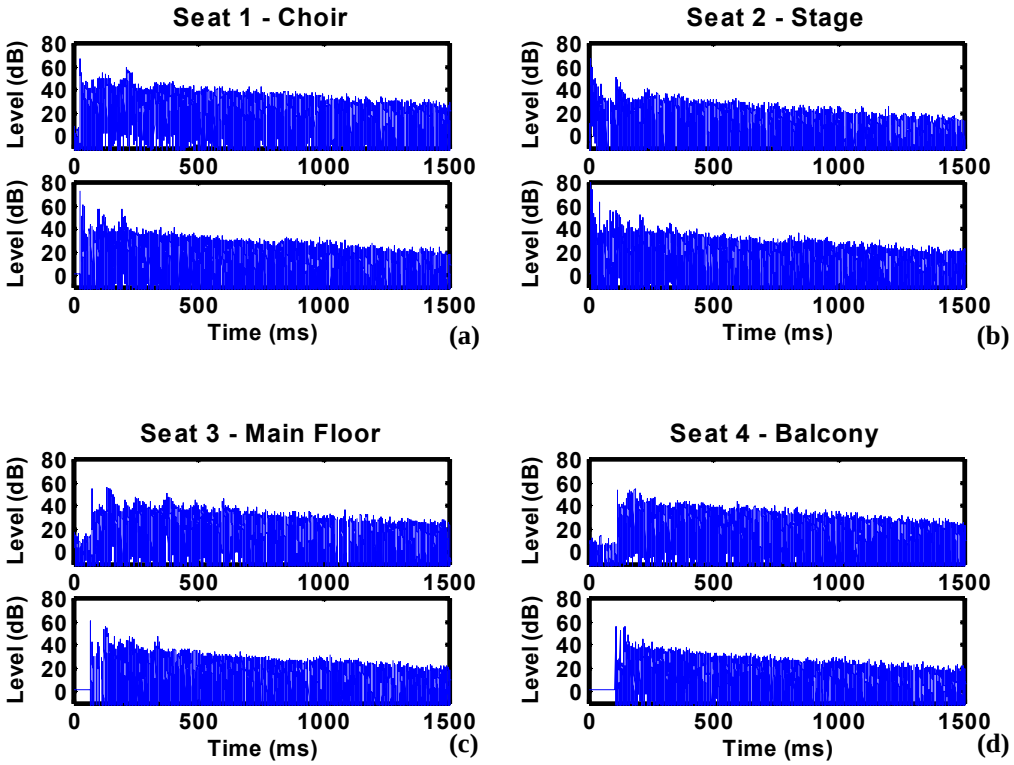

FIG. 6.5. Plots of log-squared impulse responses from the CATT™ model with the source at center stage, compared to the measured responses at the same receiver locations. (a) Response for seat 1, in the choir loft. (b) Response for seat 2, on stage. (c) Response for seat 3, on the main floor. (d) Response for seat 4, in the balcony. For each seat, the measured impulse response is on top and the exported CATT™ impulse response is on bottom. The receivers were at the locations shown in Fig. 2.7.

6.3.2 Objective Parameters

To further evaluate the computer model, the various impulse responses for the source at center stage were exported and processed in Matlab® to produce the architectural acoustics parameters. To check the various absorption coefficients in Table 6.1, the parameter values were calculated for eleven receiver locations distributed throughout the hall. Table 6.2 shows the average values obtained for each set of absorption coefficients. The effects of the excessive absorption from the third absorption coefficient ($\alpha 3$) for unoccupied pews are shown by the very short RT and EDT values, and the higher clarity values. For the $\alpha 2$ coefficients, the average RT value is closest to

the measured value, but the rest of parameter values are farther from the measured values than the first set of coefficients ($\alpha 1$). Overall, the parameter values for the model with the $\alpha 1$ coefficients come closest to the measured parameter values, so these coefficients were used the models.

Table 6.2. Average parameter values for the CATT model for the three different sets of ceiling and pew absorption coefficients in Table 6.1. These values are based on 11 receiver locations distributed throughout the hall.

	RT	EDT	C80	ECM_O	ECS_O	STI	C50
$\overline{P}$ (measured)	3.87	4.63	-4.2	0.91	0.87	0.45	-8.1
$\overline{P}$ (α1)	4.11	3.10	-0.7	1.11	1.09	0.48	-3.6
$\overline{P}$ (α2)	3.75	2.88	0.5	1.10	1.08	0.49	-1.6
$\overline{P}$ (α3)	2.41	1.45	3.9	1.14	1.13	0.58	1.5

Figure 6.6 shows the maps of $T10_{10\text{-}20}$ and EDT from the CATT™ model. Overall, the RT values are more uniform and slightly shorter than the measured values (see Fig. 4.2). The EDT values are also shifted lower than the measured values, but with a very similar pattern (see Fig. 4.3). The map clearly shows the areas of low values around the source and in the balcony areas at the rear of the hall. Adjusting the absorption coefficients as mentioned above did not eliminate these discrepancies. They were adjusted to bring the parameter values closer to the measured values, but they still did not match exactly. The absorption coefficients could have been modified again to bring the parameter values into closer agreement, but running the model repeatedly with modified coefficients would have taken too much time. Also, parameter values shown above were determined to be close enough to the measured values, since exact agreement between modeled and measured values was not expected.

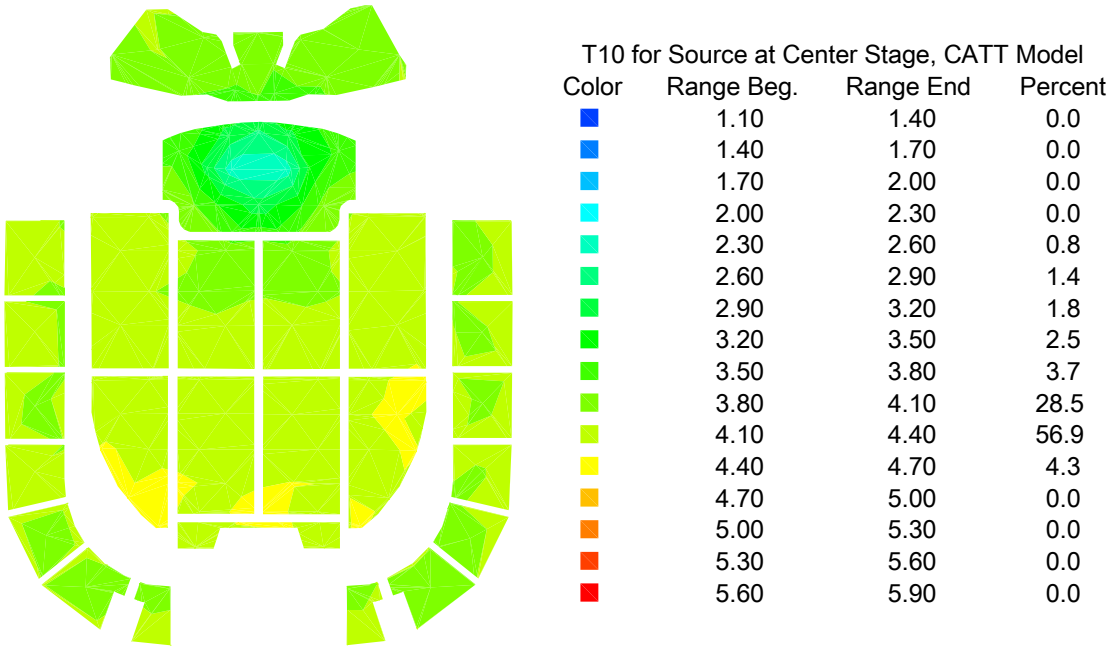

(a)

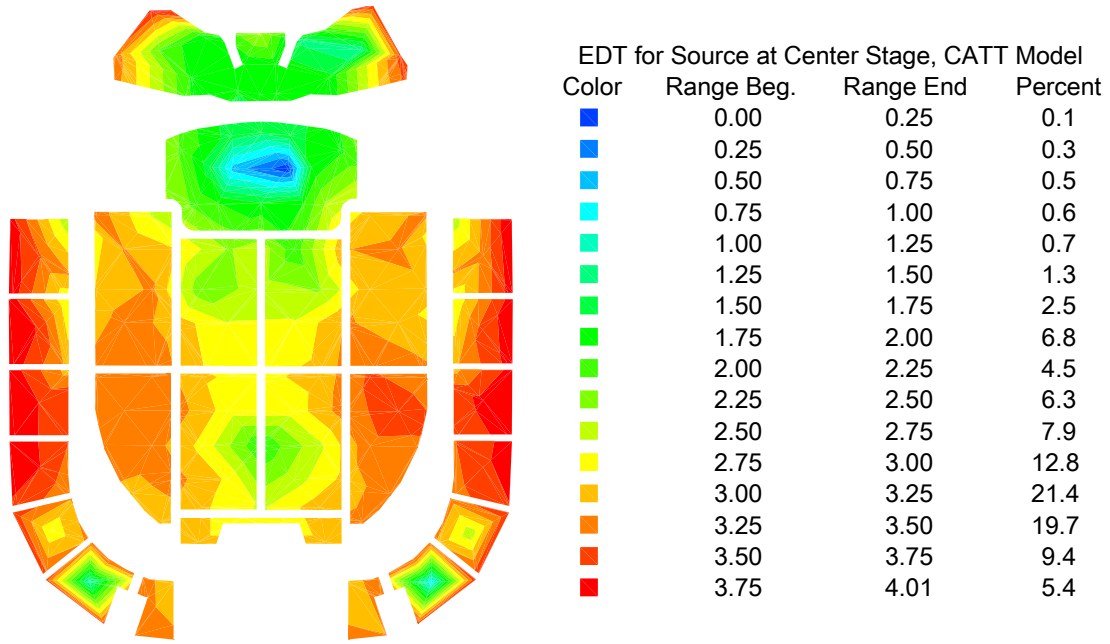

(b)

FIG. 6.6. Color maps for the CATT™ model with the source at center stage. (a) $T10_{10\text{-}20}$ map (compare to Fig. 4.2). (b) EDT map (compare to Fig. 4.3).

The color maps of the CATT™ values for C_{80} and ECM are shown in Fig. 6.7. Again, the map of C_{80} shows the focusing effects of the ceiling in the balcony at the rear of the hall and in the choir, like the map of measured values in Fig. 4.4. The ECM map shows that echoes will most likely be perceived in the middle of the hall and in the choir, which matches the measured results in Fig. 4.10. However, the areas of 10% of listeners perceiving echoes on the main floor and in the choir are not as large as those derived from the measured impulse responses. The reflections do not protrude from the CATT™ impulse response decays in these areas as much as they do from the measured impulse response decays. Appendix B contains the color maps for the rest of the CATT™ parameter values.

Table 6.3 shows the statistical values for the acoustic parameters derived from the 133 modeled impulse responses with the source at center stage. The mean values for the $T10_{10\text{-}20}$, STI, ECM and ECS are similar to the measured mean values in Table 5.1. However, the mean values for the clarity factors and the EDT from the model are closer to preferred values than the measured mean values. Once again, the receiver positions were fairly uniformly spaced throughout the seating areas, so the area-weighted mean values for the model are within a difference limen of the ordinary mean values.

Table 6.3. Statistics for parameter values derived from impulse responses with the source at center stage in the CATT™ model (compare to Table 5.1). The subscript O on the echo criteria indicates that these values were derived from impulse responses measured with an omnidirectional receiver, instead of a binaural receiver.

	RT	EDT	C80	ECM_O	ECS_O	STI	C50
Min	2.42	0.08	-7.62	0.64	0.57	0.30	-14.84
Max	4.52	4.01	7.47	1.71	1.87	0.77	7.22
$\overline{P}$	4.07	2.93	-1.10	1.09	1.09	0.48	-4.48
$\overline{P_A}$	4.08	2.92	-1.16	1.10	1.10	0.47	-4.78
s	0.36	0.77	2.85	0.26	0.32	0.09	4.04
s_A	0.35	0.73	2.83	0.25	0.31	0.09	4.16

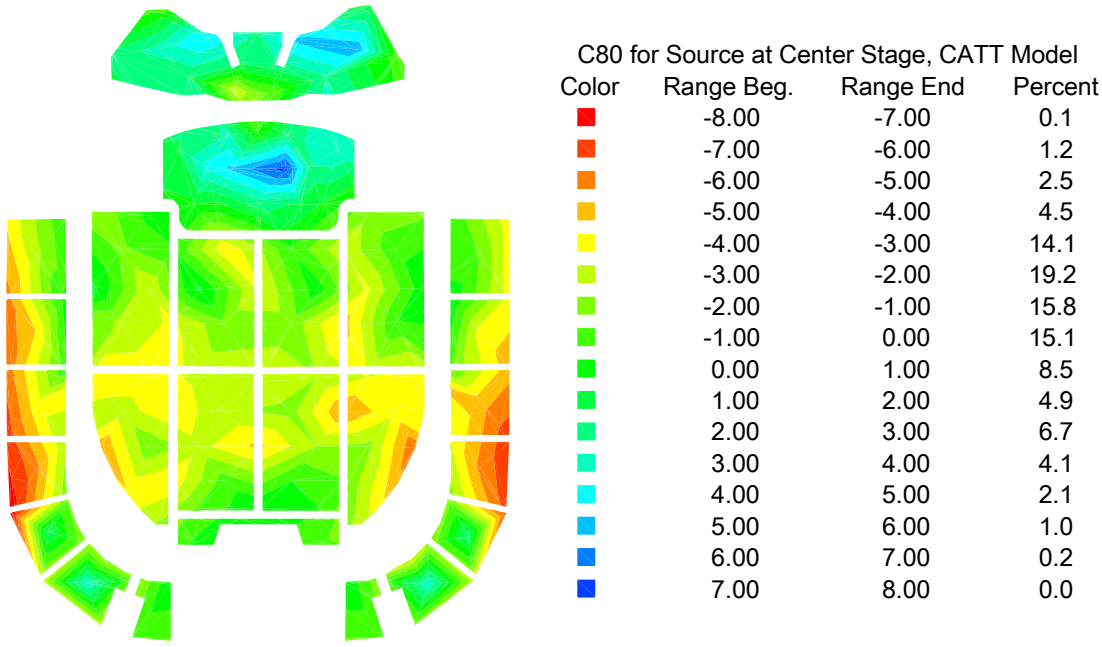

(a)

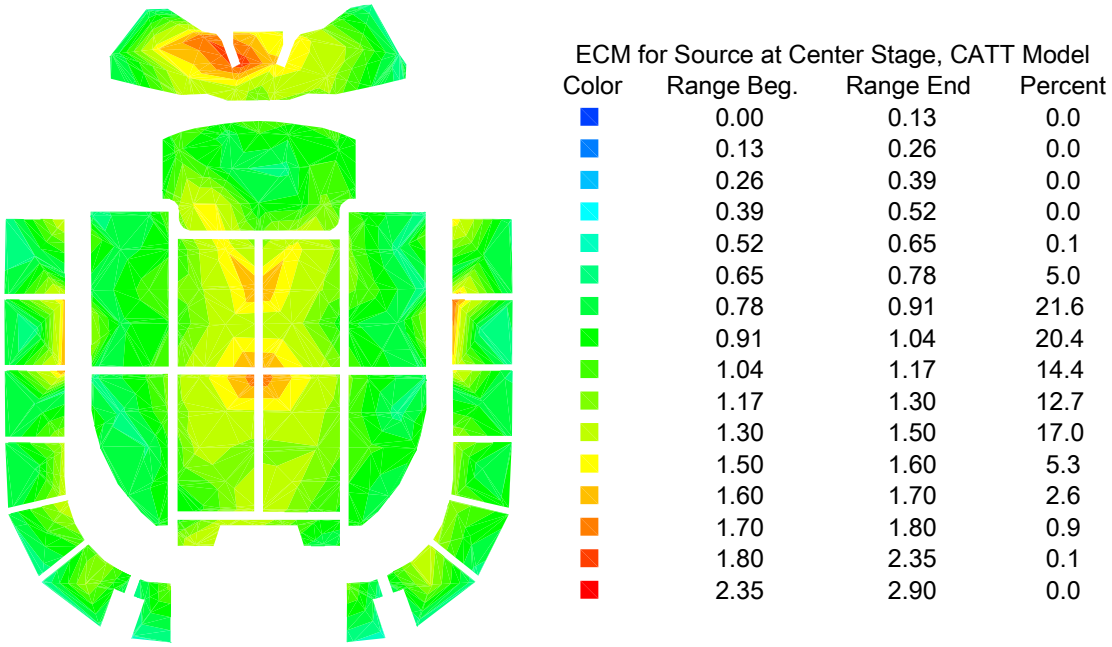

(b)

FIG. 6.7. Color maps of for the CATT™ model with the source at center stage. (a) C_{80} map (compare to Fig. 4.4). (b) ECM map (compare to Fig. 4.10). The C_{80} map shows the same focusing effects in the rear balcony sections as the map of the measured results.

6.3.3 Auralizations

The computer model was also useful for hearing what the hall would sound like at different receiver positions for various source locations. This was done by convolving binaural impulse responses from the model with speech or music recorded in an anechoic chamber, thus creating the auralizations. Listening to the auralizations was a way of subjectively checking the accuracy of the model. The primary focus of listening in this study was to assess the overall length and frequency dependence of the reverberation in the hall. The auralizations typically had more high frequency content than the actual Tabernacle, but this is consistent with observations made by Smith.[67] With the omnidirectional source, the auralizations had a longer reverberation time than what would be heard for someone talking in the Tabernacle because the omnidirectional source directly excited the ceiling and other surfaces more fully than a human talker.

When listening to the auralizations for seats 2 and 3 in Fig. 6.3, the lack of clarity was noticeable, especially when compared to the auralization for the seat with higher clarity in the balcony, mentioned in Chapter 4. However, the difference was not as drastic as the measured clarity values indicated. To compare the model auralizations to the measurements, auralizations were created for the latter by converting the measured impulse responses to *.wav files and convolving them with the same dry speech as used in CATT™. Auralizations from the measurements sounded muddier. This was likely due to different spectral content in the measured impulse responses and possibly to their limited decay range. Both the measured and modeled auralizations for seat 3 are in Appendix H. In the auralizations from both the measurements and model, the echoes were not as readily perceived as the echo criteria values portray in Fig. 4.11.

7 Historical Computer Models

Since the Tabernacle was first completed in 1867, it has been through many changes. Initially, the hall was much more reverberant than it is today. When Truman O. Angell, designer of the interior, attended the first session of General Conference in the Tabernacle, he found that "the bustle and noise made by the people destroyed the words of the speaker." President Brigham Young and Angell came to the same conclusion: everyone would be able to hear the speaker if the congregation would hold still.[68] In 1870, a balcony was built in the Tabernacle to allow more church members to attend General Conference. According to Elder George A. Smith, the "acoustic properties of the Tabernacle [were] evidently improved by the erection of the gallery," but people still needed to quit shuffling their feet in order to hear what was being said. The Deseret News said, "Speakers were heard better at this Conference than at any previous one held in the New Tabernacle."[69] The chambers on either side of the organ case and the 350-seat choir loft were also added after the original construction of the Tabernacle, in 1915[70] and between 1930 and 1960, respectively. The temporary orchestra stage shown in Fig. 1.1(a) was the most recent change to the Tabernacle, made in 2002, before the start of the current seismic renovation.

In 1922, Wayne B. Hales measured the reverberation time of the Tabernacle using various organ pipes as the source. For his study, he also investigated the echoes, distribution of sound intensity, and speech intelligibility in the hall. He found that hearing was best directly in front of the speaker and better in the balcony than under the balcony. Hales also observed that having an audience in the hall increased intelligibility, as this decreased the reverberation time.[71] In 1963, Vern O. Knudsen published research

he did with Harvey Fletcher and William Woolf on the acoustics of the Tabernacle, which used a starter pistol as the source. He found that a flutter echo could be heard from one side balcony when the source was in the other side balcony. Another observation he made was that the reverberation time in the hall changed drastically depending on the size of the audience in the hall.[72]

Another interesting change to the Tabernacle interior involved the hanging of evergreen trees from the ceiling to decorate for the Sabbath School Union Jubilee in 1875 (see Fig. 7.1). The photograph of the Tabernacle decorated with evergreen trees (courtesy of the Grow family) was recently published in an article by Walker, Holzapfel, and Lambert in BYU Studies.[73] Evergreen trees were brought in to create an inverted garden in the Tabernacle to brighten up the interior. The authors of the article mentioned that the fir trees were still hanging from the ceiling almost 10 years later, even though they were completely dried out. They speculated that the trees might have been left up so long to "muffle the echoing acoustics in the building." In order to characterize the early hall configurations and to test this theory, a computer model of the Tabernacle was created with a smaller organ case, smaller choir loft, and extended balcony to match the features of the building at the time. As options to the model, virtual fir trees were added to the ceiling and the balcony was removed for comparison.

7.1 Evergreen Tree Absorption Measurements

To determine how much the fir trees affected the acoustics in the Tabernacle, their sound absorption coefficients had to be measured, so they could be applied to the model. The trees shown the photograph were most likely white fir trees,[74,75] but the Noble fir

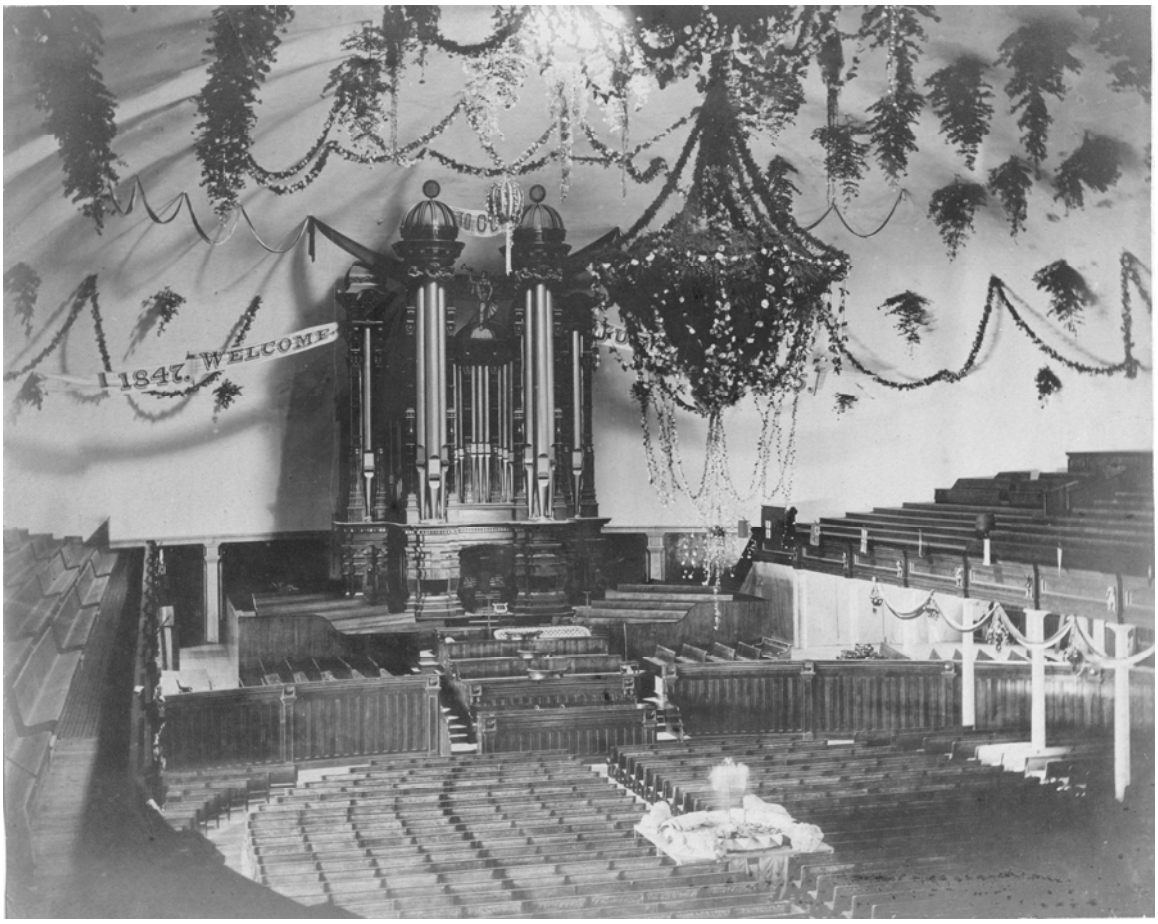

FIG. 7.1. Photograph of the interior of the Tabernacle with evergreen trees hanging from the ceiling for the Sabbath School Union Jubilee in 1875. Courtesy BYU Studies 42, p. 65 (2003).

trees were measured because of their availability. As shown in Fig. 7.2, four trees were measured in the reverberation chamber at BYU in accordance with ISO 354.[76] This standard requires that the test specimens be placed at least 1 m from any chamber boundary or diffuser, 1 m from any microphone, and 2 m from each other. To measure the absorption coefficient of the trees, the integrated impulse response method was used because it requires fewer measurements and takes less time than the interrupted noise method. With this method, ISO 354 states that the chamber can be excited with a pseudo-random test signal, so the MLS from the TEF was used to measure the impulse response of the room with and without the trees in place. To calculate the absorption

FIG. 7.2. Four Noble Fir trees and the dodecahedron loudspeaker in the reverberation chamber for sound absorption measurements during December 2004.

coefficient for each octave band of interest, the reverberation time was first calculated for each of these bands. The test specimens absorbed sound and reduced the reverberation time in the chamber. The absorption coefficient was then calculated from this reduction in reverberation time. For the integrated impulse response method, the reverberation time is measured from a decay curve that is calculated using reverse integration of the squared impulse response, as described in Chapter 4.

The octave-band impulse responses were generated by filtering the broadband impulse response with appropriate digital filters in Matlab®.[77] From the octave band reverberation times, the frequency-dependent absorption coefficient was calculated according to the following procedure. First, the equivalent sound absorption area was

calculated for the chamber with and without the test specimen in place using the following equation:

$$A_n = \frac{55.3V}{cT_n} - 4Vm_n, \tag{7.1}$$

where V is the volume of the empty chamber in cubic meters, c is the speed of sound in meters per second, T_n is the reverberation time in seconds, m_n is the air attenuation in decibels per kilometer, and the subscript n refers to the chamber configuration (n = 1 for the empty chamber and n = 2 for the chamber with the fir trees). The equivalent sound absorption area of all four fir trees was then

$$A_T = A_2 - A_1 = 55.3V\left(\frac{1}{c_2T_2} - \frac{1}{c_1T_1}\right) - 4V\left(m_2 - m_1\right). \tag{7.2}$$

An effective absorption coefficient for an individual tree was then calculated by dividing the sound absorption area for all of the trees by four, then calculating

$$\alpha_s = \frac{A_T}{S_n}, \tag{7.3}$$

where S_n in this case was the area of each face in the model that fir tree absorption coefficient was applied to. Table 7.1 shows the coefficients for each octave band from 125 Hz to 4000 Hz. All of the coefficients are less than 1 because the extrapolated $\alpha_{3.15}$ coefficient value was .99 for the 16 kHz octave band. Since the fir tree absorption coefficients were applied to ceiling faces according to where a tree was hanging in the photograph, the absorption area for one tree was divided by the area of each of these ceiling faces to calculate the absorption coefficients, as shown in Table 7.1. Since these measurements were taken in December, the humidity in the empty chamber was below the minimum required value of 30%. As a result, the measured absorption coefficients

were only approximations of the coefficients that would be measured according to the standard.

Table 7.1. Measured total absorption areas (in m^2) for the Noble Fir trees in the chamber and absorption coefficients for each size of ceiling face used for the fir trees in the CATT™ model. The subscripts on each absorption coefficient, α, indicate the area of that face in m^2.

	125 Hz	250 Hz	500 Hz	1000 Hz	2000 Hz	4000 Hz
A	4.115	3.874	3.870	3.983	4.626	3.648
$A_{per\ tree}$ (A/4)	0.087	0.098	0.139	0.293	0.771	1.599
$\alpha_{3.15}$	0.03	0.03	0.04	0.09	0.25	0.51
$\alpha_{4.86}$	0.02	0.02	0.03	0.06	0.16	0.33
$\alpha_{5.69}$	0.02	0.02	0.02	0.05	0.14	0.28
$\alpha_{6.75}$	0.01	0.01	0.02	0.04	0.11	0.24

7.2 CATT-Acoustic™ Models

To create the historical computer models of the Tabernacle in CATT™, with or without the evergreen trees, the model for the current configuration was modified. The side chambers of the organ case were deleted and the entire organ case was moved down and toward the exterior wall, since this change was noticed when comparing pictures of the current organ case and historical pictures of the organ case. This shift was determined when trying to line up the extended audience area with the rostrum in the model. The other major modification was to extend the balcony and main floor seating areas toward the organ case, as shown in the picture of the hall in Fig. 7.1. The absorption coefficients for the seating areas were also changed to occupied coefficients, to compare the results of the historical models to historical comments made about the acoustics of the Tabernacle during general conference. Figure 7.3 shows the inside of the computer model from approximately the same angle as the picture in Fig. 7.1, with the source at the pulpit. The fir tree absorption coefficients were applied to some faces in the ceiling at the front of the hall, according to where the trees were shown hanging from the

ceiling in Fig. 7.1. The tree coefficients were only applied to ceiling faces in the front of the hall under the assumption that the trees hanging did not extend beyond the limits of the photograph toward the back of the hall. It is possible that the trees were hanging from the ceiling farther back in the hall, but there was no historical evidence available to support this idea. The fir tree absorption coefficients were applied to the faces shown in green in Fig. 7.3, where the rest of the faces on the ceiling still have the same plaster absorption coefficient used in the model of the hall as it stood in 2004.

Since the trees are made up of thin fir needles, the scattering coefficient *d* was assumed to be fairly low for the lower octave bands and increase with increasing frequency. All of the absorption and scattering coefficients used in the computer models are listed in Appendix C.

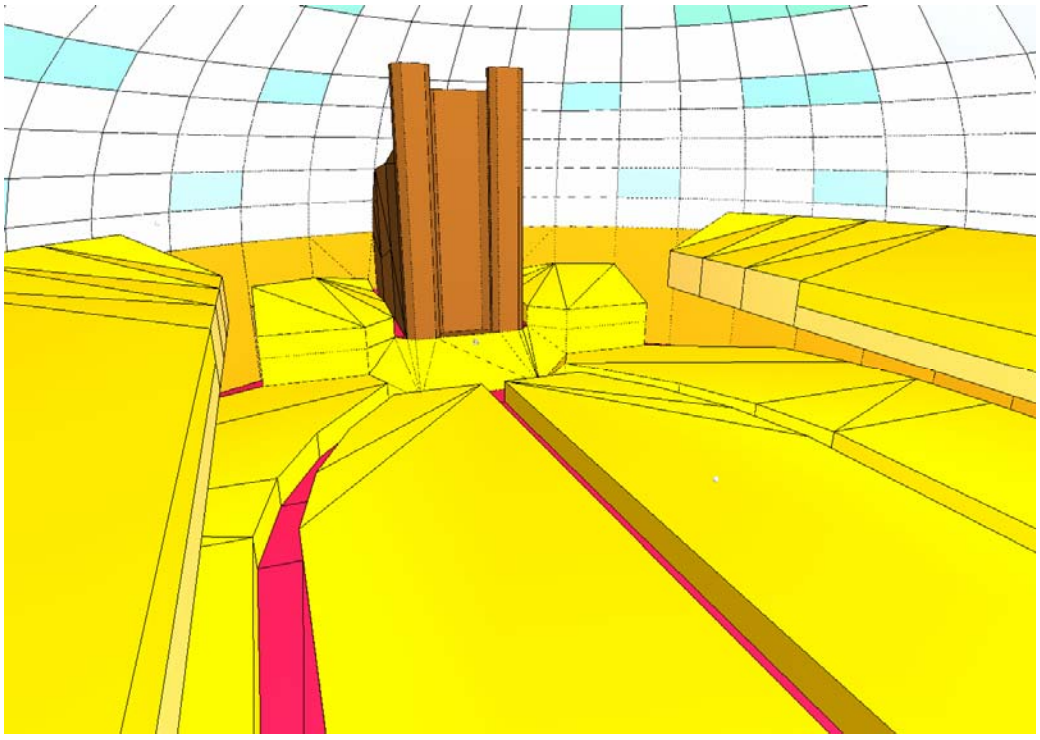

FIG. 7.3. The interior of the CATT™ computer model of the Tabernacle, including the fir tree absorption coefficients, shown by the green patches on the ceiling.

Another computer model was created to investigate the acoustical effects of removing the balcony from the Tabernacle (i.e., as in the original Tabernacle configuration). As shown in Fig. 7.4, this model was created from the fir tree model by deleting the balcony and replacing the fir tree absorption and scattering coefficients with the coefficients for the plaster, like the rest of the ceiling. The results of the model were compared to the historical model with the balcony in place.

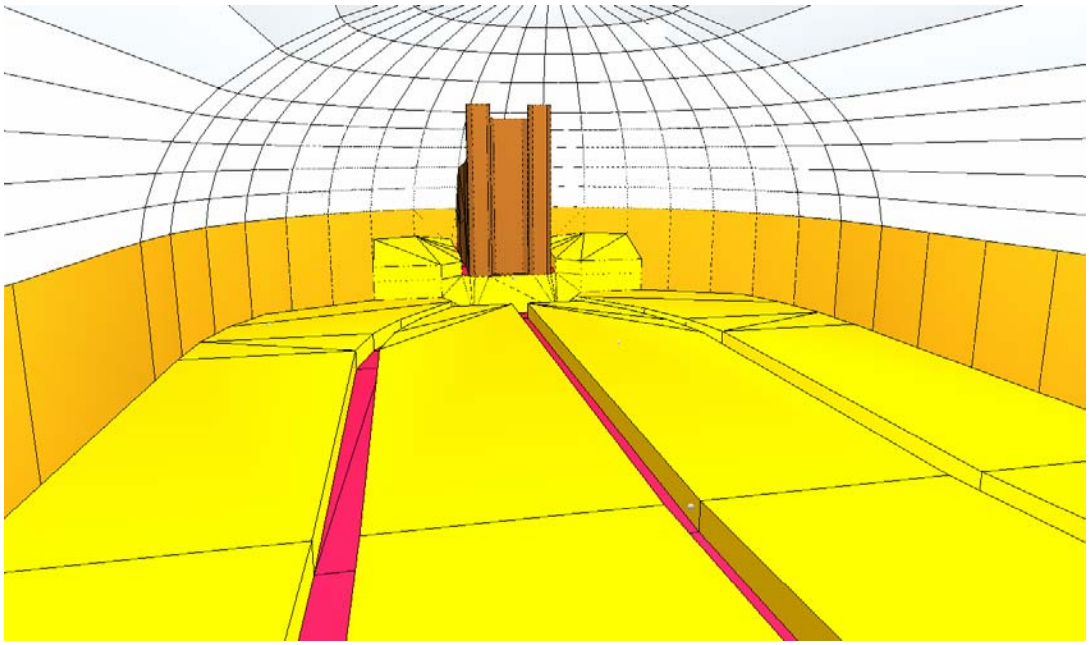

FIG. 7.4. Interior of the CATT™ computer model of the Tabernacle without the balcony.

7.3 Analysis of Historical Computer Models

7.3.1 Objective Parameters

To study the historical computer models of the Tabernacle, only a few receiver positions (8 or 11, depending on the model, since 3 positions were in the balcony) were selected instead of mapping values over the entire hall (see Fig. 7.5). Specifically, the RT, EDT, STI, clarity factors, and echo criteria were derived from the model responses

for these receiver locations that were at approximately the same locations as given in Hales' study. Tables 7.3 through 7.5 show the range and ordinary mean values for all receiver locations for these parameters using the different historical models. Since the receiver positions are no longer uniformly spaced, the statistics could be skewed.

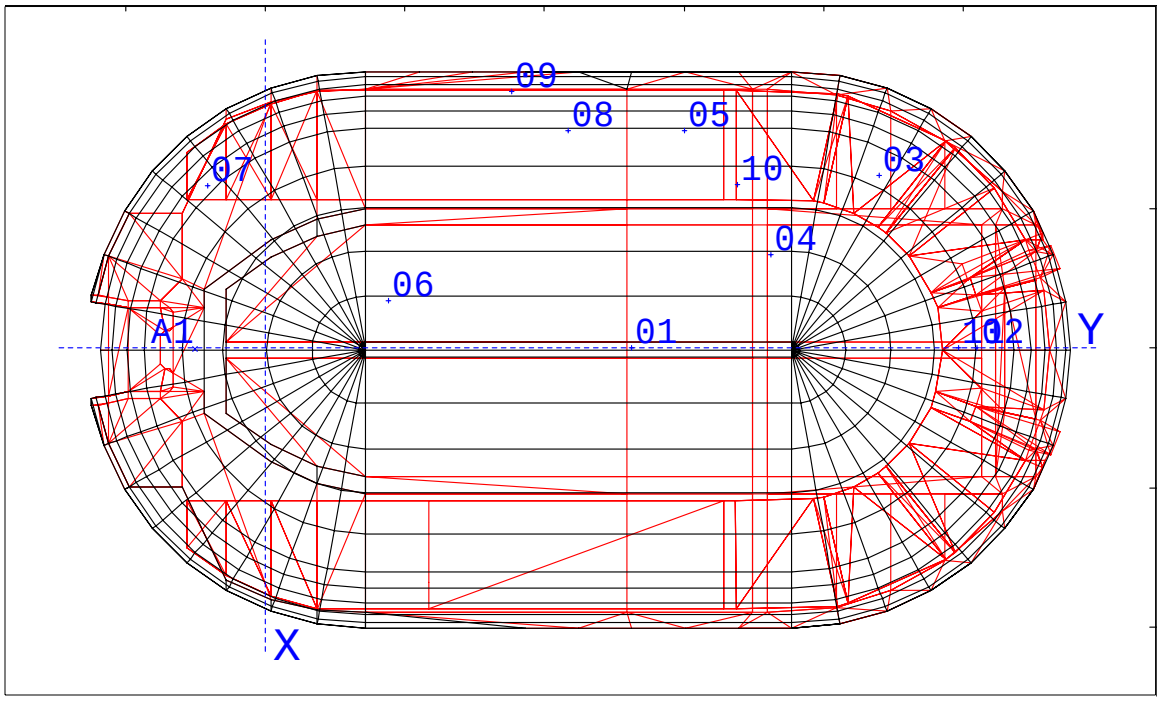

FIG. 7.5. CATT™ drawing of historical model, including the balcony. The crosses by the blue numbers show the receiver locations. Receivers 09 through 11 are in the balcony. A1 on the left indicates the source position.

Table 7.2. Table of statistics for the historical CATT™ computer model with no balcony, as shown in Fig. 7.4.

	RT	EDT	C_{80}	ECM	ECS	STI	C_{50}
Min	3.72	1.28	-5.7	0.62	0.69	0.34	-9.7
Max	4.16	4.23	5.0	1.21	1.06	0.69	3.2
$\overline{P}$	3.98	2.78	0.3	0.88	0.86	0.46	-3.3
s	0.18	0.86	3.7	0.20	0.13	0.12	4.3

The mean values of the RT and EDT in Tables 7.2 and 7.3 show that the addition of the balcony significantly decreased the average values for both of these parameters. This supports the historical comments that the addition of the balcony improved the acoustics,

making it easier to understand the speaker. Despite these results, the mean STI value decreased slightly with the addition of the balcony, but it was still within a difference limen of the value for no balcony, and easily within the same subjective range.

Table 7.3. Table of statistics for the historical CATT™ computer model of the Tabernacle with the balcony in place and no fir trees hanging from the ceiling.

	RT	EDT	C_{80}	ECM	ECS	STI	C_{50}
Min	1.91	0.97	-11.7	0.64	0.72	0.33	-13.1
Max	3.37	2.45	6.2	1.41	1.31	0.73	4.8
$\overline{P}$	2.86	1.74	1.0	0.89	0.91	0.43	-2.1
s	0.45	0.38	5.0	0.28	0.20	0.12	5.2

Table 7.4. Table of statistics for the historical CATT™ computer model of the Tabernacle with the balcony in place and fir trees hanging from the ceiling as shown in Fig. 7.1

	RT	EDT	C_{80}	ECM	ECS	STI	C_{50}
Min	1.97	0.98	-12.2	0.61	0.68	0.40	-13.7
Max	3.47	2.44	6.5	1.50	1.34	0.81	4.7
$\overline{P}$	2.93	1.71	1.0	0.85	0.86	0.54	-2.1
s	0.48	0.40	5.2	0.30	0.22	0.11	5.2

The mean values in Tables 7.3 and 7.4 show the effects of the fir trees hanging from the ceiling. According to the STI, there was a slight increase in speech intelligibility in the hall with the addition of the fir trees. The increase in the low frequency reverberation with the addition of the trees shows that the low frequency absorption coefficients for the trees should have been increased to model the plaster ceiling above them, which acts as a diaphragmatic absorber due to the large air space behind it. However, there does not seem to be much change in the hall according to the values of rest of the parameters. Almost all of the changes in the mean parameter values are less than a difference limen, so the change would be inaudible.

When compared with mean values for the current hall configuration in Table 6.3, the mean values for the computer model without the balcony show the effects of adding the balcony and including audience absorption. Interestingly, the RT is about the same, but the EDT for the model without the balcony is significantly shorter. While the current model would be expected to have shorter RT because the balcony is included, the average RT value is similar to the historical model because the current model is unoccupied and the historical model is occupied. The mean clarity factor and echo criteria values also show the significance of adding audience absorption, since both the clarity factors and the echo criteria for the historical model without the balcony are closer to preferred values than the values for the current model. The mean values in Tables 6.3 and 7.3 show the effects adding audience absorption. These effects are shown in the shorter RT and EDT values in Table 7.3. This is also why the clarity factors and STI are higher in Table 7.3.

Figure 7.6 shows the unoccupied reverberation times measured at different frequencies by Hales is his study of the acoustics of the Tabernacle.[1] The reverberation time values are the results of averaging 10 different measurements which he took at different frequencies by playing different organ pipes and measuring the time it took for the note to become inaudible. Compared to the measured results shown in Fig. D.1, Hales' results are noticeably longer for the lower octave bands, but similar for the 4000 Hz band. Knudsen and Fletcher measured an unoccupied reverberation time of about 4 seconds at 1000 Hz, which is lower than Hales' result, but higher than the current results.[3] The shorter reverberation time measured by Knudsen and Fletcher was most likely due to the increased absorption in the Tabernacle provided by the expansion of the choir loft between the times of Hales' and Knudsen's and Fletcher's measurements.

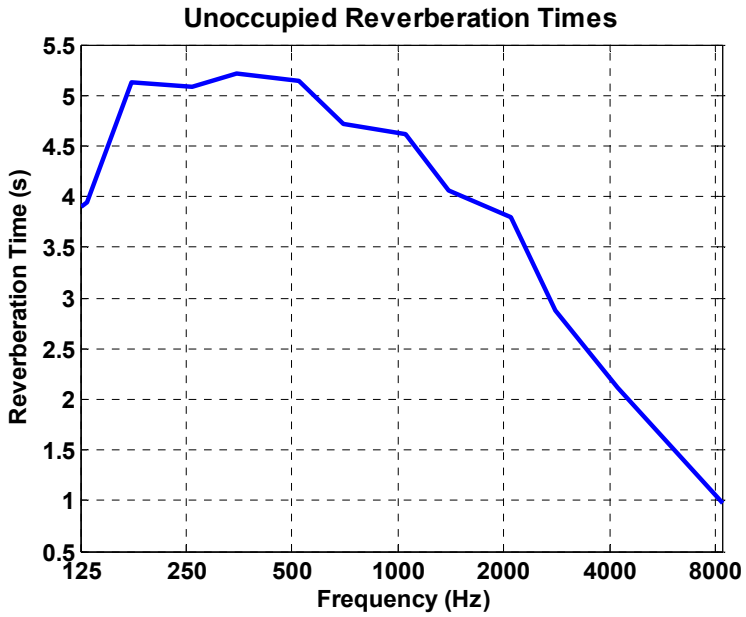

FIG. 7.6. Unoccupied reverberation times measured by Wayne B. Hales (Compare to Fig. D.1).

7.3.2 Auralizations

To hear possible differences between the historical models, auralizations were created for a few different seats. First, the model without the balcony was compared to the model with the balcony and no trees, for seats 1 and 7 in Fig. 7.5. For seat 1, the model with the balcony seemed only slightly less reverberant than the model without the balcony (see Appendix H). However, for seat 7, which was closer to the rostrum, there was less reverberance and a more noticeable improvement in the acoustics with the addition of the balcony. Without the balcony, there was a very distinct and distracting echo at this seat that was not present in the auralization from the model with the balcony. This correlates with the historical comments, since Elder George A. Smith would probably have been listening from a rostrum position closer to seat 7 than seat 1. The

most noticeable differences were heard for seats under the balcony (i.e., seats 2, 3, 5, and 8).

To find out how the trees affected the acoustics of the Tabernacle, auralizations from the model without the trees were compared to auralizations from the model with the fir tree absorption coefficients on parts of the ceiling. For seats 1 and 7 (Fig. 7.5), the auralizations for the model with the trees were more intelligible but still about as reverberant as the auralizations for the model without the trees. An auralization for seat 1 is in Appendix H. The beginning of the auralization sounded drier, but then the reverberation of the hall seemed to come back. There was only a slight difference between the auralizations from the different models for seat 11 in the balcony. Therefore, it seems likely that the trees hanging from the ceiling helped the acoustics of the Tabernacle and increased intelligibility to an extent, but it is still debatable whether they were effective almost ten years later, when they were dried out.

8 Conclusions

The acoustics of the Tabernacle have been characterized by measuring many impulse responses of the hall with multiple source positions and a high spatial density of receiver positions. These impulse responses were used to produce several architectural acoustics parameters that were mapped over drawings of the seating areas. Notably, it was shown that the limits set by ISO 3382 for calculating the reverberation time do not always accurately capture the reverberant tail of the impulse response. This is especially true for impulse responses with strong early reflections and limited decay ranges. The maps showed the spatial variation of the parameters throughout the hall, which was further quantified using ordinary and area-weighted statistics. An algorithm was developed to determine the minimum number of receiver positions required to characterize the acoustics of the Tabernacle.

The statistical results showed that the area-weighted mean and standard deviation did not differ greatly from the ordinary mean and standard deviation, since the receiver locations were spaced fairly evenly throughout the hall. While the required number of receiver positions varied for each parameter, the convergence results suggested that at least 123 receiver positions were needed to characterize the Tabernacle for *all* parameters investigated in this study. Accordingly, measurement of only a few seats in the Tabernacle would fail to account for the spatial variation in the sound field as quantified by the various parameters. Depending on which few seats were measured, the hall could be shown to behave much better or worse than it really does. This is why it is inappropriate to compare different halls using architectural acoustics parameters

measured at only a few seats. This concept was specifically demonstrated by comparing the Tabernacle to the Boston Symphony Hall.

An EASE® computer model of the Tabernacle was helpful for studying the focusing effects of the ceiling through ray-tracing. It was especially helpful as a means of increasing understanding of spatial variation of clarity in the hall. Ray-tracing for the areas of exceptionally high and low clarity values showed that the ceiling was the source of strong clusters of reflections that increased clarity at some positions and decreased it at others. The differences in clarity could also be heard in auralizations from a CATT-Acoustic™ model. The model was used to show that parameter values and auralizations generally agreed with historical comments about the improvement of the acoustics of the Tabernacle with the addition of the balcony. Another model was used to simulate the presence of fir trees hung for the ceiling. Auralizations and parameter values indicated that the fir trees increased intelligibility in the Tabernacle to some degree.

The broad implications of this study are limited by the fact that the results are specific to the Tabernacle, which has a very unique geometry. Many architectural acoustics parameters have been developed for concert hall acoustics and some of the measured values could be thrown off by the fact that the focusing effects of the ceiling produced clusters of reflections that were stronger than the direct sound. The spatial variation of many parameters was probably an extreme case because of the concave ceiling. Fewer than 123 receiver positions would likely be acceptable to characterize other halls. However, this statement cannot be made with certainty because comparative high spatial density data is not currently available for other halls. Another limitation is

that the measurements were made in the Tabernacle when it was unoccupied. An audience would have changed the absorption in the room dramatically.

The parameter values for the various seating areas in the Tabernacle will be useful to the Church of Jesus Christ of Latter-day Saints as a baseline for comparison with similar values after its seismic renovation is completed. This will allow a comprehensive evaluation of any acoustical changes in the Tabernacle. The computer models could be used by the Church to test new materials in the Tabernacle during the course of renovation or for understanding other historical comments about the acoustics. Microphone placement for broadcasts and recording, and speaker placement for sound reinforcement systems could also be tested in the current CATT™ model. Since the spatial variation of the parameter values is so large in the Tabernacle, the parameter maps could be used as guidelines for listening to different acoustic conditions, such as higher or lower clarity.

In a general sense, the various parameter maps are useful for showing correlations and relationships between different architectural acoustics parameters. Spatial variation shown by these maps and the corresponding statistics actually indicate the need for a new parameter to characterize spatial uniformity of sound fields in halls. One step in this direction would be to apply the convergence algorithm to other halls to establish how many receiver locations are necessary to adequately characterize their acoustics. By properly implementing the findings, accurate comparisons of halls could be made. Specifically, to add value to the idea of convergence of the standard deviation of parameters, high-density measurements of a few shoebox-shaped halls could be conducted to establish a preferred maximum standard deviation value of a hall.

To further quantify the spatial variation of the sound fields in halls, additional steps should be taken. A new spatial variation parameter would complement other parameters by quantifying their uniformities throughout the halls. If there is a small amount of variation in the sound field, then an average of the parameters for only a few seats would be sufficient for comparing different halls. More research is required to further establish this parameter. One possibility would be taking standard deviations of various orthogonal parameters then combining these values in a weighted average to obtain a composite index for the hall. The average would need to be properly weighted because all of the parameters are not on the same scale. This weighting could be related to the difference limen for each parameter to weight variations in each parameter equitably. It would be affected by several hall characteristics, including the shape of the hall, the amount of diffusion in the hall, and how seating areas are arranged in relation to other surfaces. Another area of research to be studied in more detail is the convergence of the architectural acoustics parameters for other halls. As mentioned previously, the Tabernacle is likely an extreme case for spatial variation, so in order to get a better idea of the minimum number of receiver positions needed to characterize typical halls, it would be helpful to perform high-density measurements in more commonly shaped rooms. Measurements in shoebox-shaped halls would provide valuable insights and quite possibly show that fewer than 123 receiver locations are typically required.

References

[1] W. B. Hales, *Graduate Thesis on the Acoustics of the Salt Lake Tabernacle*, M.S. Thesis, University of Utah, 1922, pp. 20-21.

[2] W. B. Hales, "Acoustics of the Salt Lake Tabernacle," J. Acoust. Soc. Am. **2**, 280-292 (1930).

[3] V. O. Knudsen, "Architectural Acoustics," Sci. Am. **209**, 78-92 (1963).

[4] D. Romboy, "Tabernacle to Close for Renovation," Deseret News, B01, September 18, 2004.

[5] "Tabernacle to Close for Renovation," LDS Church News, p. 4, October 16, 2004.

[6] W. C. Sabine, *Collected Papers on Acoustics*. (Dover, New York, 1964), Chap. 1, p. 3.

[7] M. R. Schroeder, "New Method of Measuring Reverberation Time," J. Acoust. Soc. Am. **37**, 409-412 (1965).

[8] W. Ahnert and H.-P. Tennhardt, "Acoustics for Auditoriums and Concert Halls," in *Handbook for Sound Engineers,* 2nd ed. edited by G. M. Ballou (Focal Press, Woburn, MA, 2002), Chap. 6, pp. 111-126.

[9] J.S. Bradley and R. E. Halliwell, "Making Auditorium Acoustics More Quantitative," Sound and Vib. **23**, 16-23 (1989).

[10] L. L. Beranek, *Concert Halls and Opera Houses: Music, Acoustics and Architecture.* 2nd ed. (Springer-Verlag, New York, 2004).

[11] P. S. Kovitz and F. M. Becker, "Time Delay Spectrometry and Maximum-Length Sequence Measurements: A Comparison in Practical Applications," AES 95th Convention, 2003, Preprint 3702, pp. 1-24.

[12] S. Muller and P. Massarani, "Transfer-Function Measurement with Sweeps," J. Audio Eng. Soc., **49**, 443-471 (2001).

[13] L.L. Beranek, *Concert Halls and Opera Houses: Music, Acoustics and Architecture*. 2nd ed. (Springer-Verlag, New York, 2004), App. 1, p. 577.

[14] J. S. Bradley, "A Comparison of Three Classical Concert Halls," J. Acoust. Soc. Am. **89**, 1176-1192 (1991).

[15] X. Pelorson, J-P. Vian, and J-D Polack, "On the Variability of Room Acoustical Parameters: Reproducibility and Statistical Validity," Appl. Acoust. **37**, 175-198 (1992).

[16] H. Kuttruff, *Room Acoustics*, 4th ed. (Spon Press, New York, 2000), Chap. 9, p. 306.

[17] M. Kleiner, B. Dalenback and P. Svensson, "Auralization – An Overview," J. Audio Eng. Soc. **41**, 861-874 (1993).

[18] B. Dalenback, M. Kleiner and P. Svensson, "Audibility of Changes in Geometric Shape, Source Directivity, and Absorptive Treatment – Experiments in Auralization," J. Audio Eng. Soc. **41**, 905-913 (1993).

[19] H. Kuttruff, "Auralization of Impulse Response Modeled on the Basis of Ray-Tracing Results," J. Audio Eng. Soc. **41**, 876-879 (1993).

[20] *Sound Lab MLS Maximum Length Sequence Software User's Manual*, (Crown International, Elkhart, IN, 1994) pp. B-1–B-21.

[21] M. R. Schroeder, "Integrated-impulse Method Measuring Sound Decay Without Using Impulses," J. Acoust. Soc. Am. **66**, 497-500 (1979).

[22] L. L. Beranek, "Balanced Noise-criterion (NCB) Curves," J. Acoust. Soc. Am. **86**, 650-664 (1989).

[23] L. L. Beranek, *Concert Halls and Opera Houses: Music, Acoustics and Architecture.* 2nd ed. (Springer-Verlag, New York, 2004), Chap. 4, p. 534.

[24] ISO 3382:1997(E). "Acoustics – Measurement of the Reverberation Time of Rooms with Reference to other Acoustical Parameters." (International Organization for Standardization, Geneva, Switzerland, 1997).

[25] L. L. Beranek, *Concert Halls and Opera Houses: Music, Acoustics and Architecture.* 2nd ed. (Springer-Verlag, New York, 2004), Chap. 2, p. 20-23.

[26] W. Ahnert and H.-P. Tennhardt, "Acoustics for Auditoriums and Concert Halls," in *Handbook for Sound Engineers,* edited by G. M. Ballou (Focal Press, Woburn, MA, 2002), Chap. 6, pp. 123-124.

[27] L. L. Beranek, *Concert Halls and Opera Houses: Music, Acoustics and Architecture.* 2nd ed. (Springer-Verlag, New York, 2004), Chap. 4, pp. 536, 538-539.

[28] W. Ahnert and H.-P. Tennhardt, "Acoustics for Auditoriums and Concert Halls," in *Handbook for Sound Engineers,* 2nd ed. edited by G. M. Ballou (Focal Press, Woburn, MA, 2002), Chap. 6, p. 125.

[29] L. L. Beranek, *Concert Halls and Opera Houses: Music, Acoustics and Architecture.* 2nd ed. (Springer-Verlag, New York, 2004), Chap. 4, pp. 536-537.

[30] T. Houtgast and H. J. M. Steeneken, "A Review of the MTF Concept in Room Acoustics and its use for Estimating Speech Intelligibility in Auditoria," J. Acoust. Soc. Am. **77**, 1069-1077 (1985).

[31] W. Ahnert and H.-P. Tennhardt, "Acoustics for Auditoriums and Concert Halls," in *Handbook for Sound Engineers,* 2nd ed. edited by G. M. Ballou (Focal Press, Woburn, MA, 2002), Chap. 6, pp. 118-119.

[32] L. Dietsch, and W. Kraak, "Ein Objectives Kriterium zur Erfassung von Echostorungen bei Musik- und Sprachdarbietungen,"[An Objective Criterion for Measuring Echo Disturbances during Presentation of Music and Speech], Acustica **60**, 205-216 (1986).

[33] H. Kuttruff, *Room Acoustics*, 4th ed. (Spon Press, New York, 2000), Chap. 4, pp. 205-207.

[34] L. L. Beranek, *Concert Halls and Opera Houses: Music, Acoustics and Architecture.* 2nd ed. (Springer-Verlag, New York, 2004), App. 3, pp. 615-616.

[35] A.V. Oppenheim and R. W. Schafer, *Discrete-Time Signal Processing.* (Prentice-Hall, Inc., Englewood Cliffs, NJ, 1989), Chaps. 2, 3, pp. 10, 80.

[36] Salas, Hille. *Calculus: One and Several Variables*, 8th ed. edited by G. J. Etgen (John Wiley & Sons, Inc., New York, 1999), Chap. 5, pp. 264-265.

[37] A.V. Oppenheim and R. W. Schafer, *Discrete-Time Signal Processing.* (Prentice-Hall, Inc., Englewood Cliffs, NJ, 1975), Chap. 1, p. 29.

[38] L. L. Beranek, *Concert Halls and Opera Houses: Music, Acoustics and Architecture.* 2nd ed. (Springer-Verlag, New York, 2004), App. 3, p. 615.

[39] M. R. Schroeder, "New Method of Measuring Reverberation Time," J. Acoust. Soc. Am. **37**, 409-412 (1965).

[40] L. L. Beranek, *Concert Halls and Opera Houses: Music, Acoustics and Architecture.* 2nd ed. (Springer-Verlag, New York, 2004), Chap. 4, p. 536.

[41] L. L. Beranek, *Concert Halls and Opera Houses: Music, Acoustics and Architecture.* 2nd ed. (Springer-Verlag, New York, 2004), Chap. 2, p. 23.

[42] L. L. Beranek, *Concert Halls and Opera Houses: Music, Acoustics and Architecture.* 2nd ed. (Springer-Verlag, New York, 2004), App. 3, p. 617.

[43] F. Becker, "A Do-It Yourselfer's Guide to Computing the Speech Transmission Index," Syn-Aud-Con, Tech Topic **26,** (1998).

[44] T. Houtgast and H. J. M. Steeneken, "A Review of the MTF Concept in Room Acoustics and its use for Estimating Speech Intelligibility in Auditoria," J. Acoust. Soc. Am. 77, 1069-1077 (1985).

[45] M. R. Schroeder, "Modulation Transfer Functions: Definition and Measurement," Acustica **49**, 179-182 (1981).

[46] T. Houtgast and H. J. M. Steeneken, "The Modulation Transfer Function in Room Acoustics," B & K Tech. Rev. **3,** 11 (1985).

[47] P. Mapp, "Designing for Speech Intelligibilty," in *Handbook for Sound Engineers,* edited by G. M. Ballou (Focal Press, Woburn, MA, 2002), Chap. 36, p. 1271.

[48] X. Pelorson, J-P. Vian, and J-D Polack, "On the Variability of Room Acoustical Parameters: Reproducibility and Statistical Validity," Appl. Acoust. **37**, 175-198 (1992).

[49] H. Smith, *Geometric Acoustic Modeling of the LDS Conference Center*, M.S. Thesis, Brigham Young University, 2004, p. 62.

[50] L. L. Beranek, *Concert Halls and Opera Houses: Music, Acoustics and Architecture.* 2nd ed. (Springer-Verlag, New York, 2004), App. 2, p. 586.

[51] L. L. Beranek, *Concert Halls and Opera Houses: Music, Acoustics and Architecture.* 2nd ed. (Springer-Verlag, New York, 2004), App. 3, p. 626.

[52] J. Holloman, "Salt Lake Tabernacle Acoustical Mapping Project, Listener Evaluation, February 2004", unpublished.

[53] J. Holloman, personal communication, September 15, 2005.

[54] H. Kuttruff, *Room Acoustics*. (Spon Press, New York, 2000), Chap. 9, pp. 300-301.

[55] T. J. Cox and P. D'Antonio, *Acoustic Absorbers and Diffusers: Theory, design and application*. (Spon Press, New York, 2004) p. 87.

[56] H. Kuttruff, *Room Acoustics*. (Spon Press, New York, 2000), Chap. 9, pp.303-306.

[57] *CATT-Acoustic v8: Room Acoustics Prediction and Desktop Auralization User's Manual*, (CATT, Gothenburg, Sweden, 2002) pp. 2-71–2-73.

[58] B.-I. L. Dalenback, "Room Acoustic Prediction Based on a Unified Treatment of Diffuse and Specular Reflection," J. Acoust. Soc. Am. **100**, 899-909 (1996).

[59] L. L. Beranek, *Concert Halls and Opera Houses: Music, Acoustics and Architecture.* 2nd ed. (Springer-Verlag, New York, 2004), App. 3, pp. 639-640.

[60] C. Davis and D. Davis, *Sound System Engineering*. (Elsevier, Burlington, MA, 1997), Chap. 7, p. 158-160.

[61] H. Smith, *Geometric Acoustic Modeling of the LDS Conference Center*, M.S. Thesis, Brigham Young University, 2004, pp. 167-169.

[62] A. Lawrence, *Architectural Acoustics*. (Elsevier Pub. Co. Ltd.,London, 1970), App. 3, p. 201.

[63] R. E. Borg and D. G. Stork, *The Physics of Sound,* 2nd ed. (Prentice Hall, Englewood Cliffs, NJ, 1995), Chap. 8, p. 230.

[64] D. E. Hall, *Musical Acoustics*. (Brooks/Cole, Pacific Grove, CA, 2002), Chap. 15, p. 331.

[65] T. J. Cox and P. D'Antonio, *Acoustic Absorbers and Diffusers: Theory, design and application*. (Spon Press, New York, 2004), App. A, pp. 375-378.

[66] L. L. Beranek and T. Hidaka, "Sound absorption in concert halls by seats, occupied and unoccupied, and by the hall's interior surfaces," J. Acoust. Soc. Am. **104**, 3169-3177 (1998).

[67] H. Smith, *Geometric Acoustic Modeling of the LDS Conference Center*, M. S. Thesis, Brigham Young University, 2004. p. 124.

[68] S. L. Grow, *A Historical Study of the Construction of the Salt Lake Tabernacle*, M.S. Thesis, Brigham Young University, 1947. (This thesis also includes four different accounts for how the shape of the Tabernacle might have been determined, if the reader is interested.)

[69] P. H. Peterson, "Accommodating the Saints at General Conference," BYU Studies **41**, 4-39 (2002).

[70] S. L. Grow, *A Tabernacle in the Desert.* (Deseret Book Company, Salt Lake City, 1958), Chap. 4, p. 78.

[71] W. B. Hales, "Acoustics of the Salt Lake Tabernacle," J. Acoust. Soc. Am. **2**, 280-292 (1930).

[72] V. O. Knudsen, "Architectural Acoustics," Sci. Am. **209**, 78-92 (1963).

[73] R. W. Walker, R. N. Holzapfel, and J. S. Lambert, "Salt Lake Tabernacle Interior Photograph: Sabbath School Jubilee, July 1875," BYU Studies **42**, 65-74 (2003).

[74] P. Allen, personal communication, December 15, 2004.

[75] B. Gardner, personal communication, December 17, 2004.

[76] ISO 354 (2003). "Acoustics – Measurement of Sound Absorption in a Reverberation Room." (International Organization for Standardization, Geneva, Switzerland, 2003).

[77] Christopher Couvreur, Matlab® code "octdsgn.m" (Faculte Polytechnique de Mons (Belgium), 1997). This code was downloaded from the file exchange at http://www.mathworks.com and was still available as of November 21, 2005.

Appendix A – Matlab® Code

NCB.m

```
%Program for plotting NCB curves and calculating the
%NCB values for measurements taken by the LD 824 sound-level meters.
%Adapted from code by Gordon Dix, dataplot_NCB.m

clear;close all;clc;
warning('off', 'all')
k=1;
s=what;
numfiles=length(s.mat);
fc=[16 31.5 63 125 250 500 1000 2000 4000 8000]; %octave band center frequencies
headerSPL=31;
headerthird=121;

for k=1:numfiles-3 % this for loop processes each file separately
   g=char(s.mat(k)); % get the file name and convert
   %it into a character string
   p=1;
   while ((g(p))~='.') % search through the string
      %and figure out where the .mat starts
      p=p+1;
   end

   g=g(1:p-3);% get rid of the .mat extension and last two letters (source-mic desc)
   [SPL_A,SPL_C,SPL_flat]=textread([g '.slmdl'],'%*s %f %f %f',1,'delimiter',',','headerlines',headerSPL);
   [t1 t2 t3 t4 t5 t6 t7 t8 t9 t10 t11 t12 t13 t14 t15 t16 t17...
      t18 t19 t20 t21 t22 t23 t24 t25 t26 t27 t28 t29 t30 t31 t32 t33]...
      =textread([g '.slmdl'],'%*s %f %f %f %f %f %f %f %f %f %f %f %f %f %f %f %f %f %f %f %f %f %f %f
%f %f %f %f %f %f %f %f %f %f %f %f',1,'delimiter',',','headerlines',headerthird);
   third=[t1 t2 t3 t4 t5 t6 t7 t8 t9 t10 t11 t12 t13 t14 t15 t16 t17...
      t18 t19 t20 t21 t22 t23 t24 t25 t26 t27 t28 t29 t30 t31 t32 t33];

   %NCB values (dB) from Beranek, JASA (1989), each column is a row from Table IV.
   %NCB-10
   NCB(:,1)=[78;59;43;30;21;15;12;8;5;2];
   %NCB-15
   NCB(:,2)=[79;61;45;34;26;20;17;13;10;7];
   %NCB-20
   NCB(:,3)=[80;63;49;38;30;25;22;18;15;12];
   %NCB-25
   NCB(:,4)=[81;66;52;42;35;30;27;23;20;17];
   %NCB-30
   NCB(:,5)=[82;69;55;46;40;35;32;28;25;22];
   %NCB-35
   NCB(:,6)=[84;71;58;50;44;40;37;33;30;27];
   %NCB-40
   NCB(:,7)=[85;74;62;54;49;45;42;38;35;32];
   %NCB-45
   NCB(:,8)=[87;76;65;58;53;50;47;43;40;37];
   %NCB-50
   NCB(:,9)=[89;79;69;62;58;55;52;49;46;43];
```

```
    %NCB-55
    NCB(:,10)=[92;82;72;67;63;60;57;54;51;48];
    %NCB-60
    NCB(:,11)=[94;85;76;71;67;64;62;59;56;53];
    %NCB-65
    NCB(:,12)=[97;88;79;75;72;69;66;64;61;58];

    %Sum third-octave data into octave data for comparing with NCB curves
    for n=1:length(fc)
       octdata(n)=10*log10(10^(0.1*third(n*3-2))+10^(0.1*third(n*3-1))+10^(0.1*third(n*3)));
       diffdata(n,:)=NCB(n,:)-octdata(n);
       for nn=1:length(NCB)
          if diffdata(n,nn) > 0
             nindex(nn)=nn;
          else
             nindex(nn)=13;
          end
       end
       [topn(n),nindex2]=min(nindex); %function of fc
       diffs(n)=diffdata(nindex2);
    end

    [highn,findex]=max(topn);
    dstore=10*ones(size(topn));
    for cc=1:length(topn)
       if topn(cc)==max(topn)
          dstore(cc)=diffdata(cc,topn(cc));
       end
    end
    [mindif,aindex]=min(dstore);
    ndif=NCB(aindex,max(topn))-octdata(aindex);
    nrange=NCB(aindex,max(topn))-NCB(aindex,max(topn)-1);
    nratio=(nrange-ndif)/nrange;
    ncvalue=round(5*nratio+max(topn)*5);
    semilogx(fc,NCB,'k',fc,octdata,'b:')
    set(gca,'XTick',fc,'XTickLabel',fc)
    xlim([fc(1) fc(end)])
    title('Balanced Noise Criterion (NCB)')
    for m=1:length(NCB)
       text(4250,NCB(10,m)+5,num2str((m+1)*5))
    end
    text(2500,90,['NC-' num2str(ncvalue)])
end
```

OMNI_final.m

```
%Architectural acoustics parameter code
%Written for Sarah Rollins' thesis on the Salt Lake Tabernacle
%--October 17, 2005--
%This loads the impulse response files and finds the indices of the direct
%sound and the beginning of noise, then calls functions to calculate the
%architectural acoustics parameters.
%This function must be in the same directory as the impulse response files.

clear;close all;clc;
warning('off', 'all')
s=what;
numfiles=length(s.mat);
fc=[125 250 500 1000 2000 4000 8000]; %octave-band center frequencies
numoct=length(fc); %number of octave band filters

for k=1:numfiles % this for loop processes each file separately

   g=char(s.mat(k)); % get the file name and convert
   %it into a character string
   p=1;
   while ((g(p))~='.') % search through the string
      %and figure out where the .mat starts
      p=p+1;
   end
   if g(1)=='z'
      break
   end
   g=g(1:p-1);% get rid of the .mat extension
   IRfile=load(g); % load the file

   S_Rate=IRfile.samplingfrequency;
   IRdata=IRfile.data; %impulse response (IR)
   tms=(1:length(IRdata))/S_Rate*1000; %time in ms
   N=length(IRdata);

   for c=1:numoct+1

      if c==numoct+1
         IRdata_filt(:,numoct+1)=IRdata;
      else
         [b,a]=octdsgn(fc(c),S_Rate,3);
         IRdata_filt(:,c)=filter(b,a,IRdata);
      end
      lsqIR_filt=10*log10(IRdata_filt(:,c).^2/(2e-5)); %log-squared impulse response

      %Find the arrival of the direct sound, to pass the index to the
      %parameter functions
      %Search the first fifth of the impulse response
      ms200=200*S_Rate/1000;
      dmean=max(lsqIR_filt)-20; % direct sound must be at least 20 dB above the noise at
                                % the beginning of the IR
      nn=find(lsqIR_filt >= dmean);
```

```
    direct(c)=nn(1);
    %Find noise level, to know when to truncate the impulse response

    %Set the noise level as the maximum value for the last quarter of the loq-squared IR
    lastqu=round(.75*length(lsqIR_filt));
    nlev=max(lsqIR_filt(lastqu:end));
    nline=nlev*ones(size(tms));

    %Skim across the envelope of the impulse response-finding the max value
    %in dm step size windows
    start500n=find(tms==500);
    dm=S_Rate/1000*50; %50 ms step size, looking for max
    mn=1;
    for m=start500n:dm:lastqu-1
       decaymax(mn)=max(lsqIR_filt(m:m+dm-1));
       mn=mn+1;
    end

    %Find when the moving average of the log-squared IR drops below the max
    %of the noise
    dmm=1; %1 sample step size, looking for where IR drops belows noise level
    for mm=1:length(decaymax)/dmm
       decaymean=mean(decaymax((mm-1)*dmm+1:mm*dmm));
       if decaymean < nlev
          truncptn(c)=start500n+dm*dmm*mm-dm*dmm;
          break;
       end
    end

end
%This seat had a weird dip in the response, so the truncation point was
%set manually.
if k==12
       truncptn(end)=1650*48;
end
IRdata2=IRdata_filt;

%************ Parameter Functions ******************
fprintf('k=%g\n',k)
%Schroeder Integration - T60, EDT
if mod(k,1)==0
   fprintf('Calculating RT, EDT...\n')
end
[T60iso(k,:),T60L2(k,:),T60L3(k,:),T60drL(k,:),EDT(k,:)]=schr_f (S_Rate,IRdata2,direct,truncptn,g);
%Intelligibility - STI, RASTI
if mod(k,1)==0
   fprintf('Calculating STI, RASTI...\n')
end
[STI(k),RASTI(k)]=sti_f(S_Rate,IRdata2,direct,truncptn);

%Clarity - C80, C50
if mod(k,1)==0
   fprintf('Calculating C80,C50...\n')
end
[C80(k,:),C50(k,:)]=clarity_f(S_Rate,IRdata2,direct,truncptn);
```

```
    %Echo Criterion – Dietsch
    if mod(k,1)==0
        fprintf('Calculating Dietsch Echo Criteria...\n')
    end
    [ECmu(:,k),ECsp(:,k)]=EC_Dietsch_f(S_Rate,IRdata2,direct,truncptn);

end

schr=[T60iso/1000,T60L2/1000,T60L3/1000,T60drL/1000,EDT/1000];
intel=[STI' RASTI'];
clar=[C80 C50];
echoes=[ECsp' ECmu'];
pvalues=[schr intel clar echoes]; %combine all parameter values for all seats into one matrix
dlmwrite('values.xls',pvalues,'\t')

%Receiver areas - read in from text file
areas=dlmread('areas.txt','\t');
areatot=sum(areas); %total area

%Parameter values
[numseats,numparam]=size(pvalues);

for n=1:numparam
    %Ordinary mean
    omean(n)=mean(pvalues(:,n));

    %Area-weighted mean
    amean(n)=sum((areas.*pvalues(:,n))./areatot);

    %Ordinary standard deviation
    ostd(n)=std(pvalues(:,n));

    %Area-weighted standard deviation
    Ldiff=pvalues(:,n)-amean(n);
    stdarg=areas(n).*(Ldiff.^2);
    astd(n)=sqrt((sum(stdarg))/areatot);
end

stats=[min(pvalues)' max(pvalues)' omean' amean' ostd' astd'];
dlmwrite('stats.xls',stats,'\t')
```

schr_f.m

```
function [RTiso,RT,RT2,RT3] = schr_f(S_Rate,IRdata,direct,truncptn,g)
%Code for calculating RT and EDT using Schroeder integration
%RT - ISO 3382 method (5 to 35/25 dB down), 10 to 20 dB down, 10 to 15 dB down
%and 15 to 35/25 dB down

fs=S_Rate;
[N,numoct]=size(IRdata);
T=1/fs; %sampling period
starttime=direct;
endtime=truncptn(end);

for c=1:numoct
   endtime=truncptn(c);
   dt=1/fs*1000; %delta t in ms
   tms=(1:endtime)*dt; %time in milliseconds, n/(FS/1000)
   tmsfull=(1:N)*dt;
   starttime=direct(c);
   data=IRdata(:,c);
   impdata=data.^2;
   clear schrint tendB;

   schrint(endtime:-1:1)=cumsum(impdata(endtime:-1:1));
   pschr=10*log10(schrint./max(abs(schrint)));

   last4th=round(.75*length(pschr));
   dh=1;
   %Determine an approximation for the end of the linear part of the Schroeder curve
   for h=last4th:dh:length(pschr)
      temp(h)=abs(pschr(h)-pschr(h-dh));
      if temp(h) > abs(pschr(last4th)-(pschr(last4th-dh)))%+.03
         ends=h;
         break;
      else
         ends=length(pschr);
      end
   end
   %Calculate the T60 from Schroeder curve between 5 dB down and 35 dB down
   %unless the decay range is too small, then use 5 dB down to 25 dB down
   %**REF: ISO 3382:1997(E), pp 9,14**
   dBdown5=max(pschr)-5;
   dBdown35=max(pschr)-35;
   dBdown25=max(pschr)-25;
   dBdown15=max(pschr)-15; %for Early Decay Time
   dBdown10=max(pschr)-10;
   dBdown20=max(pschr)-20;

   if pschr(ends)>dBdown35
      dBdown=dBdown25;
   else
      dBdown=dBdown35;
   end
```

```
dif5=abs(pschr-dBdown5);
dif10=abs(pschr-dBdown10);
dift5=abs(pschr-dBdown);
fivedB=find(dif5==min(dif5));
tendB=find(dif10==min(dif10));
tfivedB=find(dift5==min(dift5));

%Calculate T60 from Schroeder integration curve
%Find a and b for the least squares regression line
x=tms(fivedB:tfivedB);%(2400:4800);
y=pschr(fivedB:tfivedB);%(2400:4800);

N=length(x);%different N from index 'n' above
a=(mean(y)*sum(x.^2)-mean(x)*sum(x.*y))/(sum(x.^2)-N*mean(x)^2);
b=(sum(x.*y)-N*mean(x)*mean(y))/(sum(x.^2)-N*mean(x)^2);
regline=a+b*x;
T30(c)=(max(pschr)-60-a)/b;


%Find the 15 dB down point
x2beg=tms(tfivedB)+dt;
n=1;
diften5=10*ones(1,length(pschr));
dif20=10*ones(1,length(pschr));

diften5=abs(pschr-dBdown15);
dif20=abs(pschr-dBdown20);
tenfivedB=find(diften5==min(diften5));
twentydB=find(dif20==min(dif20));

%Try looking at the slope farther down the Schroeder curve, after the
%clusters of reflections

%---Look at 10 dB down to 15 dB down ----
xL=tms(tendB:tenfivedB);
yL=pschr(tendB:tenfivedB);

NL=length(xL);%different N from index 'n' above
aL=(mean(yL)*sum(xL.^2)-mean(xL)*sum(xL.*yL))/(sum(xL.^2)-NL*mean(xL)^2);
bL=(sum(xL.*yL)-NL*mean(xL)*mean(yL))/(sum(xL.^2)-NL*mean(xL)^2);
reglineL=aL+bL*xL;
T30_late1(c)=(max(pschr)-60-aL)/bL;

%---Look at 10 dB down to 20 dB down ----
xL2=tms(tendB:twentydB);
yL2=pschr(tendB:twentydB);

NL2=length(xL2);%different N from index 'n' above
aL2=(mean(yL2)*sum(xL2.^2)-mean(xL2)*sum(xL2.*yL2))/(sum(xL2.^2)-NL2*mean(xL2)^2);
bL2=(sum(xL2.*yL2)-NL2*mean(xL2)*mean(yL2))/(sum(xL2.^2)-NL2*mean(xL2)^2);
reglineL2=aL2+bL2*xL2;
T30_late2(c)=(max(pschr)-60-aL2)/bL2;

%---Look at 15 dB down to 25 or 35 dB down ----
xL3=tms(tenfivedB:tfivedB);
yL3=pschr(tenfivedB:tfivedB);
```

```
    NL3=length(xL3);%different N from index 'n' above
    aL3=(mean(yL3)*sum(xL3.^2)-mean(xL3)*sum(xL3.*yL3))/(sum(xL3.^2)-NL3*mean(xL3)^2);
    bL3=(sum(xL3.*yL3)-NL3*mean(xL3)*mean(yL3))/(sum(xL3.^2)-NL3*mean(xL3)^2);
    reglineL3=aL3+bL3*xL3;
    T30_late3(c)=(max(pschr)-60-aL3)/bL3;

    %********** Early Decay Time (EDT) *********************
%   Calculate EDT from 0 to -10dB on IR, on Schroeder curve
    x2=tms(1:tendB);
    y2=pschr(1:tendB);

    N2=length(x2);%different N from index 'n' above
    a2=(mean(y2)*sum(x2.^2)-mean(x2)*sum(x2.*y2))/(sum(x2.^2)-N2*mean(x2)^2);
    b2=(sum(x2.*y2)-N2*mean(x2)*mean(y2))/(sum(x2.^2)-N2*mean(x2)^2);

    regline2=a2+b2*x2;
    EDT(c)=(max(pschr)-60-a2)/b2;

end

%Plot Schroeder curve and fit to check the math
%Comment out the lines below if you do not want a plot of the impulse response and Schroeder curve for
%every file.
figure
subplot(2,2,1)
plot(tms,10*log10(impdata(1:length(tms))/T-10),'b',tms,pschr,'r',x,regline,'g--*','LineWidth',2.5)
title('RT (5 dB to 25/35 dB)', 'FontSize',14,'FontWeight','bold')
aa=gca;
set(gca,'XLimMode','manual','YLimMode','manual',...
    'FontSize',12,'LineWidth',2.5,'FontWeight','bold')
ylim([-50 0])
xlabel('\bf Time (ms)', 'FontSize',12)
ylabel('\bf Log-Squared Pressure (dB)','FontSize',12)
hold on;
text(.35*max(tms),max(pschr)-5,['RT = ' num2str(T30(end)/1000) ' s'],'FontWeight','bold','FontSize',14);

subplot(2,2,2)
plot(tms,10*log10(impdata(1:length(tms))/T-10),'b',tms,pschr,'r',xL,reglineL,'g--*','LineWidth',2.5)
title('RT (10 dB to 15 dB)', 'FontSize',14,'FontWeight','bold')
aa=gca;
set(aa,'XLimMode','manual','YLimMode','manual',...
    'FontSize',12,'LineWidth',2.5,'FontWeight','bold')
ylim([-55 0])
xlabel('\bf Time (ms)', 'FontSize',12)
ylabel('\bf Log-Squared Pressure (dB)','FontSize',12)
hold on;
text(.35*max(tms),max(pschr)-5,['RT = ' num2str(T30_late1(end)/1000) '
s'],'FontWeight','bold','FontSize',14);

subplot(2,2,3)
plot(tms,10*log10(impdata(1:length(tms))/T-10),'b',tms,pschr,'r',xL2,reglineL2,'g--*','LineWidth',2.5)
title('RT (10 dB to 20 dB)', 'FontSize',14,'FontWeight','bold')
aa=gca;
set(aa,'XLimMode','manual','YLimMode','manual',...
    'FontSize',12,'LineWidth',2.5,'FontWeight','bold')
```

```
ylim([-55 0])
xlabel('\bf Time (ms)', 'FontSize',12)
ylabel('\bf Log-Squared Pressure (dB)','FontSize',12)
hold on;
text(.35*max(tms),max(pschr)-5,['RT = ' num2str(T30_late2(end)/1000) '
s'],'FontWeight','bold','FontSize',14);

subplot(2,2,4)
plot(tms,10*log10(impdata(1:length(tms))/T-10),'b',tms,pschr,'r',xL3,reglineL3,'g--*','LineWidth',2.5)
title('RT (15 dB to 25/35 dB)', 'FontSize',14,'FontWeight','bold')
aa=gca;
set(aa,'XLimMode','manual','YLimMode','manual',...
    'FontSize',12,'LineWidth',2.5,'FontWeight','bold')
ylim([-55 0])
xlabel('\bf Time (ms)', 'FontSize',12)
ylabel('\bf Log-Squared Pressure (dB)','FontSize',12)
hold on;
text(.35*max(tms),max(pschr)-5,['RT = ' num2str(T30_late3(end)/1000) '
s'],'FontWeight','bold','FontSize',14);

end
RTiso=T30;
RT=T30_late1; %10 to 15 dB down
RT2=T30_late2; %10 to 20 dB down
RT3=T30_late3; %15 to 25/35 dB down
EDT;
```

sti_f.m

```
function [STI, RASTI]=sti_f(S_Rate,IRdata,direct,truncptn)
%Program for calculating speech intelligibility factors, STI and RASTI
%Reference: "A Do-It-Yourselfer's Guide to Computing the
%Speech Transmission Index," by Farrel Becker, Syn-Aud-Con

fs=S_Rate;
[N,numoct]=size(IRdata);
df=1/(N/fs);
f=0:df:fs-df;
dt=1/fs;
fmod=[0.63, 0.7938, 1.0001, 1.2601, 1.5876, 2.0003, 2.5202,...
      3.1752, 4.0005, 5.0403, 6.3504, 8.0010, 10.0806, 12.5];
nummod=length(fmod);%number of modulation frequencies, STI

for n=1:(numoct-1) %do not include broadband data

   %Step 1: Square the impulse response
   impdata=IRdata(:,n).^2;

   %Step 2: Integrate the squared impulse response to get the total energy
   intdata=sum(impdata);

   %Step 3: Compute the Fourier transform of the squared impulse response
   fdata1=fft(impdata);
   fdata=fdata1(1:length(impdata)/2);

   %Step 4: Normalize the envelope spectrum
   cmtf=fdata./intdata; %this is the complex modulation transfer function (CMTF)

   %Step 5: Take the magnitude of the CMTF -> MTF
   magcmtf=sqrt(real(cmtf).^2+imag(cmtf).^2);
   %save MTF for 500 Hz and 2 kHz, for RASTI calculations
   if n==3
      magcmtfr(:,1)=magcmtf;
   elseif n==5
      magcmtfr(:,2)=magcmtf;
   end

   %Step 7: Generate matrix of 98 m-values for 14 modulation frequencies
   %and 7 octave bands
   for m=1:nummod
      diffarray=abs(f-fmod(m));
      [a,freqn]=min(diffarray);
      mF(m,n)=magcmtf(freqn); %m-values, rows:modulation frequencies, columns:octave bands

      %Step 8: Convert each of the 98 m values into an "apparent signal to noise
      %ratio" (S/N) in dB
      SNapp(m,n)=10*log10(mF(m,n)/(1-mF(m,n)));

      %Step 9: Limit the Range, 30 dB
      if SNapp(m,n) > 15
         SNapp(m,n)=15;
```

```
      elseif SNapp(m,n) < -15
         SNapp(m,n)=-15;
      end
   end

end

%Steps 7-9 for RASTI
fmod5=[1 2 4 8]; %modulation frequencies for the 500 Hz octave band
nummod5=length(fmod5); %number of modulation frequencies for the 500 Hz octave band
fmod2k=[0.7 1.4 2.8 5.6 11.2]; %modulation frequencies for the 2 kHz octave band
nummod2k=length(fmod2k); %number of modulation frequencies for the 2 kHz octave band
fmodr=[fmod5 fmod2k];
nummodr=length(fmodr);

for k=1:nummodr

   diffarrayr=abs(f-fmodr(k));
   [a,freqn]=min(diffarrayr);
   if k >= 1 && k <= 4
      mFr=magcmtfr(freqn,1); %m-values, rows:modulation frequencies, columns:octave bands
      %Step 8: Convert each of the 98 m values into an "apparent signal to noise
      %ratio" (S/N) in dB
      SNappr(k,1)=10*log10(mFr/(1-mFr));
      %Step 9: Limit the Range, 30 dB
      if SNappr(k,1) > 15
         SNappr(k,1)=15;
      elseif SNappr(k,1) < -15
         SNappr(k,1)=-15;
      end
   else
      mFr=magcmtfr(freqn,2);
      SNappr(k,2)=10*log10(mFr/(1-mFr));
      %Step 9: Limit the Range, 30 dB
      if SNappr(k,2) > 15
         SNappr(k,2)=15;
      elseif SNappr(k,2) < -15
         SNappr(k,2)=-15;
      end
   end

end
%Step 10: Compute the mean (S/N) for each octave band
meanSN=mean(SNapp);%STI

meanSNr=mean(SNappr);%RASTI

%Step 11: Weight the octave mean (S/N) values
w=[0.13 0.14 0.11 0.12 0.19 0.17 0.14];
weighted=w.*meanSN;
SNfin=sum(weighted);
STI=(SNfin+15)/30;
%Step 11: Compute the unweighted mean of the 2 (S/N) values
SNfinr=mean(meanSNr);

RASTI=(SNfinr+15)/30;
```

clarity_f.m

```
function [C80,C50]=clarity_f(S_Rate,IRdata,direct,truncptn)
%program to calculate clarity factors

fs=S_Rate; %sampling frequency
[N,numoct]=size(IRdata);

%Calculate sampling period, T
T=1/fs;

data=IRdata;

start=direct;
last=truncptn-1;

for a=1:numoct
   sqimp=data(:,a).^2;
   %Find the index for 80 ms after the direct sound
   n80ms=round(start(a)+80/T/1000);
   C80(a)=10*log10(sum(sqimp(start:n80ms))./sum(sqimp(n80ms:last)));
   %Find the index for 50 ms after the direct sound
   n50ms=round(start(a)+50/T/1000);
   C50(a)=10*log10(sum(sqimp(start:n50ms))./sum(sqimp(n50ms:last)));

end
```

EC_Dietsch_f.m

```
function [ECsp, ECmu]=EC_Dietsch_f(S_Rate,IRdata,direct,truncptn)
%Program to calculate the Echo Criterion by Dietsch and Kraak
%REF: Room Acoustics, by Heinrich Kuttruff, p 205-207

if direct(4) > direct(5)
   startnMU=direct(5);
else
   startnMU=direct(4);
end
startnSP=direct(4); %start point for integration for speech, t=0
endnSP=startnSP+24000; %direct + 500 ms
endnMU=startnMU+24000; %direct + 500 ms

fs=S_Rate;
tms=(1:length(IRdata))/48;
IRdataSP=IRdata(:,4);
IRdataMU=IRdata(:,4)+IRdata(:,5);

%Dietsch Echo Criterion
dtau=1;
tau=1:dtau:(endnSP-startnSP);

%**SPEECH**
nsp=2/3;
dtausp=9; %in ms
dtaus=48*dtausp;

tsnumS=abs(IRdataSP(startnSP:endnSP)).^nsp.*(startnSP:endnSP)'./48;
tsdenS=abs(IRdataSP(startnSP:endnSP)).^nsp;
tsSP=cumsum(tsnumS)./cumsum(tsdenS);
Nsp=length(tsSP);

for m=1:48*dtausp
   EKnumS((m:dtaus:Nsp-dtaus),m)=tsSP((m:dtaus:Nsp-dtaus)+dtaus)-tsSP(m:dtaus:Nsp-dtaus);
end

%**MUSIC**
nmu=1;
dtaumu=14; %in ms
dtaum=48*dtaumu; % in samples

tsnumM=abs(IRdataMU(startnMU:endnMU)).^nmu.*(startnMU:endnMU)'./48;
tsdenM=abs(IRdataMU(startnMU:endnMU)).^nmu;
tsMU=cumsum(tsnumM)./cumsum(tsdenM);
Nmu=length(tsMU);

for m=1:48*dtaumu
   EKnumM((m:dtaum:Nmu-dtaum),m)=tsMU((m:dtaum:Nmu-dtaum)+dtaum)-tsMU(m:dtaum:Nmu-
dtaum);
end

EKs=EKnumS./dtausp;    EKm=EKnumM./dtaumu;
ECsp=max(max(EKs));   ECmu=max(max(EKm));
```

ST1.m

```
%ST1, Stage Support Factor
%Reference: Beranek, p.617
clear; close all; clc

s=what;
names=s.mat;

for n=1:length(names)
   g=char(names(n)); % get the file name and convert
   %it into a character string
   p=1;
   while ((g(p))~='.') % search through the string
      %and figure out where the .mat starts
      p=p+1;
   end

   g=g(1:p-1);% get rid of the .mat extension and 'C' or 'D'
   IRfile=load(g); % load the omni file

   S_Rate=IRfile.samplingfrequency;
   IRdata=IRfile.data;
   tms=(1:length(IRdata))/S_Rate*1000; %time in ms
   N=length(IRdata);

   lsqIR=10*log10(IRdata.^2);
   %Find the arrival of the direct sound, to pass the index to the
   %parameter functions
   %Search the first fifth of the impulse response
   firstfif=round(.2*length(lsqIR));
   dmean=mean(lsqIR(10:60));

   for dn=1:firstfif
      if lsqIR(dn) > dmean + 40
         direct=dn;
         break;
      end
   end

   figure
   plot(tms,lsqIR,'b',tms(direct),lsqIR(direct),'r*')

   ms00=direct;
   ms10=direct+10*S_Rate/1000;
   ms20=direct+20*S_Rate/1000;
   ms100=direct+100*S_Rate/1000;
   sqdata=IRdata.^2;

   num=sum(sqdata(ms20:ms100)); %integrand numerator
   den=sum(sqdata(ms00:ms10));  %integrand denominator

   ST1value(n)=10*log10(num./den);
end
dlmwrite('ST1.xls',ST1value,'\t')
```

converge.m

```
%Convergence Program - shows the convergence of various statistics for parameter values
%as the number of receiver positions increases
close all; clear;

load('zdata.mat') % numseats x numparam
[numseats,numparam]=size(pvalues);
seatselect=dlmread('seatselect.txt','\t'); % numseats x 1
areas=dlmread('areas_con.txt','\t'); %numseats x numseats
Narray=seatselect;
x=1:numseats;

%Just Noticeable Difference Limen for each parameter,
%from Heather Smith's thesis, p.62
rtjnd=.05*ones(1,8); %JND, for each octave band
edtjnd=.05*ones(1,8); %JND, for each octave band
C80jnd=.5*ones(1,8); %JND, for each octave band
C50jnd=1*ones(1,8); %JND, for each octave band
STIjnd=.03*ones(1,2); %JND, for STI, use the same for RASTI
jnd=[rtjnd edtjnd STIjnd C80jnd C50jnd];
% jnd=[rtjnd rtjnd rtjnd rtjnd edtjnd];
% jnd=rtjnd;
% jnd=[C80jnd C50jnd];

%Label for each parameter
pchar=['T10_{125 Hz} (s)    ';'T10_{250 Hz} (s)    ';'T10_{500 Hz} (s)    ';'T10_{1000 Hz} (s)   ';
'T10_{2000 Hz} (s)   ';'T10_{4000 Hz} (s)   ';'T10_{8000 Hz} (s)   ';'T10_{broadband} (s) ';...
      'EDT_{125 Hz} (s)    ';'EDT_{250 Hz} (s)    ';'EDT_{500 Hz} (s)    ';'EDT_{1000 Hz} (s)   ';
'EDT_{2000 Hz} (s)   ';'EDT_{4000 Hz} (s)   ';'EDT_{8000 Hz} (s)   ';...
      'EDT_{broadband} (s) ';'STI               ';'RASTI              ';'C80_{125 Hz} (dB)   ';'C80_{250 Hz}
(dB)   ';'C80_{500 Hz} (dB)   ';'C80_{1000 Hz} (dB)  ';'C80_{2000 Hz} (dB)  ';...
      'C80_{4000 Hz} (dB)  ';'C80_{8000 Hz} (dB)  ';'C80_{broadband} (dB)';'C50_{125 Hz} (dB)   ';
'C50_{250 Hz} (dB)   ';'C50_{500 Hz} (dB)   ';'C50_{1000 Hz} (dB)  ';'C50_{2000 Hz} (dB)  ';...
      'C50_{4000 Hz} (dB)  ';'C50_{8000 Hz} (dB)  ';'C50_{broadband} (dB)'];
plabel=cellstr(pchar);

%**Calculate ordinary and area-weighted statistics for decreasing numbers of seats ***
pp=1;
for p=[8 16 17 26 34]  %subtract 2 to exclude EC values(no JND values published)
   for n=1:numseats
      omean(n,p)=mean(pvalues(Narray(1:n),p));
      ostd(n,p)=std(pvalues(Narray(1:n),p));

      %Area-weighted mean
      areatot=sum(areas(:,numseats-n+1));
      amean(n,p)=sum((areas(1:n,numseats-n+1).*pvalues(Narray(1:n),p))./areatot);

      %Area-weighted standard deviation
      Ldiff=pvalues(Narray(1:n),p)-amean(n,p);
      stdarg=areas(1:n,numseats-n+1).*(Ldiff.^2);
      astd(n,p)=sqrt((sum(stdarg))/areatot);

   end
```

```
for m=1:numseats
   %Determine minimum number of seats required using means
   if omean(m,p) < omean(numseats,p)-jnd(p) || omean(m,p) > omean(numseats,p)+jnd(p)
      outlimo(m)=m;
   else
      outlimo(m)=2;
   end
   if amean(m,p) < amean(numseats,p)-jnd(p) || amean(m,p) > amean(numseats,p)+jnd(p)
      outlima(m)=m;
   else
      outlima(m)=2;
   end
   %Determine minimum number of seats required using standard deviations
   if ostd(m,p) < ostd(numseats,p)-jnd(p) || ostd(m,p) > ostd(numseats,p)+jnd(p)
      stdlimo(m)=m;
   else
      stdlimo(m)=2;
   end
   if astd(m,p) < astd(numseats,p)-jnd(p) || astd(m,p) > astd(numseats,p)+jnd(p)
      stdlima(m)=m;
   else
      stdlima(m)=2;
   end
end

%**Plotting the convergence for increasing numbers of seats
minseatso(p)=max(outlimo)+1;
minseatsa(p)=max(outlima)+1;
minseatsos(p)=max(stdlimo)+1;
minseatsas(p)=max(stdlima)+1;

figure
subplot(2,2,1)
minlim=ones(numseats,1)*(omean(numseats,p)-jnd(p));
maxlim=ones(numseats,1)*(omean(numseats,p)+jnd(p));
plot(x,omean(:,p),'k',x,minlim,'b--',x,maxlim,'b--',...
   minseatso(p),omean(minseatso(p),p),'ro',...
   'LineWidth',2.5,'MarkerSize',10)
title('Ordinary Mean','FontSize',14)
xlabel('Number of Seats','FontSize',12)
ylabel(plabel{p},'FontSize',12)
aa=gca;
set(aa,'XLimMode','manual','YLimMode','manual',...
      'XLim',[2,numseats],'FontSize',12,'LineWidth',2.5)

subplot(2,2,2)
minlim=ones(numseats,1)*(ostd(numseats,p)-jnd(p));
maxlim=ones(numseats,1)*(ostd(numseats,p)+jnd(p));
plot(x,ostd(:,p),'k',x,minlim,'b--',x,maxlim,'b--',...
   minseatsos(p),ostd(minseatsos(p),p),'ro',...
   'LineWidth',2.5,'MarkerSize',10)
title('Ordinary Standard Deviation','FontSize',14)
xlabel('Number of Seats','FontSize',12)
ylabel(plabel{p},'FontSize',12)
aa=gca;
set(aa,'XLimMode','manual','YLimMode','manual',...
```

```
        'XLim',[2,numseats],'FontSize',12,'LineWidth',2.5)

    subplot(2,2,3)
    minlim=ones(numseats,1)*(amean(numseats,p)-jnd(p));
    maxlim=ones(numseats,1)*(amean(numseats,p)+jnd(p));
    plot(x,amean(:,p),'k',x,minlim,'b--',x,maxlim,'b--',...
       minseatsa(p),amean(minseatsa(p),p),'ro',...
       'LineWidth',2.5,'MarkerSize',10)
    title('Area-Weighted Mean','FontSize',14)
    xlabel('Number of Seats','FontSize',12)
    ylabel(plabel{p},'FontSize',12)
    aa=gca;
    set(aa,'XLimMode','manual','YLimMode','manual',...
         'XLim',[2,numseats],'FontSize',12,'LineWidth',2.5)

    subplot(2,2,4)
    minlim=ones(numseats,1)*(astd(numseats,p)-jnd(p));
    maxlim=ones(numseats,1)*(astd(numseats,p)+jnd(p));
    plot(x,astd(:,p),'k',x,minlim,'b--',x,maxlim,'b--',...
       minseatsas(p),astd(minseatsas(p),p),'ro',...
       'LineWidth',2.5,'MarkerSize',10)
    title('Area-Weighted Standard Deviation','FontSize',14)
    xlabel('Number of Seats','FontSize',12)
    ylabel(plabel{p},'FontSize',12)
    aa=gca;
    set(aa,'XLimMode','manual','YLimMode','manual',...
         'XLim',[2,numseats],'FontSize',12,'LineWidth',2.5)
    mins(pp,:)=[minseatso(p) minseatsa(p) minseatsos(p) minseatsas(p)];
    clear outlimo outlima stdlimo stdlima
    pp=pp+1;
end
```

Appendix B – Other Data Maps

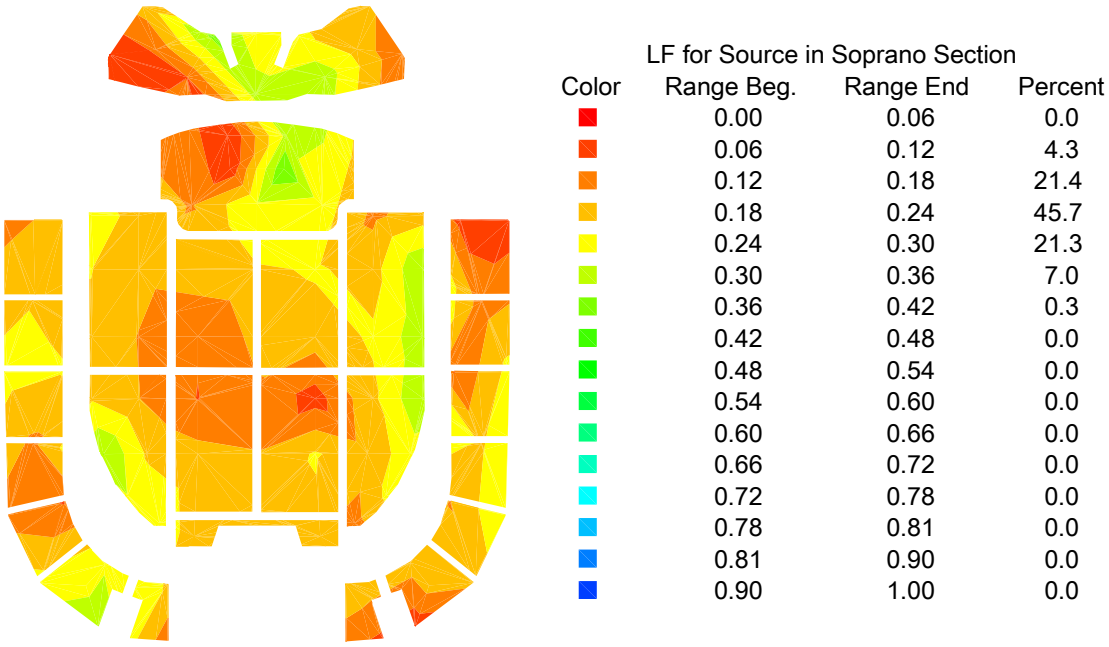

LF for Source in Soprano Section

Color	Range Beg.	Range End	Percent
	0.00	0.06	0.0
	0.06	0.12	4.3
	0.12	0.18	21.4
	0.18	0.24	45.7
	0.24	0.30	21.3
	0.30	0.36	7.0
	0.36	0.42	0.3
	0.42	0.48	0.0
	0.48	0.54	0.0
	0.54	0.60	0.0
	0.60	0.66	0.0
	0.66	0.72	0.0
	0.72	0.78	0.0
	0.78	0.81	0.0
	0.81	0.90	0.0
	0.90	1.00	0.0

FIG. B.1. Color map of LF for the source in the choir soprano section.

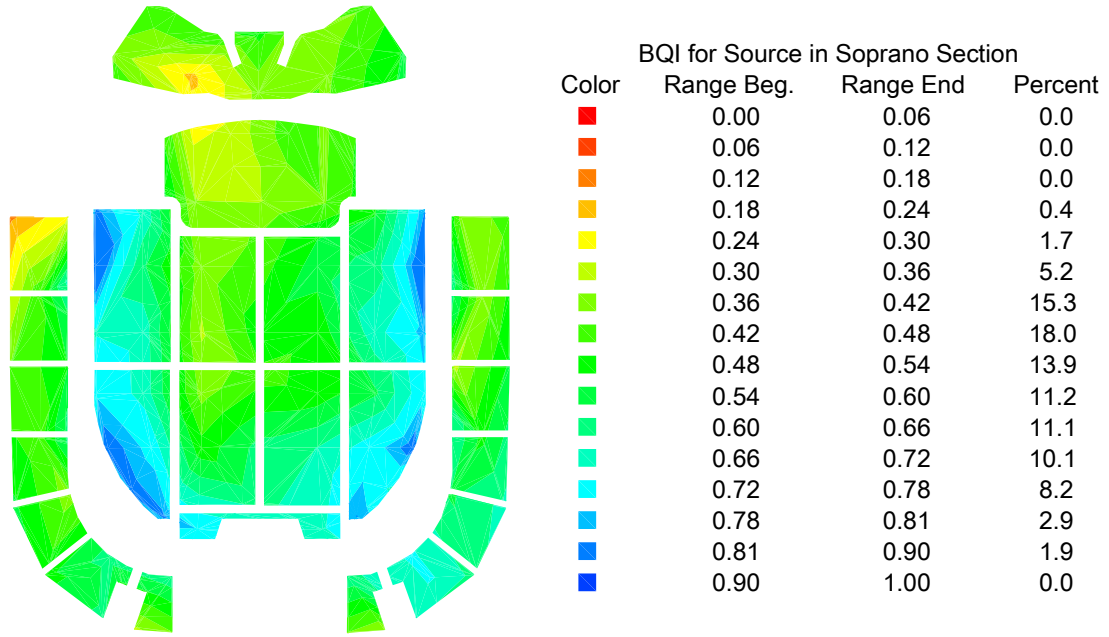

BQI for Source in Soprano Section

Color	Range Beg.	Range End	Percent
	0.00	0.06	0.0
	0.06	0.12	0.0
	0.12	0.18	0.0
	0.18	0.24	0.4
	0.24	0.30	1.7
	0.30	0.36	5.2
	0.36	0.42	15.3
	0.42	0.48	18.0
	0.48	0.54	13.9
	0.54	0.60	11.2
	0.60	0.66	11.1
	0.66	0.72	10.1
	0.72	0.78	8.2
	0.78	0.81	2.9
	0.81	0.90	1.9
	0.90	1.00	0.0

FIG. B.2. Color map of BQI for the source in the choir soprano section.

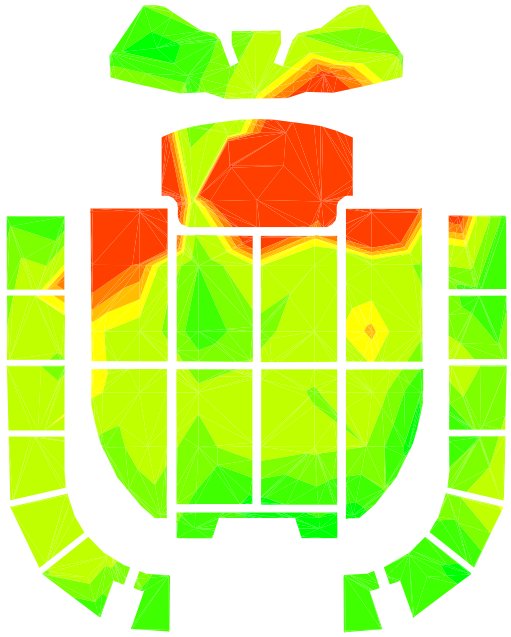

ECS for Source in Choir Soprano Section

Color	Range Beg.	Range End	Percent
	0.00	0.08	0.0
	0.08	0.16	0.0
	0.16	0.24	0.0
	0.24	0.32	0.0
	0.32	0.40	0.0
	0.40	0.48	0.0
	0.48	0.56	0.0
	0.56	0.64	2.0
	0.64	0.72	15.7
	0.72	0.80	20.6
	0.80	0.90	40.0
	0.90	0.93	4.0
	0.93	0.96	2.2
	0.96	1.00	2.3
	1.00	1.50	13.1
	1.50	2.00	0.0

FIG. B.3. Color map of ECS for the source in the choir soprano section.

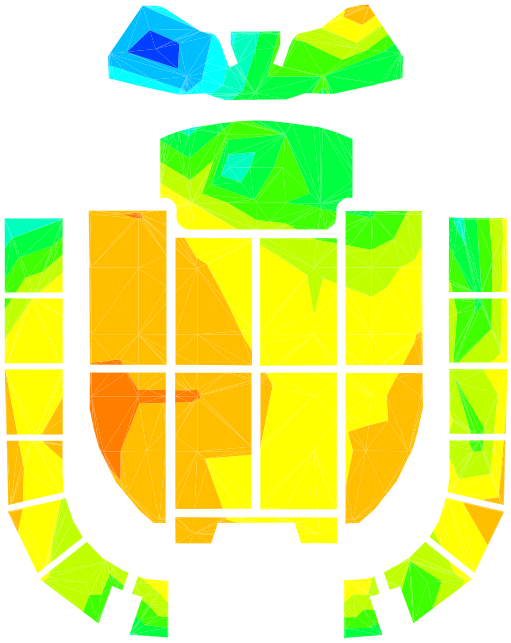

STI for Source in Choir Soprano Section

Color	Range Beg.	Range End	Percent
	0.20	0.25	0.0
	0.25	0.30	0.0
	0.30	0.35	2.6
	0.35	0.40	25.5
	0.40	0.45	30.6
	0.45	0.50	14.1
	0.50	0.55	11.1
	0.55	0.60	9.7
	0.60	0.65	1.8
	0.65	0.70	1.2
	0.70	0.75	2.6
	0.75	0.80	0.7

FIG. B.4. Color map of STI for the source in the choir soprano section.

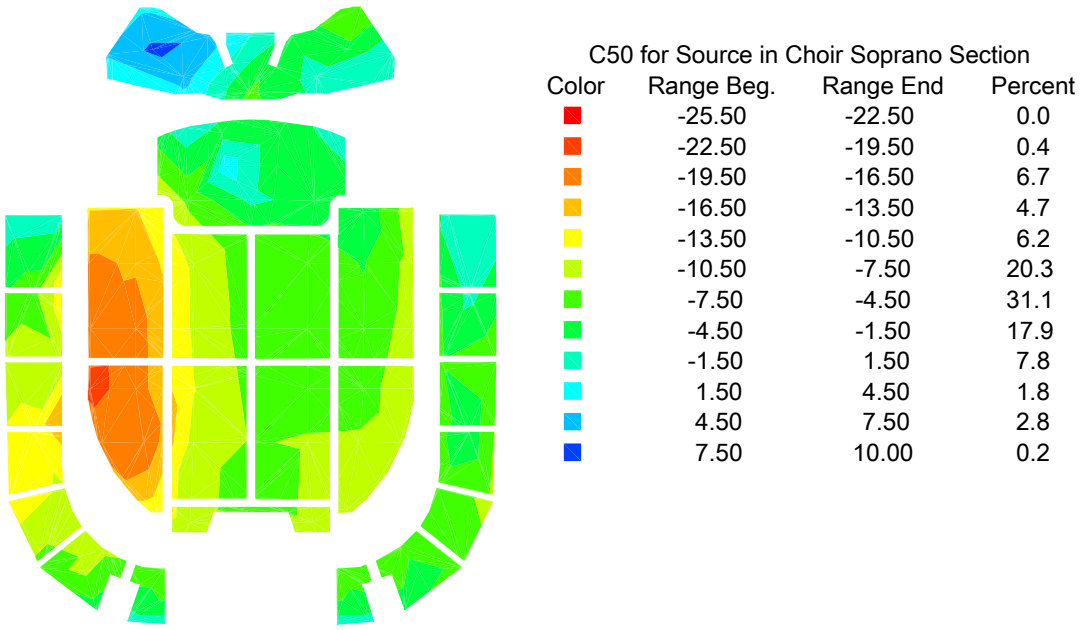

FIG. B.5. Color map of C50 for the source in the choir soprano section.

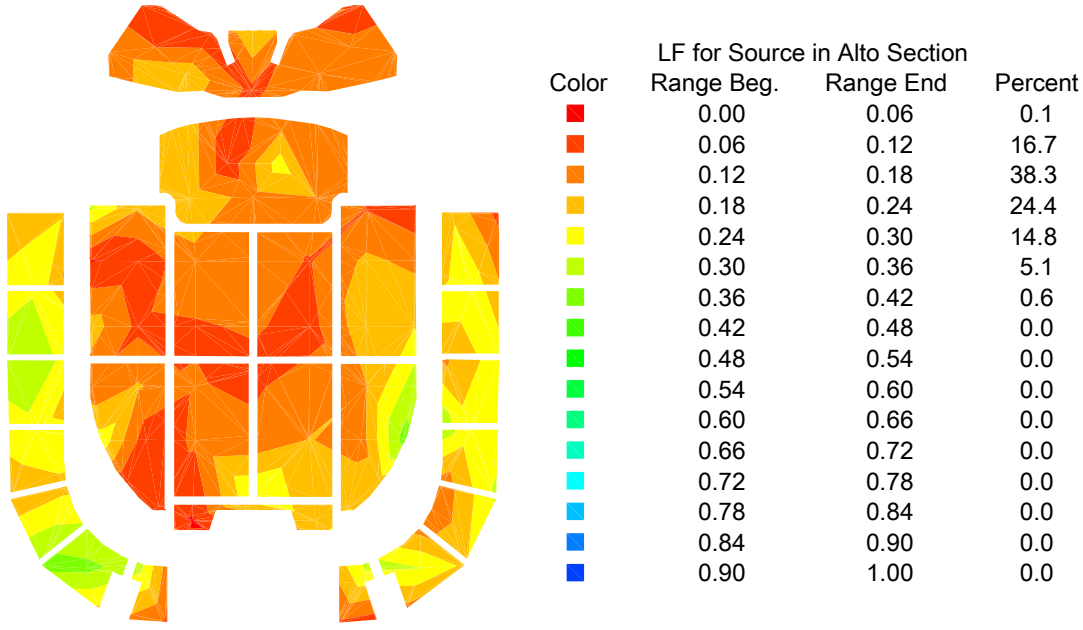

FIG. B.6. Color map of LF for the source in the choir alto section.

BQI for Source in Alto Section

Color	Range Beg.	Range End	Percent
	0.00	0.06	0.0
	0.06	0.12	0.0
	0.12	0.18	0.0
	0.18	0.24	1.1
	0.24	0.30	3.4
	0.30	0.36	5.9
	0.36	0.42	10.3
	0.42	0.48	19.2
	0.48	0.54	15.7
	0.54	0.60	17.4
	0.60	0.66	15.0
	0.66	0.72	8.1
	0.72	0.78	3.6
	0.78	0.84	0.3
	0.84	0.90	0.0
	0.90	1.00	0.0

FIG. B.7. Color map of BQI for the source in the choir alto section.

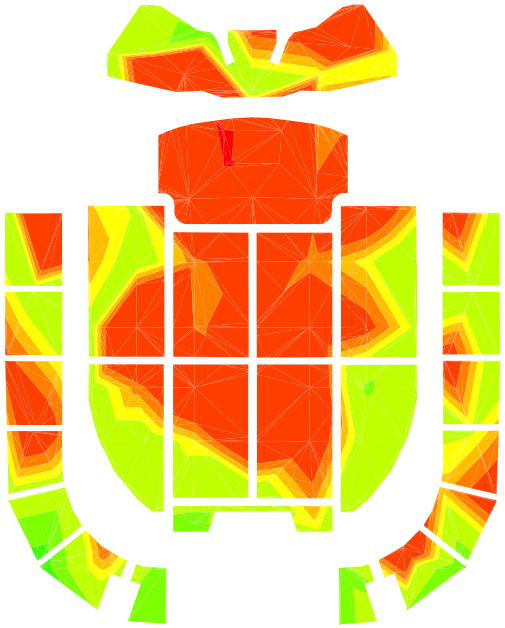

ECS for Source in the Choir Alto Section

Color	Range Beg.	Range End	Percent
	0.00	0.08	0.0
	0.08	0.16	0.0
	0.16	0.24	0.0
	0.24	0.32	0.0
	0.32	0.40	0.0
	0.40	0.48	0.0
	0.48	0.56	0.0
	0.56	0.64	0.0
	0.64	0.72	0.2
	0.72	0.80	4.1
	0.80	0.90	26.8
	0.90	0.93	9.7
	0.93	0.96	7.9
	0.96	1.00	10.2
	1.00	1.50	40.8
	1.50	2.00	0.3

FIG. B.8. Color map of ECS for the source in the choir alto section.

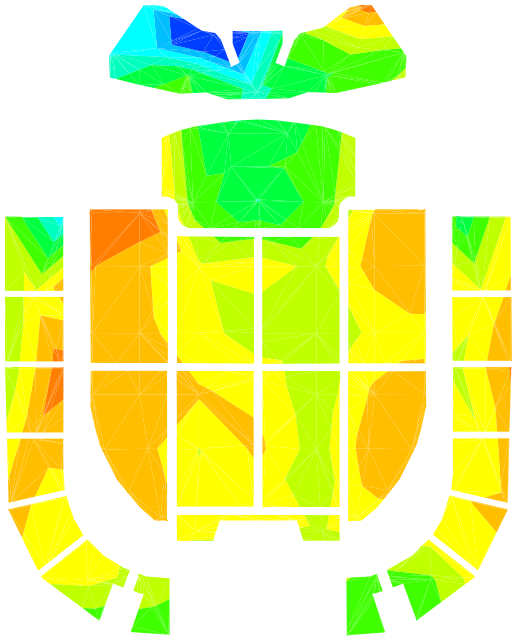

STI for Source in Choir Alto Section

Color	Range Beg.	Range End	Percent
	0.20	0.25	0.0
	0.25	0.30	0.0
	0.30	0.35	2.1
	0.35	0.40	23.9
	0.40	0.45	31.9
	0.45	0.50	18.4
	0.50	0.55	10.8
	0.55	0.60	7.7
	0.60	0.65	1.6
	0.65	0.70	1.7
	0.70	0.75	0.9
	0.75	0.90	0.9

FIG. B.9. Color map of STI for the source in the choir alto section.

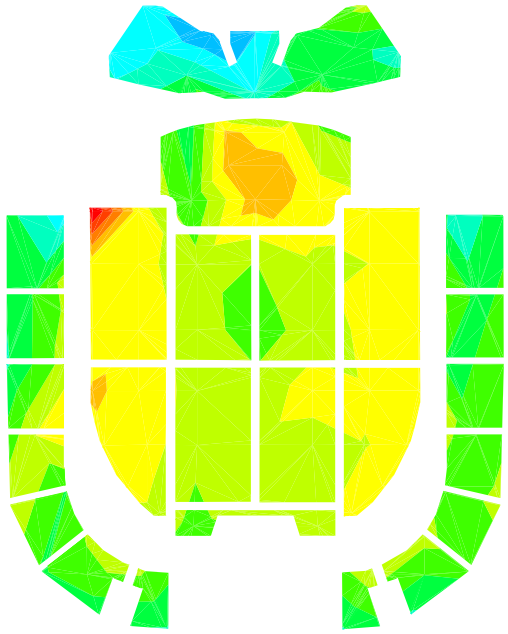

C50 for Source in Choir Alto Section

Color	Range Beg.	Range End	Percent
	-25.50	-22.50	0.1
	-22.50	-19.50	0.1
	-19.50	-16.50	0.2
	-16.50	-13.50	3.1
	-13.50	-10.50	28.5
	-10.50	-7.50	29.1
	-7.50	-4.50	18.8
	-4.50	-1.50	12.2
	-1.50	1.50	3.8
	1.50	4.50	3.3
	4.50	7.50	0.9
	7.50	10.00	0.0

FIG. B.10. Color map of C50 for the source in the choir alto section.

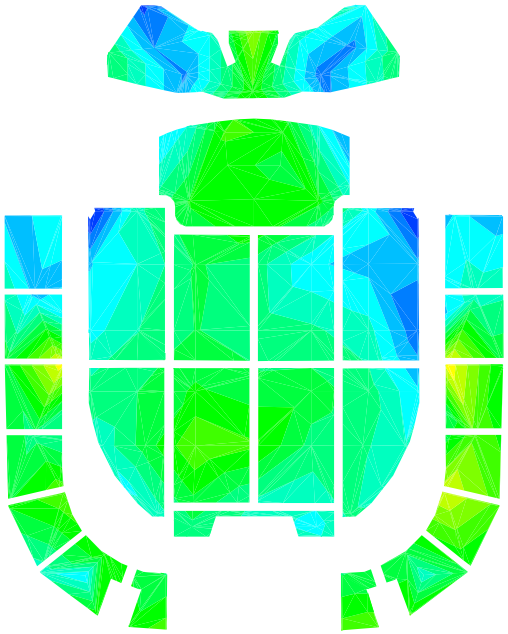

C80 for Source through the Sound System

Color	Range Beg.	Range End	Percent
	-11.20	-10.00	0.0
	-10.00	-9.00	0.0
	-9.00	-8.00	0.0
	-8.00	-7.00	0.0
	-7.00	-6.00	0.1
	-6.00	-5.00	0.8
	-5.00	-4.00	2.3
	-4.00	-3.00	5.7
	-3.00	-2.00	15.1
	-2.00	-1.00	17.5
	-1.00	0.00	20.5
	0.00	1.00	14.8
	1.00	2.00	13.0
	2.00	3.00	7.7
	3.00	4.00	2.2
	4.00	5.00	0.3

FIG. B.11. Color map of C80 for the source through the sound system.

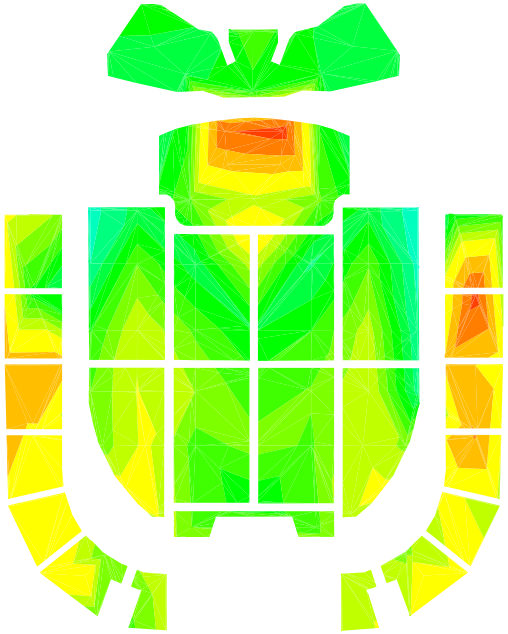

ECM for Source through the Sound System

Color	Range Beg.	Range End	Percent
	0.00	0.09	0.0
	0.09	0.18	0.0
	0.18	0.27	0.0
	0.27	0.36	0.0
	0.36	0.45	0.7
	0.45	0.54	2.2
	0.54	0.63	12.1
	0.63	0.72	13.3
	0.72	0.81	15.2
	0.81	0.90	15.2
	0.90	1.00	16.0
	1.00	1.20	15.6
	1.20	1.40	7.3
	1.40	1.60	2.1
	1.60	1.80	0.3
	1.80	2.00	0.0

FIG. B.12. Color map of ECM for the source through the sound system.

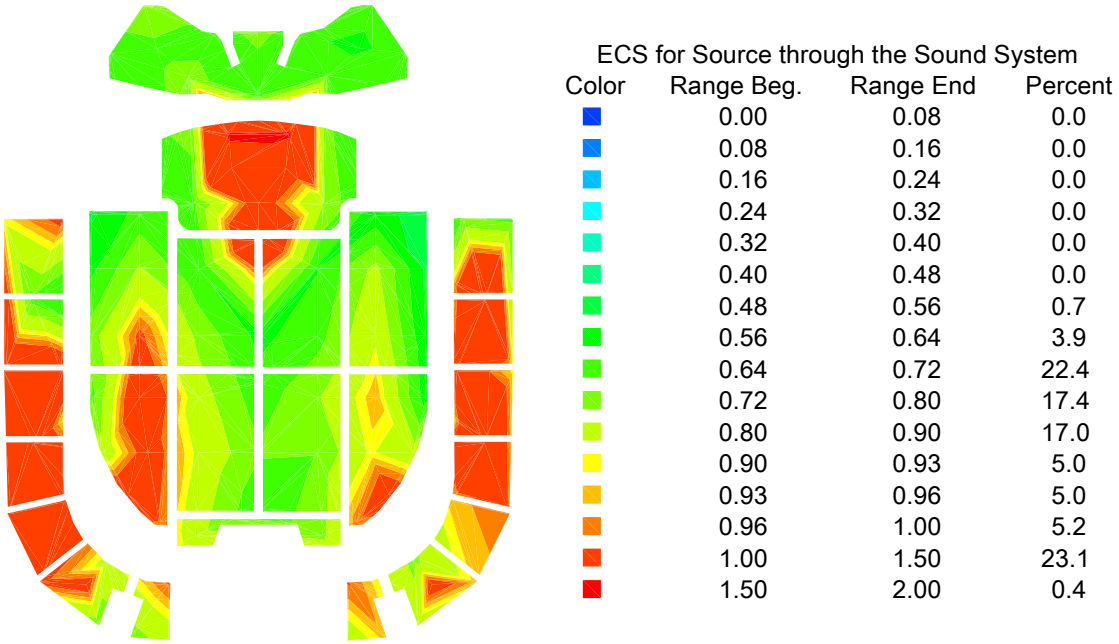

FIG. B.13. Color map of ECS for the source through the sound system.

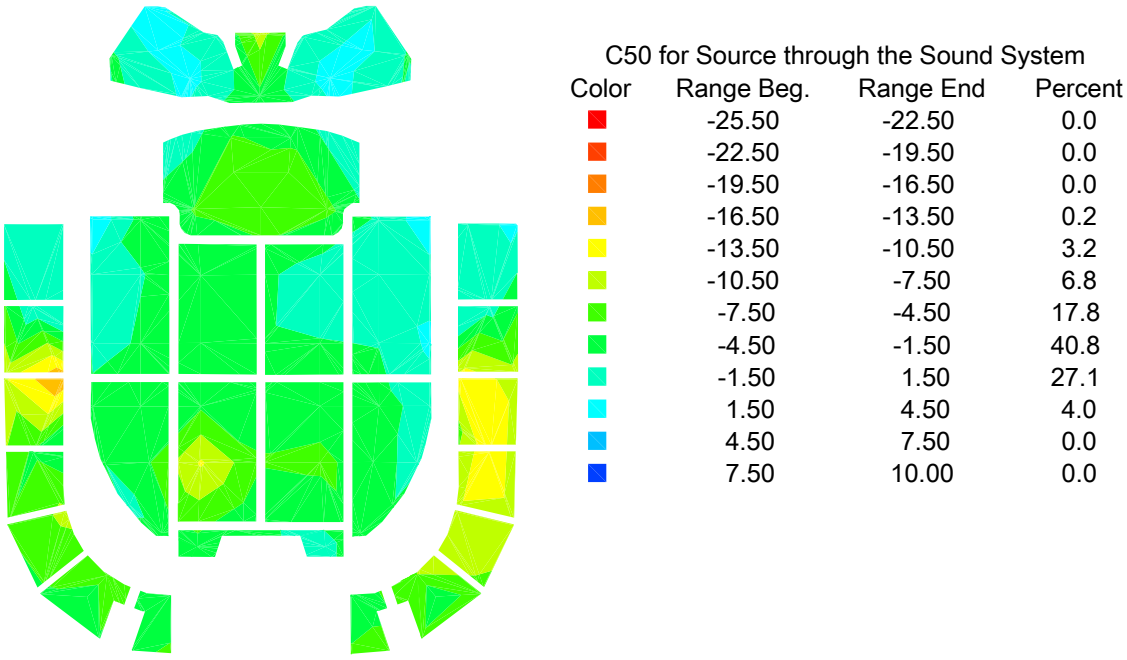

FIG. B.14. Color map of C50 for the source through the sound system.

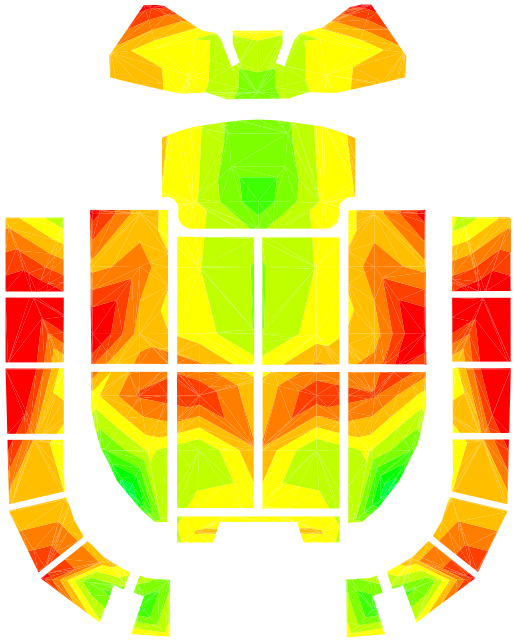

T10 for Source at the Pulpit

Color	Range Beg.	Range End	Percent
	1.10	1.35	0.0
	1.35	1.30	0.0
	1.60	1.85	0.0
	1.85	2.10	0.0
	2.10	2.35	0.0
	2.35	2.60	0.0
	2.60	2.85	0.2
	2.85	3.10	0.5
	3.10	3.35	1.8
	3.35	3.60	7.2
	3.60	3.85	17.9
	3.85	4.10	21.3
	4.10	4.35	21.2
	4.35	4.60	14.2
	4.60	4.85	8.2
	4.85	5.90	7.4

FIG. B.15. Color map of $T10_{10\text{-}20}$ for the source at the pulpit.

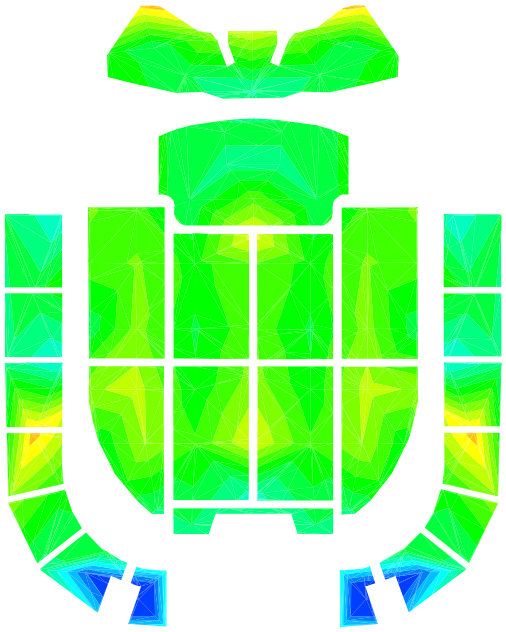

C80 for Source at the Pulpit

Color	Range Beg.	Range End	Percent
	-11.20	-10.00	0.0
	-10.00	-9.00	0.0
	-9.00	-8.00	0.0
	-8.00	-7.00	0.2
	-7.00	-6.00	1.4
	-6.00	-5.00	4.3
	-5.00	-4.00	12.9
	-4.00	-3.00	24.0
	-3.00	-2.00	20.4
	-2.00	-1.00	20.6
	-1.00	0.00	9.8
	0.00	1.00	1.9
	1.00	2.00	1.0
	2.00	3.00	1.2
	3.00	4.00	1.0
	4.00	8.00	1.1

FIG. B.16. Color map of C80 for the source at the pulpit.

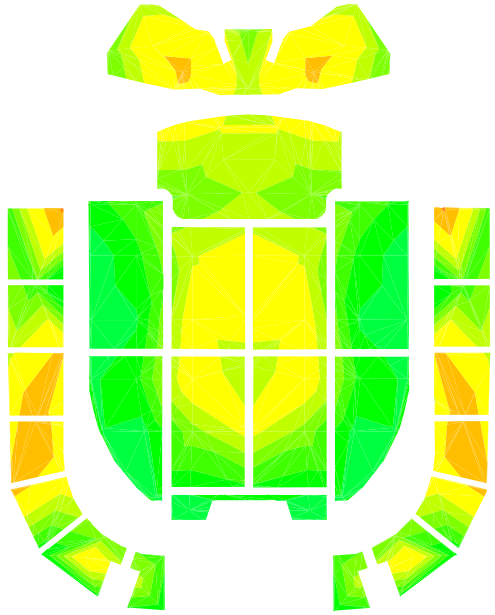

ECM for Source at the Pulpit

Color	Range Beg.	Range End	Percent
	0.00	0.09	0.0
	0.09	0.18	0.0
	0.18	0.27	0.0
	0.27	0.36	0.0
	0.36	0.45	0.0
	0.45	0.54	0.0
	0.54	0.63	10.4
	0.63	0.72	12.5
	0.72	0.81	10.8
	0.81	0.90	13.4
	0.90	1.00	19.4
	1.00	1.20	27.7
	1.20	1.40	5.8
	1.40	1.60	0.0
	1.60	1.80	0.0
	1.80	2.00	0.0

FIG. B.17. Color map of ECM for the source at the pulpit.

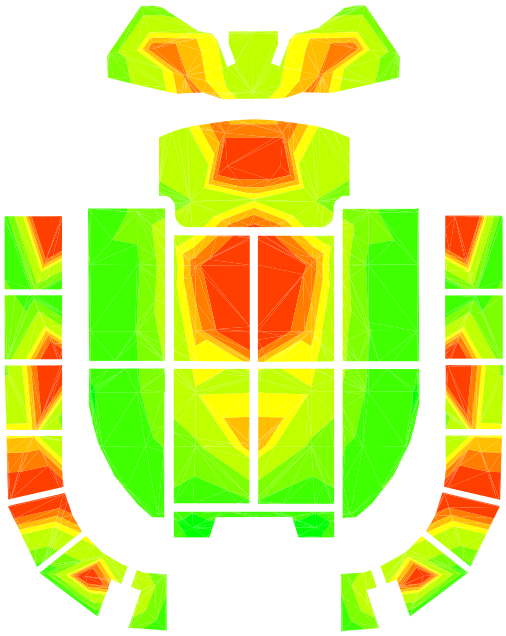

ECS for Source at the Pulpit

Color	Range Beg.	Range End	Percent
	0.00	0.08	0.0
	0.08	0.16	0.0
	0.16	0.24	0.0
	0.24	0.32	0.0
	0.32	0.40	0.0
	0.40	0.48	0.0
	0.48	0.56	0.0
	0.56	0.64	0.9
	0.64	0.72	22.5
	0.72	0.80	15.8
	0.80	0.90	24.6
	0.90	0.93	9.6
	0.93	0.96	7.6
	0.96	1.00	7.3
	1.00	1.50	11.8
	1.50	2.00	0.0

FIG. B.18. Color map of ECS for the source at the pulpit.

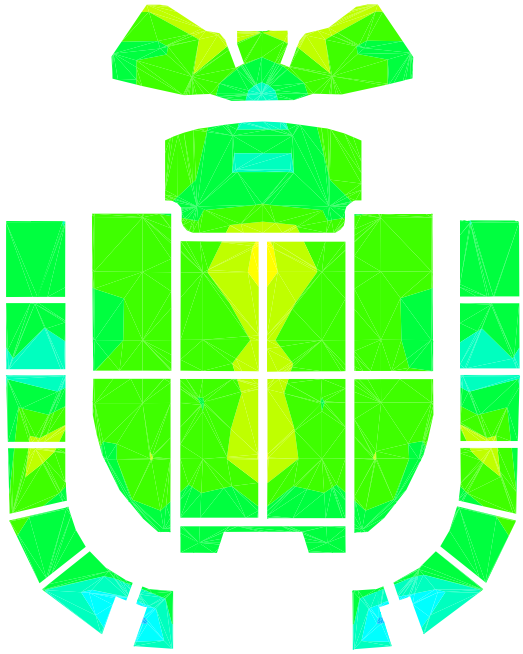

C50 for Source at the Pulpit

Color	Range Beg.	Range End	Percent
	-25.50	-22.50	0.0
	-22.50	-19.50	0.0
	-19.50	-16.50	0.0
	-16.50	-13.50	0.0
	-13.50	-10.50	0.4
	-10.50	-7.50	9.7
	-7.50	-4.50	50.0
	-4.50	-1.50	31.6
	-1.50	1.50	6.8
	1.50	4.50	1.5
	4.50	7.50	0.0
	7.50	10.00	0.0

FIG. B.19. Color map of C50 for the source at the pulpit.

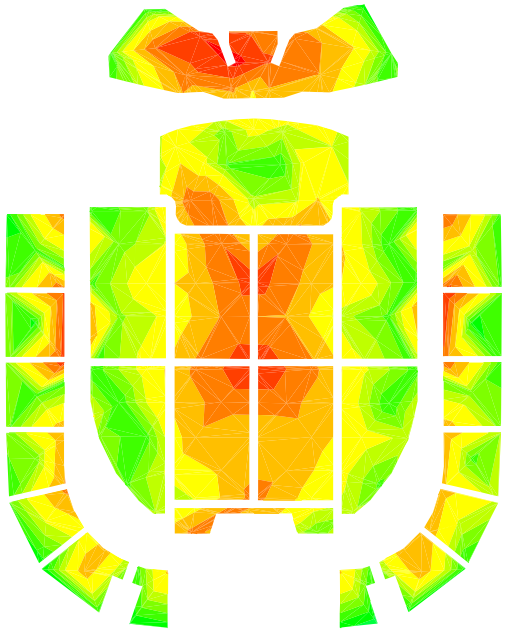

ECM for Source at Center Stage, CATT Model

Color	Range Beg.	Range End	Percent
	0.00	0.09	0.0
	0.09	0.18	0.0
	0.18	0.27	0.0
	0.27	0.36	0.0
	0.36	0.45	0.0
	0.45	0.54	0.0
	0.54	0.63	0.0
	0.63	0.72	0.8
	0.72	0.81	9.0
	0.81	0.90	15.2
	0.90	1.00	16.1
	1.00	1.20	23.1
	1.20	1.40	19.6
	1.40	1.60	12.6
	1.60	1.80	3.4
	1.80	2.00	0.1

FIG. B.20. Color map of ECM for the CATT™ model with the source at center stage.

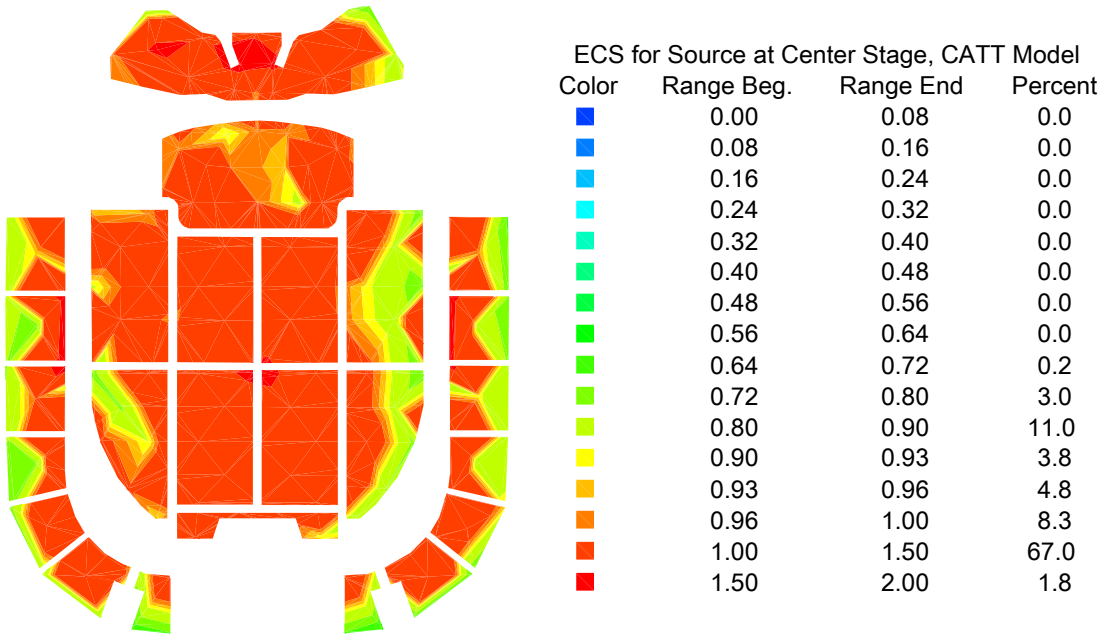

FIG. B.21. Color map of ECS for the CATT™ model with the source at center stage.

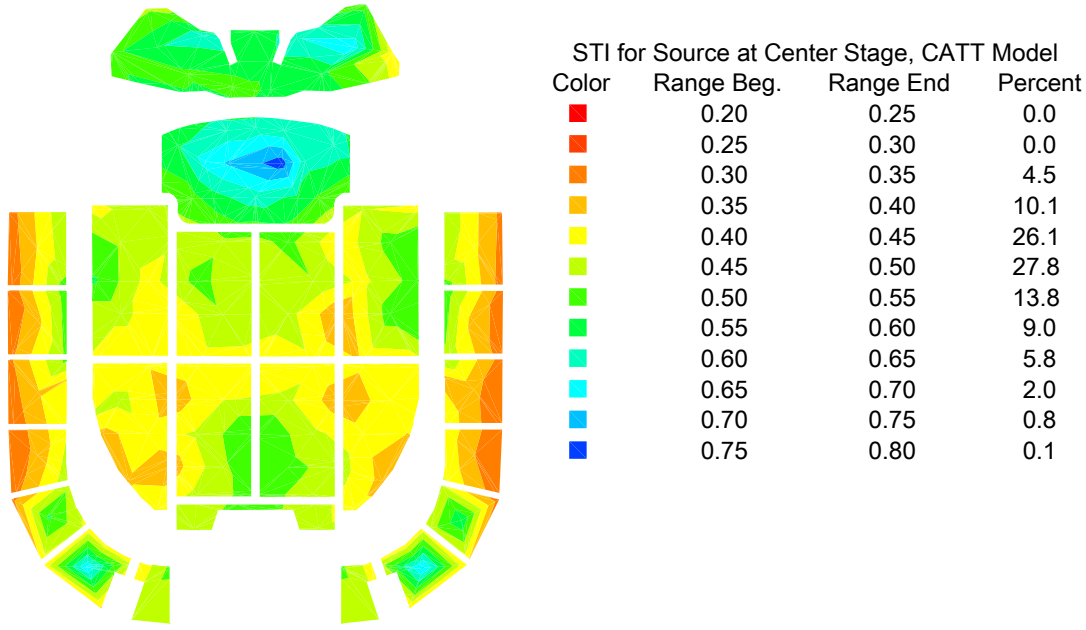

FIG. B.22. Color map of STI for the CATT™ model with the source at center stage.

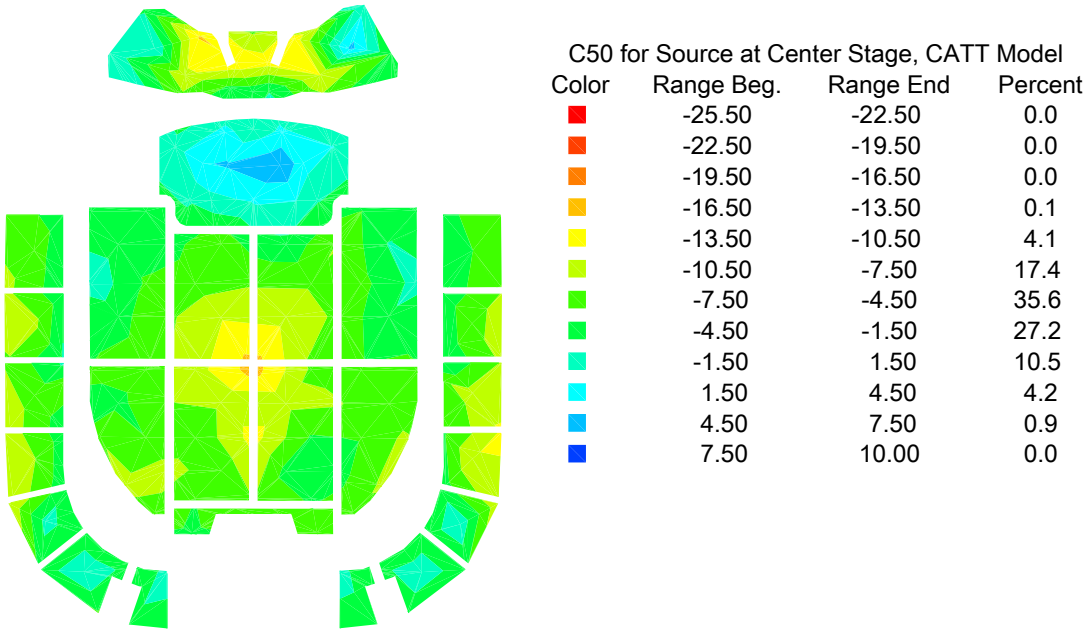

FIG. B.23. Color map of C50 for the CATT™ model with the source at center stage.

Appendix C – Absorption and Scattering Coefficients used in CATT™ Model

Table C.1 Absorption coefficients used in the CATT model, in terms of percentages.

Material Name (Description)	125 Hz	250 Hz	500 Hz	1000 Hz	2000 Hz	4000 Hz
BLACKCURT (Stage Curtain)[1]	7	31	49	65	60	50
BSEATS (Balcony Seats, Occupied)[2]	15	20	25	30	50	50
BSEATS_UN (Balcony Seats, Unoccupied)[2]	4.3	6.3	7	8	14	15
CEIL_PLASTER3 (Ceiling Plaster)[3]	15	12	8	6	4	2
CSEATS (Choir Seats)[4]	26	38	48	55	55	54
DARKWOOD (Organ Case)[4]	28	22	19	16	8	6
GLASS (Cry Room Window)[1]	35	25	18	12	7	4
LINO (Linoleum -Choir, Balcony)[1]	1	2	2	3	4	5
MSEATS (Main Floor Seats, Occupied)[2]	15	20	25	30	50	50
MSEATS_UN (Main Floor Seats, Unoccupied)[2]	4.3	6.3	7	8	14	15
PINETREESA (Trees, 3.15 m^2 Ceiling Faces)	2.7	3	4.4	9.3	25	51
PINETREESB (Trees, 4.86 m^2 Ceiling Faces)	1.7	2	2.9	6	16	33
PINETREESC (Trees, 5.69 m^2 Ceiling Faces)	1.5	1.7	2.4	5	14	28
PINETREESD (Trees, 6.75 m^2 Ceiling Faces)	1.2	1.5	2	4.3	11	24
PINEWALLEXT (Exterior Walls)[4]	25	18	11	8	7	6
PINEWALLINT (Interior Walls - Stage, Stairs)[4]	32	10	8	6	4	2
PINEWIN (Exterior Walls with Windows)[1]	32	24	18	11	9	8
REDCARPET (Comm.Carpet - Main Floor, Choir)[4]	2	4	8	20	35	40
RSEATS (Rostrum Seats, by the Stage)[2]	15	20	25	30	50	45
SWOOD (Stage Floor)[4]	10	7	6	6	6	6

Table C.2. Published values for absorption coefficients that are different from Table C.1. The numbers 2 and 3 in the descriptions for the unoccupied seating and plaster coefficients correspond to the second and third absorption coefficients shown in Table 6.1.

Material Name (Description)	125 Hz	250 Hz	500 Hz	1000 Hz	2000 Hz	4000 Hz
BLACKCURT (Stage Curtain)[5]	5	7	13	22	32	35
BSEATS (Balcony Seats, Occupied)[5]	57	61	75	85	91	86
BSEATS_UN (Balcony Seats, Unoccupied, 2)[6]	2	2	3	6	6	5
BSEATS_UN (Balcony Seats, Unoccupied, 3)[1]	30	36	41	46	66	66
CEIL_PLASTER3 (plaster on laths, air space, 2)[5]	30	10	10	5	4	5
CEIL_PLASTER3 (rough plaster on lath, 3)[5]	2	3	4	5	4	3
CSEATS (Choir Seats)[7]	54	62	68	70	68	66
DARKWOOD (Organ Case)[4]	28	22	19	13	8	6
LINO (Linoleum -Choir, Balcony)[5]	2	3	3	3	3	2
MSEATS (Main Floor Seats, Occupied)[5]	57	61	75	86	91	86
MSEATS_UN (Main Floor Seats, Unoccupied, 2)[6]	2	3	3	6	6	5
MSEATS_UN (Main Floor Seats, Unoccupied, 3)[1]	30	36	41	46	66	66
PINEWALLEXT (Exterior Walls)[4]	25	18	11	8	7	6
PINEWALLINT (Interior Walls - Stage, Stairs)[1]	28	22	19	13	8	6
RSEATS (Rostrum Seats, by the Stage)[7]	15	20	25	30	50	45

Table C.3. Scattering coefficients used in the CATT model, in terms of percentages. All of these coefficients were determined by modifying similar coefficients in Heather Smith's thesis.[8]

Material Name (Description)	125 Hz	250 Hz	500 Hz	1000 Hz	2000 Hz	4000 Hz
BLACKCURT (Stage Curtain)	15	15	15	15	15	15
BSEATS (Balcony Seats, Occupied)	30	40	50	60	70	70
BSEATS_UN (Balcony Seats, Unoccupied)	30	40	50	60	70	70
CEIL_PLASTER3 (Ceiling Plaster)	30	30	30	30	30	30
CSEATS (Choir Seats)	30	40	50	60	70	70
DARKWOOD (Organ Case)	10	15	30	65	80	80
GLASS (Cry Room Window)	10	10	10	10	10	10
LINO (Linoleum Flooring - Choir, Balcony)	10	10	10	10	10	10
MSEATS (Main Floor Seats, Occupied)	30	40	50	60	70	70
MSEATS_UN (Main Floor Seats, Unoccupied)	30	40	50	60	70	70
PINETREESA (Trees, 3.15 m^2 Ceiling Faces)	20	20	20	20	23	30
PINETREESB (Trees, 4.86 m^2 Ceiling Faces)	20	20	20	20	23	30
PINETREESC (Trees, 5.69 m^2 Ceiling Faces)	20	20	20	20	23	30
PINETREESD (Trees, 6.75 m^2 Ceiling Faces)	20	20	20	20	23	30
PINEWALLEXT (Exterior Walls)	20	20	20	20	20	20
PINEWALLINT (Interior Walls - Stage, Stairs)	10	10	10	10	10	10
PINEWIN (Exterior Walls with Windows)	20	20	20	20	20	20
REDCARPET (Commercial Carpet - Main Floor, Choir)	15	15	15	15	15	15
RSEATS (Rostrum Seats, by the Stage)	30	40	50	60	70	70
SWOOD (Stage Floor)	10	10	10	10	10	10

References

[1] C. Davis and D. Davis, *Sound System Engineering*, 2nd ed. (Elsevier, Burlington, MA, 1997), Chap. 7, p. 158-160.

[2] R. E. Borg and D. G. Stork, *The Physics of Sound*, 2nd ed. (Prentice Hall, Englewood Cliffs, NJ, 1995), Chap. 8, p. 230.

[3] A. Lawrence, *Architectural Acoustics*. (Elsevier Pub. Co. Ltd.,London, 1970), App. 3, p. 201.

[4] L. L. Beranek, *Concert Halls and Opera Houses: Music, Acoustics and Architecture*. 2nd ed. (Springer-Verlag, New York, 2004), App. 3, pp. 639-640.

[5] T. J. Cox and P. D'Antonio, *Acoustic Absorbers and Diffusers: Theory, design and application*. (Spon Press, New York, 2004), App. A, pp. 375-378. This reference also contains an absorption coefficient for pews, 100% occupied.

[6] D. E. Hall, *Musical Acoustics*. (Brooks/Cole, Pacific Grove, CA, 2002), Chap. 15, p. 331.

[7] L. L. Beranek and T. Hidaka, "Sound absorption in concert halls by seats, occupied and unoccupied, and by the hall's interior surfaces," J. Acoust. Soc. Am. **104**, 3169-3177 (1998).

[8] H Smith, *Geometric Acoustic Modeling of the LDS Conference Center*, M. S. Thesis, Brigham Young University, 2004. p. 124.

Appendix D – Data from Kirkegaard Associates

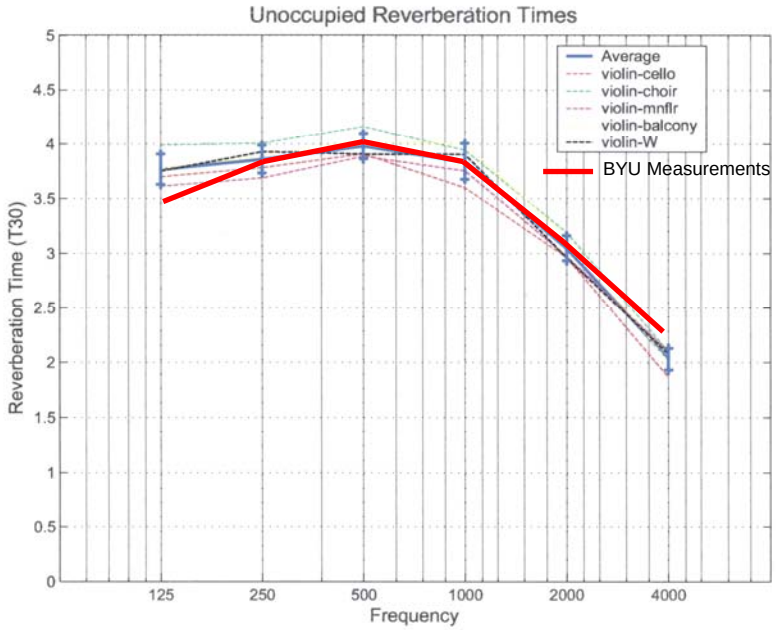

FIG. D.1. Graph showing unoccupied reverberation times measured by Tim Gulsrud of Kirkegaard Associates. The times shown for the BYU measurements were the times calculated according to ISO 3382. For the Kirkegaard measurements, the dodecahedron loudspeaker was on stage near the violinists.

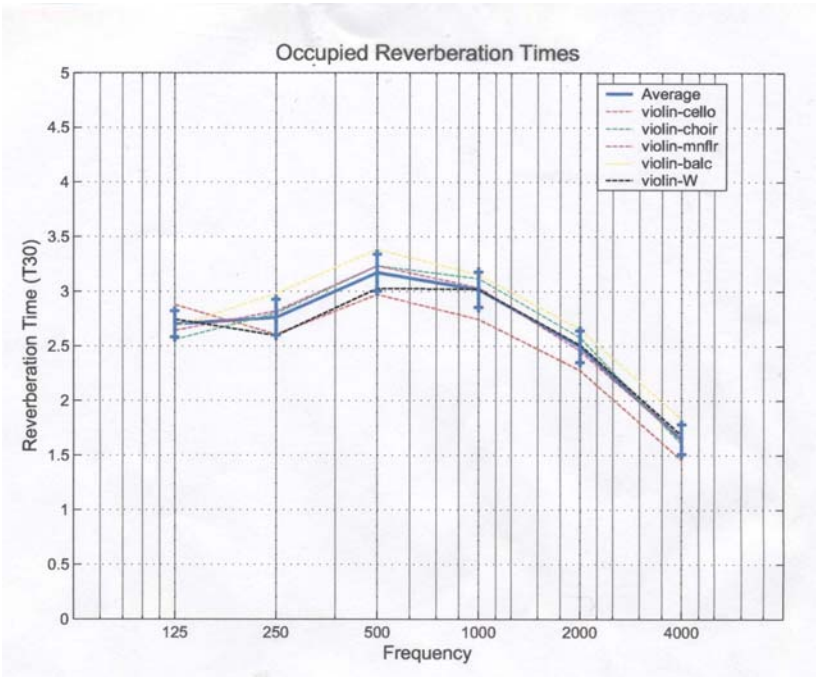

FIG. D.2. Reverberation times measured in the Tabernacle right before a concert to measure the occupied condition. The audience filled the main floor, but only a few seats in the balcony.

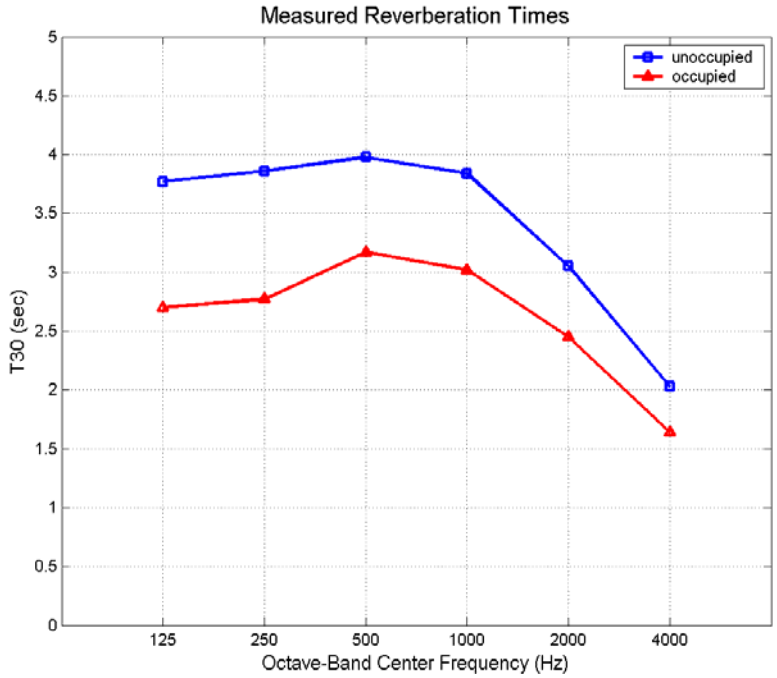

FIG. D.3. Comparison of the unoccupied reverberation times to the occupied reverberation times, to show the difference of having an audience in the Tabernacle.

All of these plots were created by Tim Gulsrud of Kirkegaard Associates.

Appendix E – Subjective Survey Form, by Jon Holloman

Salt Lake Tabernacle Acoustical Mapping Project
Listener Evaluation February 2004

Parameter

Reverberation Time	Too short	*1 2 3 4 5 6 7*	Too long
Mid-frequency strength factor	Too little	*1 2 3 4 5 6 7*	Too much
Low-frequency strength factor	Too little	*1 2 3 4 5 6 7*	Too much
First reflection	Not noticeable	*1 2 3 4 5 6 7*	Too strong
Binaural quality factor (Is the sound even in both ears?)	Not even	*1 2 3 4 5 6 7*	Even
Envelopment factor (Do you feel included as part of the performance?)	Too close	*1 2 3 4 5 6 7*	Too Distant
Bass ratio (Is there enough bass energy to balance the highs and mids?)	Not enough	*1 2 3 4 5 6 7*	Too much
Clarity factor	Unclear	*1 2 3 4 5 6 7*	Clear

Comments: _____

_____

Ambient noise	Not noticeable	*1 2 3 4 5 6 7*	Too much
Stage support factor (Choir and Orch)	While you are performing, can you hear well enough to maintain pitch, rhythm and blend?		
	NO	*1 2 3 4 5 6 7*	YES

Comments: _____

_____

Evaluator: _____Seat Position_____

Is there an audience present? _____

Appendix F – Comparison of Auralizations

Table F.1. Auralizations for receiver location toward the front of the main floor (seat 3 in Fig. 2.7).

Measured	Current Model	No Balcony	Balcony	Trees